INFORMATION TO USERS

This manuscript has been reproduced from the microfilm master. UMI films the text directly from the original or copy submitted. Thus, some thesis and dissertation copies are in typewriter face, while others may be from any type of computer printer.

The quality of this reproduction is dependent upon the quality of the copy submitted. Broken or indistinct print, colored or poor quality illustrations and photographs, print bleedthrough, substandard margins, and improper alignment can adversely affect reproduction.

In the unlikely event that the author did not send UMI a complete manuscript and there are missing pages, these will be noted. Also, if unauthorized copyright material had to be removed, a note will indicate the deletion.

Oversize materials (e.g., maps, drawings, charts) are reproduced by sectioning the original, beginning at the upper left-hand corner and continuing from left to right in equal sections with small overlaps. Each original is also photographed in one exposure and is included in reduced form at the back of the book.

Photographs included in the original manuscript have been reproduced xerographically in this copy. Higher quality 6" x 9" black and white photographic prints are available for any photographs or illustrations appearing in this copy for an additional charge. Contact UMI directly to order.

UMI®

Bell & Howell Information and Learning
300 North Zeeb Road, Ann Arbor, MI 48106-1346 USA
800-521-0600

Identification and Characterization of an Operon Affecting Detachment of *Streptococcus mutans* from Biofilms.

by

Neeraj Vats

Submitted in partial fulfillment of the requirements for the degree of Doctor of Philosophy

at

Dalhousie University
Halifax, Nova Scotia
March 24, 2000

DALHOUSIE UNIVERSITY

FACULTY OF GRADUATE STUDIES

The undersigned hereby certify that they have read and recommend to the Faculty of Graduate Studies for acceptance a thesis entitled "Identification and Characterization of an Operon Affecting Detachment of *Streptococcus mutans* from Biofilms"

by Neeraj Vats

in partial fulfillment of the requirements for the degree of Doctor of Philosophy.

Dated: March 24, 2000

External Examiner

Research Supervisor

Examining Committee

DALHOUSIE UNIVERSITY

DATE: March 24, 2000

AUTHOR: Neeraj Vats

TITLE: Identification and Chraracterization of an Operon Affecting Detachment of *Streptococcus mutans* from Biofilms

DEPARTMENT OR SCHOOL: Microbiology and Immunology

DEGREE: Ph.D. CONVOCATION: May YEAR: 2000

Permission is herewith granted to Dalhousie University to circulate and to have copied for non-commercial purposes, at its discretion, the above title upon the request of individuals or instructions.

Signature of Author

Dedicated to the memory of my loving grandmother, and my kind cousin Rahual.

TABLE OF CONTENTS

RESULTS

LIST OF FIGURES

LIST OF TABLES

ABSTRACT

Streptococcus mutans adheres to enamel and may subsequently cause caries. A previously characterized surface protein releasing enzyme (SPRE), capable of detaching cells from model biofilms may be a means to detach cells from enamel prior to the development of caries. This work was undertaken to characterize the SPRE activity, and identify gene(s) responsible for, or affecting the activity or production of SPRE. Characterization of SPRE required development of a model system to assay detachment. In detachment experiments biofilms were formed on epon-hydroxyapatite (EHA) rods, which mimicked enamel. To mirror conditions in the oral cavity and to provide a specific mechanism for adherence EHA rods were conditioned with saliva or salivary agglutinin (SA). Stable biofilms were formed after 1 hour. Detachment was determined to be temperature dependent, and had a pH optimum of 5.5-6.0. In comparison to the controls, crude SPRE preparations were able to induce detachment of significantly greater percentages of cells from model biofilm. The susceptibility of SPRE to inactivation by pronase, suggested detachment was an active enzyme mediated process. A pool of transposon mutants was produced and screened. A putative SPRE defective mutant was isolated. In contrast to the wild type, SPRE prepared from the mutant lacked the ability to detach cells from biofilms. Genetic characterization revealed a single transposon insertion adjacent to the -35 region of an operon encoding a P-type ATPase similar to CopA and CopB of *Enterococcus hirae*. The ATPase conferred high level (8 mM) copper resistance to *S. mutans*. The transposon insertion was postulated to allow increased expression of the operon by decreasing the affinity of a negative regulator, CopY, for its binding site overlapping the promoter. Increased expression of the ATPase in the mutant was believed to lower intracellular copper concentrations which may negatively effect SPRE.

ABBREVIATIONS

AEP	Acquired enamel pellicle
ATP	Adenosine triphosphate
BSA	Bovine serum albumin
CAT	Chloramphenicol acetyltransferase
DNA	Deoxyribonucleic acid
DEPC	Diethylpyrocarbonate
EHA	Epon-hydroxyapatite
ELISA	Enzyme-linked immunosorbent assay
HA	Hydroxyapatite
IgG	Immunoglobulin G
MIC	Minimal inhibitory concentration
ORF	Open reading frame
PBS	Phosphate buffered saline
PBP	Penicillin binding protein
PBST	Phosphate buffered saline / Tween 20
PCR	Polymerase chain reaction
PTS	Phosphoenolpyruvate: sugar phosphotransferase system
RNA	Ribonucleic acid
RCB	Resting cell buffer
SA	Salivary agglutinin
SPRE	Surface protein releasing enzyme
sIgA	Secretory immunoglobulin A

ACKNOWLEDGEMENTS

I would like thank my supervisor Dr. Lee; he had all the attributes expected from a supervisor, most importantly, patience and knowledge. Additionally, his infectious enthusiasm and belief that anything was possible got me through many tough spots. I would also like to thank the members my supervisory committee, Drs. Hoffman, Mahony and Ryding for support and helpful suggestions. I would particularly like to thank Dr. Hoffman and the members of his research group for welcoming me into their lab and for all of the help they gave me with the molecular biological techniques; without them I would still be in the lab struggling with libraries and RNA.

I also wish to thank past and present members of Dr. Lee's lab for their help and friendship. Without them graduate school would have been a long, lonely pursuit.

I would also like to extend my thanks to the members of the Department of Microbiology and Immunology, for all of your help from the time I began my bachelors degree to suggestions for writing this thesis.

Most importantly I have to thank my family for everything! If it wasn't for their love, support, and encouragement non of this would have been possible.

Thanks also to everyone at Freewheeling for the good times.

Last, but not least, Karen. Your warm smile made all the difference.

LITERATURE REVIEW

Biofilms.

Many bacterial diseases require that the pathogen adhere to host surfaces. Adherent bacteria may persist on a surface to form adherent microcolonies called biofilms which are composed of bacterial cells and their products as well as components from the surrounding environment (44). The adherent microcolonies may exist as a monolayer or develop into multiple layers containing one or numerous bacterial species.

Biofilms are of great importance not only in disease but also in industrial processes. Biofilm formation can hamper industrial process by causing corrosion, increasing resistance to flow in water pipes, and reducing heat transfer on the water-cooled side of heat exchangers. In Cystics fibrosis (CF), *Pseudomonas aeruginosa*, can adhere to alveolar epithelial cells and embed themselves in an exopolymer composed of alginate (44). *P. aeruginosa* biofilms within the lungs CF patients may augment the disease state of CF by increasing the turbidity or thickness of the already thick mucous in the lung (143). Additionally, *Staphylococcus epidermidis* infection associated with implanted biomaterials may result in bacterial sepsis or endocarditis (66). In the human oral cavity, adherent microbial biomass on tooth surfaces is referred to as dental plaque, which is a multi-species biofilm composed of bacterial cells, their products and salivary components. Under specific conditions, dental plaque may lead to the formation of dental caries and other diseases (133).

The ubiquity of biofilms and significant effects biofilms have on their environments has prompted significant research into biofilm formation and biofilm processes. In general, biofilm formation is a four-step process: **(i)** The formation of a conditioned surface which involves the

coating of a surface with organic molecules with which bacteria may interact. This step may not be necessary if the biofilm is to be formed on an organic surface such as the epithelium. **(ii)** Reversible adherence of bacteria to the surface through weak interactions such as Van der Wals or hydrophobic interactions. **(iii)** Irreversible bacterial adherence to the surface which requires specific interactions between macromolecules on the bacterial surface such as surface proteins, carbohydrates, and pili or fimbriae with material on the conditioned surface. **(iv)** Growth of the adherent cells to form microcolonies on the immobilised surface (213). Once established, biofilms are extremely difficult to eradicate. Biofilm bacteria have been described as more resistant to biocides, antiseptics, antibiotics, antagonistic environmental factors and host defence systems (44, 68).

Dental plaque is an oral biofilm.

Dental plaque is a multispecies biofilm which forms on the hard surfaces of the oral cavity (133). The enamel is formed of tightly packed hydroxyapatite crystals, the spaces between which are filled with water and organic molecules. With the exception of the small areas between the hydroxyapatite crystals, the enamel is composed of entirely inorganic components, and is conditioned with organic molecules before biofilm formation may proceed. Saliva bathing the teeth fulfils this requirement by coating the teeth with a thin layer of glycoproteins, mucins and enzymes of salivary origin. This thin film of materials is commonly referred to as the acquired enamel pellicle (AEP). Bacteria subsequently adhere to the surface to form dental plaque.

By early adolescence, the flora of the mouth (particularly that of dental plaque) reaches a complex mature state in which more than 200 bacterial taxa are present (72, 147). The presence of such a diverse group of microorganisms does not mean the population is without

some form of order. Bacteria exhibit a tropism for specific sites within the oral cavity with gram-positive, facultatively anaerobic cocci and rods found in occlusal fissures and a predominance of gram-negative, strict anaerobes in deep periodontal pockets (199). *Streptococcus mutans*, for example, only colonises the tooth surface and is absent from the mouths of predentate infants (32).

Even in the case of dental plaque formation there is temporal and spatial organisation. The first bacteria to adhere to the surface are primary colonisers, bacteria which adhere to the tooth via interactions with the acquired pellicle to form a monolayer of cells. After formation of such a monolayer, the acquired pellicle is effectively masked by adherent bacteria. Subsequently adhering bacteria, i.e. secondary colonisers, must then adopt another mechanism for adhesion, i.e. different receptors must be utilised. Secondary colonisers possess intracellular adhesins which recognise and bind to epitopes on the primary colonisers in a phenomenon known as coaggregation allowing themselves to incorporate into the biofilm (108).

As previously stated, enamel is composed of hydroxyapatite crystals. The enamel surface undergoes a dynamic cycle of breakdown and rebuilding (133); however, the balance between demineralization and remineralization may be tilted in the presence of adherent acidogenic bacteria whose metabolic end products can lower the pH to a critical pH (5.0 - 5.5) below which remineralisation cannot occur. If the acid load is too great and the pH remains low for prolonged periods of time or frequently drops below the critical pH, demineralisation will soon lead to tooth decay (133). Burne *et al.* (24) summarised that caries formation is an ecologically driven process. Transition from healthy to diseased plaque correlates with changes in the environment (repeated cycles of plaque acidification) which selects bacteria which can tolerate the new environment.

Streptococcus mutans as an odontopathogen.

To identify dental pathogens (odontopathogens), one must examine the oral environment of diseased individuals and isolate odontopathogens by finding a specific bacterium or group of bacteria possessing virulence factors necessary to produce the observed outcome. To cause caries, a suspect bacterium must be capable of **(i)** attaching and accumulating to enamel, **(ii)** decreasing the near-neutral pH of the oral cavity to 5.0 - 5.5, and **(iii)** surviving and proliferating in an acidic environment.

As early as 1924, *S. mutans* was isolated from carious lesions by Clarke (41). However, the role of *S. mutans* in dental caries was discounted by investigators who could not isolate it from plaque. This was due to the fact that *S. mutans* is not a normal inhabitant of healthy dental plaques. If samples were taken from sites of carious lesions, however, a relation could be drawn between decay and the presence of *S. mutans* (133, 134).

Adherence and accumulation of *S. mutans* at the site of dental caries.

S. mutans can adhere to the pellicle by a sucrose-dependent and -independent mechanism (190).

Sucrose-independent adherence is mediated by the interaction of cell-surface proteins with components of the AEP or with salivary proteins bound to primary colonisers (16, 115, 116). One of the more important surface proteins is antigen P1. P1, a 1561 residue protein (185 kD) encoded by *spaP* (101, 125), is a member of the antigen I/II class of protein receptors of oral streptococci. P1 has been shown to interact with salivary agglutinin (SA), a high molecular weight glycoprotein (ca. 400kD) found in saliva and on the tooth surface (56, 91). The importance of P1 in facilitating adherence was illustrated by the inability of an

isogenic P1-negative mutant 834 of *S. mutans* to adhere to salivary agglutinin-coated HA-beads (126). A similar P1 isogenic mutant PC3370 was found to cause fewer carious lesions than the wild type in a rat model, suggesting P1 is a virulence factor (47).

Members of the antigen I/II class of surface proteins have been the subject of significant research. Their importance in adherence has prompted research to identify mechanisms for surface localisation and the SA-binding regions. P1 is covalently linked to the bacterial cell wall following signal sequence dependant translocation across the membrane (84). Linkage to the cell wall is mediated by conserved sequences located at the protein's C-terminus (discussed below).

Once localised at the surface, two repeating amino acid sequences within P1, an N-terminal alanine-rich (A-region) and a proline-rich (P-region), play important roles in mediating the interaction with SA (101). Using truncated P1 proteins, the importance of the A-region (amino acids 121-447) in binding to SA was first demonstrated (22, 48). Later work reaffirmed the importance of the A-region in interacting with SA, but demonstrated that the P-region may also be involved in interaction with SA (151). Munro *et al.* (150), confirmed that amino acids 816-1213, which are highly conserved among the antigen I/II family of adhesins and include the P-region, mediate the interaction with SA. Brady *et al.* (21) attempted to dissect the role of the P-region in adherence by engineering a protein with an internal deletion of the P-region. The construct was successfully produced, but the protein failed to be surface-expressed and remained in the cytoplasm. It was speculated that the internal deletion caused misfolding and subsequent aggregation of the protein in the cytoplasm.

Collectively, the results imply that the entire P1 protein plays important roles in mediating adherence of *S. mutans* to the AEP, with the P-region being particularly important. The P-region appears to play a role in surface localisation and in folding of P1 into its native conformation. When the protein adopts its tertiary structure, the A and P-regions may be

spatially close and may function co-operatively to mediate a high affinity interaction with SA.

The sucrose-dependent mechanism for adherence of *S. mutans* to the enamel is mediated by glucosyltransferases (GTF). *S. mutans* produces three GTFs of which, GTF-I and GTF-SI encoded by *gtfB* and *gtfC* respectively, produce insoluble glucans composed mainly of alpha-1,3 linked chains of glucose and shorter branches of alpha-1,6 chains (181, 210). Although the main products of GTF-SI are insoluble glucans, GTF-SI also produces soluble glucans (75). The insoluble glucan products may remain associated with the cell, deposited on the enamel, or cleared from the oral cavity. The third GTF, GTF-S, encoded by *gtfD* produces soluble glucans consisting of mainly alpha-1,6 linked glucose that may diffuse through plaque to be used as an energy source by *S. mutans* and other microorganisms (76, 85). The functional domains of these GTFs enzymes lie at their termini. At the N-terminus is the catalytic centre that binds and hydrolyzes sucrose (99, 148, 209). The C-terminus binds the growing polysaccharide chain into which the monosaccharide will be incorporated (2, 97, 220). The C-terminus is also suggested to aid in the surface localization of the enzyme (98). When surface localised, the protein may aid in bacterial adherence by binding to polysaccharides in plaque.

The three GTFs can be found in saliva and on the enamel. *In vitro* experiments demonstrated that GTFs can associate with hydroxyapatite, remain active, and produce glucans that induce adherence of *S. mutans* (176, 215). Studies with GTF knock-out mutants confirmed the importance of these enzymes in adherence. Deletion of *gtfC* resulted in the greatest impairment of adherence, and was the only enzyme that could restore adherence of a triple *gtf* knockout (208). *In vivo* experiments with similar knockouts demonstrated that *gtfB* and *gtfC*, which encode enzymes that produce insoluble glucans, had a greater impact on the ability to induce caries, perhaps due to the inability of the bacteria to accumulate on the enamel

and encapsulate themselves within a layer of polysaccharides (149, 224). The polysaccharides encapsulating biofilms may be critical for the viability of cells in the biofilm. Without polysaccharides the biofilm could grow following intercellular adhesion; however, without a porous polysaccharide layer, the biofilm would just be a dense cluster of cells which nutrients may not be able to penetrate, thus causing the plaque community to die.

Sucrose-dependent adherence may also be facilitated by cell-associated non-enzymatic glucan-binding proteins (Gbp) (172, 186). The importance of GbpA was demonstrated by an *S. mutans* isogenic mutant. In the absence of GbpA it was expected that fewer bacteria would adhere, thus decreasing the virulence. However, the results were the opposite of the expected in that virulence was increased; there was not a marked decrease in adherence, although a change in the structure of the plaque was noted (80). Plaques were now light and fluffy in contrast to the densely packed irregular-shaped plaques of the wild type. GbpA was hypothesised to mediate the formation of the dense plaques. In the absence of GbpA, the slight morphological change may have produced a more porous plaque into which more nutrients could diffuse. This would allow the plaque pH to remain low and lead to demineralisation.

Acid end product of cellular metabolism.

Fifty-five years ago, a relationship was drawn between the availability of a fermentable carbon source (e.g. glucose) and acid production (191). The pH within plaque was shown to drop markedly following rinsing with a 10% glucose solution (43, 62). Subsequent experiments demonstrated that *S. mutans* and *S. sobrinus* headed the list of acidogenic bacteria (107, 145, 146). *S. mutans* metabolizes carbohydrate solely by the Embden-Meyerhof glycolytic pathway (23, 223). Utilizing the glycolytic pathway in the presence of excessglucose *S. mutans* can catabolise more than 80% of the glucose it consumes into lactic acid (33, 197).

Nutrient acquisition.

The outcome of the acidogenic metabolism is clear, but to metabolize the carbohydrate the bacteria must first acquire the carbohydrate. *S. mutans* must compete with other inhabitants of the oral cavity for the carbohydrates available in the environment. Import of sugars is accomplished by an extremely efficient phosphoenolpyruvate: sugar phosphotransferase system (PTS). The PTS system of *S. mutans* can import and phosphorylate sugars including fructose, glucose, lactose, mannose, mannitol, sorbitol, sucrose, trehalose and xylitol. This is accomplished by the concerted effort of three components, cytoplasmic non-sugar specific enzyme I (EI) and Hpr, and a sugar specific membrane bound enzyme II (EII) complex. EI accepts a phosphate group from phosphoenolpyruvate and transfers it to the hisitidine residue on Hpr, which phosphorylates the first phosphorylation site on EII. EII has three functional domains that may or may not form a single peptide. The first phosphorylation site is on EIIA, the second on EIIB. The last functional domain, EIIC, contains the transmembrane channel through which the sugar is translocated and phosphorylated (212).

Acid tolerance.

The environment colonized by *S. mutans* is very harsh. *S. mutans* must respond to fluctuations in nutrient availability and the type of nutrient supplied. The bacterium is also faced with significant environmental stress: it must survive in an environment in which pH is being acidified as a result of its own metabolism. Adaptation to environmental stresses is not a new phenomenon. *Escherichia coli* and *Bacillus subtilis* possess alternative sigma factors functioning to regulate expression of proteins required for stationary phase of growth, growth in nutrient depleted environments, and in low pH conditions (12, 168). Evidence for a similar

adaptive response in *S. mutans* was uncovered following identification of a heat shock protein, DnaK, which appears to be regulated by a sigma factor similar to the sigma-β stress response regulator of *B. subtilis* (90). The expression of DnaK increases in response to low pH and in acid-adapted cells which suggests that an alternate sigma factor may regulate the acid response in *S. mutans*. Subsequent experiments identified 36 cellular proteins synthesized during the incubation at the intermediate pH (74). The multiple factors mediating the acidurence of *S. mutans* were also demonstrated by the identification of a variety of acid-sensitive transposon mutants (70). One of these acid-induced proteins is an endonuclease functioning in a RecA independent manor to protect acid-challenged bacteria from loss of purines and pyrimidines resulting from decreased stability of the glycosyl bond at lower pH's (132, 167).

Although some proteins are specifically expressed following exposure to low pH, *S. mutans* has inherent capabilities that allow it to tolerate acidic pH. Its glycolytic enzymes have a lower pH optimum and are capable of carrying out glycolysis at extracellular pH values as low as 4.0 (14, 78, 89, 196). The most important enzyme for acid resistance is the proton translocating ATPase (104). The ATPase of *S. mutans* has a low pH optimum and a very high activity which enable it to pump protons out of the cell and maintain a small ΔpH (0.5 -1.0 pH units) across the cell membrane (13, 14, 51, 73, 96, 193).

Detachment of biofilm cells.

Most of the work done on controlling biofilms has focused on limiting adherence or accumulation. These strategies require modifying the surface or the addition of products (e.g. surfactants) to interfere with biofilm formation (159). An alternative strategy is to retroactively remove the adherent population. However, there is limited information available on the

processes for detachment of biofilm cells. Detachment is often an "after thought" and has usually been attributed to four nonspecific processes (30): (i) Predator harvesting or grazing of cells from biofilms by protozoa. This type of removal may only come into play in complex aquatic environments. (ii) Abrasion of cells by particles from the environment. (iii) Shear-related removal caused by the flow of liquids over the biofilm, where a direct relationship between increased flow rate and detachment of biofilm cells has been observed (38). (iv) Sloughing, an event where large numbers or entire sections of biofilms detach from the surface. Sloughing may result from activities deep within the biofilm, such as cell death of primary colonizers, or changing environmental factors which weaken the structure of the biofilm.

In addition to the above, cell division may result in detachment through the loss of daughter cells (31, 118). It has been demonstrated that cells detached from growing microcolonies can recolonize the surface close to the parent colony (117). However, these studies do little to advance our capabilities to detach adherent populations. While not actually a strategy to detach biofilm cells, Costerton, *et al.* (45) used the unique combination of electric fields and antibiotics to eradicate biofilms from implanted devices. These workers exposed *P. aeruginosa* biofilms to tobramycin at concentrations usually unable to affect biofilm cells. However, when an electric field was applied the efficacy of the antibiotic was increased allowing eradication of the biofilm cells.

Significant progress came with the demonstration that biofilms could be detached from surfaces by treatment with enzymes (93, 179). Using serratiopeptidase, a metalloprotease, in combination with the antibiotic oflaxin, Selan *et al.* (179) were able to detach and kill *P. aeruginosa* and *Staphylococcus epidermidis* from biofilms. Johansen, *et al.* (93) used two enzyme strategies: the first, Pectinex Ultra SP (a multicomponent enzyme mix containing protease activity, and a wide range of carbohydrases) was used to detach *S. aureus* and *S.*

epidermidis from biofilms. The second strategy used mutanase and dextranase to detach biofilms formed on saliva-conditioned hydroxyapatite with an inoculum of an 1:1:1 mixture of *S. mutans*, *Actinomyces viscosus*, and *Fusobacterium nucleatum*.

While there are limited examples demonstrating detachment of biofilm cells by means that may be adapted for *in vivo* applications, enzymatic detachment may be one of the most promising methods.

Combating dental caries.

In combating dental biofilms, the most widely used method is tooth brushing, which limits or removes plaque by mechanical means. However, there are currently two schools of thought on finding methods to decrease the incidence of caries. These are to prevent pH drops in the oral cavity and to limit bacterial adherence to the enamel.

Physiological approach to control biofilms.

S. mutans takes over sites in the oral cavity following pH changes brought on by the release of lactic acid. When human volunteers rinsed with buffers of various pH's, neutral buffers had no effect on the populations of *S.mutans*, while low pH rinses led to an enrichment of these bacteria (194). These findings were also observed in experiments involving controlled microbial communities growing in a chemostat (19). When a neutral pH was maintained, glucose pulses had no effect on the populations of *S. mutans*. However, when the pH was allowed to fall after glucose pulses, there was an increase in the *S. mutans* population at the expense of bacteria associated with healthy plaques.

Some researchers have attempted to prevent pH changes prior to the occurrence of

ecological shifts. The most direct approach is to limit acid production by curbing the metabolism of *S. mutans*, e.g., the use of fluoride to impair glycolysis. Studies on microbial communities in a chemostat demonstrated that low levels of fluoride have no effect on proportions of individual species at neutral pH (20). At lower pH, fluoride could limit selection of *S. mutans*, thus reducing the acid production by the community and allowing acid-sensitive organisms to persist. Further biofilm studies also showed that the incorporation of fluoride into the substratum limited growth and accumulation of adherent populations (131). Other antibacterial compounds such as chlorhexidine and Triclosan, which interfere with sugar transport and glycolysis, have also had success in stabilizing microbial communities (140, 175).

The advent of sugar substitutes such as aspartame, saccharin and xylitol, which have potential to inhibit bacterial growth, have positively influenced oral health (67). A fact capitalized upon by the chewing gum industry is the use of sugar substitute-containing gums to reduce the introduction of fermentable sugars into the oral cavity and thus decrease the frequency of dips in pH leading to demineralisation. Additionally, mastication from gum chewing would stimulate saliva flow which is beneficial to oral health (139). Chemostat and clinical studies using xylitol or xylitol- containing products demonstrated reduction in acid production and selective inhibition of *S. mutans* (18, 88, 195). An alternative to preventing the pH drop is to raise the pH within the oral cavity. Metabolism of arginine-containing peptides or urea by organisms such as *S. sanguis* can lead to higher pH's. Sissons (183), using an artificial mouth model, has demonstrated that the pH within the biofilm can be sustained at neutral values when supplemented with urea or arginine (184).

Limiting bacterial adherence.

Efforts have also been made to prevent the incorporation of *S. mutans* into plaque by

modifying the adhesion process. Primarily, this has been achieved by using antibodies to block adhesion of *S. mutans*. The antibodies may be applied topically or may be the product of an active immune response. Topical application of antibodies was first demonstrated in monkeys. By repeated topical applications of anti-P1 monoclonal IgG antibodies directly onto the teeth of rhesus monkeys, investigators were able to show a reduction in caries (127). In humans, reductions in *S. mutans* colonisation following application of monoclonal antibody to the teeth was also demonstrated (138). Following success with monoclonal IgG antibodies, researchers attempted similar experiments with secretory IgA (sIgA). It was believed that sIgA may be more relevant for this use as sIgA is the predominant antibody in the oral cavity. The method by which the antibody was developed is rather interesting: researchers used transgenic tobacco plants to express sIgA which recognised P1 of *S. mutans* (136, 137). The ability of the antibody to agglutinate *S. mutans* cells suggested that it may be useful in clearing agglutinated clumps of cells from the oral cavity. Even if the antibodies were capable of limiting colonisation or decreasing the prevalence of caries, this mechanism is a band-aid remedy. That is, it requires periodic use of an oral care product containing antibodies in order to prevent accumulation of the *S. mutans*. Importantly, the results did fuel the argument that sIgA can decrease bacterial adherence, and if *S. mutans* cannot adhere, it cannot cause caries.

To provide long term protection, the best strategy is to induce active immunity. Synthetic peptides of the GTF that form insoluble glucan were injected subcutanously into rats and found to be capable of eliciting an antibody response which could inhibit GTF function (187). This method for inducing active immunity was promising, but like the passive immunity strategy, it has some drawbacks. Specifically, the antigens, like the topically applied antibodies, are quickly broken down or cleared from the oral cavity so only a small proportion of the antigen may actually get to the gut-associated lymphoid tissue in order to induce mucosal

immunity. To raise antibodies to an antigen that does reach the lymphoid tissue, researchers attempted to make the antigens more immunogenic by fusing them to the B subunit of cholera toxin. Chemical association of the cholera toxin B subunit and P1 was shown to produce an antibody response capable of limiting colonisation and caries in rats (100). Later studies demonstrated that the salivary binding domain of P1 associated with the B subunit of cholera toxin had similar effects (71).

The next step in the development of a caries vaccine was the use of particulate antigens. Studies in rodents described the delivery of antigens to the Peyer's patches in liposomes (36). The liposomes were believed to slowly release their contents to provide increased exposure of the immune cells to an antigen such that a single dose may provide primary and secondary mucosal immune responses (170). It was later shown that sIgA responses were present following oral immunization of humans with GTF-containing liposomes (37). In order to insure prolonged exposure to an antigen, researchers turned to live oral vaccines in which the antigen is expressed on the cell surface of an innocuous bacterium. The bacteria would colonise the host and the surface-expressed antigen would be available for presentation to the immune system. This was first attempted with an avirulent *Samonella typhimurium* strain expressing P1. Intranasal or intragastric immunisation of mice with these strains was able to induce the production of anti-P1 sIgA (77). Later work focused on using organisms naturally present in the oral cavity to express antigens on their surfaces (124). In this example, the immune response would be mounted at the site of future challenge which may increase the success of the live vaccine.

The Gram-positive bacterial cell wall.

Beyond the membrane of gram-positive cells one finds a thick cell wall composed of

peptidoglycan surrounding the cell. The primary function of the wall is to protect the protoplast from osmotic forces, but it also maintains the shape of the cell. To function in these capacities the cell wall must be rigid but flexible. Rigidity is provided by glycan chains consisting of 5-30 repeating units of the disaccharide N-acetylmuramic acid-(Beta-1,4)-N-acetylglucosamine (NAM-NAG) (111). The D-lactyl moiety of each NAM is amide linked to a short peptide, the stem peptide, which might in turn be directly or indirectly cross-linked to a stem peptide of a neighbouring glycan strand creating a three dimensional lattice (200-202). The elasticity of the cell wall may be attributed to the cross-linking of glycan strands via the peptides where a fourfold length difference between folded and extended conformation has been demonstrated (111). While the glycan chain of the cell wall is invariant, the amino acids comprising the stem peptide can vary from one bacterium to another (111). The structure of the peptidoglycan of *S. mutans* is shown in Figure 1A.

Synthesis of peptidoglycan may be divided into three separate stages. Peptidoglycan synthesis begins in the cytoplasm where the disaccharide stem peptide monomer units are produced. In these reactions, UDP is first linked to NAG, which is subsequently converted to UDP-NAM. The stem peptide is subsequently assembled on the UDP-NAM by sequential addition of amino acids to UDP-NAM. After finding its way to the bacterial membrane the NAM-pentapeptide is then phosphodiester linked to an undecaprenyl-pyrophosphate lipid carrier to form lipid I. NAG is subsequently transferred to lipid I, forming lipid II. Amino acids, L-Ala-L-Ala-L-Lys, which may eventually crosslink stem peptides are also added to the ε amine of the lysine on the stem peptide to complete the repeating unit of the peptidoglycan (7, 81). This single unit is then translocated across the cell membrane where it can be incorporated into the cell wall (142).

Incorporation of this unit into the existing peptidoglycan leading to the maturation of the cell wall requires the concerted effort of two enzymatic activities catalyzing the formation

Figure 1. A diagrammatic representation of surface-localization and anchoring of antigen P1 and release of P1 by SPRE (surface protein-releasing enzyme) in *Streptococcus mutans*. **A.** Detailed *S. mutans* peptidoglycan structure with P1 attached to the cross-bridge. Arrows shown are targets of peptidoglycan hydrolases. 1, N-acetylglucosaminidase; 2, lytic transglycosylase; 3, N-acetylmuramyl-L-alanine amidase; 4, endopeptidases; and 5, D-alanine carboxypeptidase. **B.** Steps involved in the anchoring of P1 to the peptidoglycan and the release of P1 by SPRE. 1: Translocation of P1 across cytoplasmic membrane via the protein secretion machinery. 2: Temporary "halt" and association of the precursor P1 with the membrane by the membrane-spanning domain and charged tail. 3: The LPXTGX cleavage enzyme sortase (S), cleaves the P1 precursor between the Thr and Gly residues. 4: The linkage of the cleaved P1 to the peptidoglycan cross-bridge. 5: SPRE makes specific bond cleavage at the C-terminal anchoring structure to release P1.

A

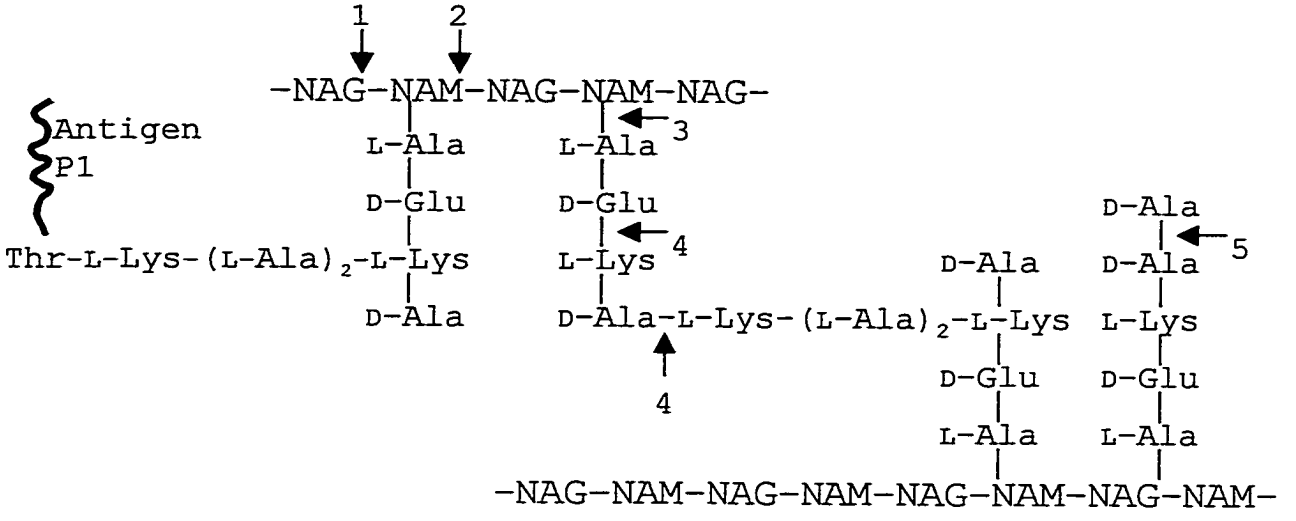
1
2
-NAG-NAM-NAG-NAM-NAG-
Antigen
P1
L-Ala
L-Ala
3
D-Glu
D-Glu
4
Thr-L-Lys-(L-Ala)2-L-Lys
L-Lys
D-Ala
D-Ala-L-Lys-(L-Ala)2-L-Lys
4
D-Ala
D-Ala
5
D-Ala
L-Lys
D-Glu
L-Ala
L-Ala
-NAG-NAM-NAG-NAM-NAG-NAM-NAG-NAM-

B

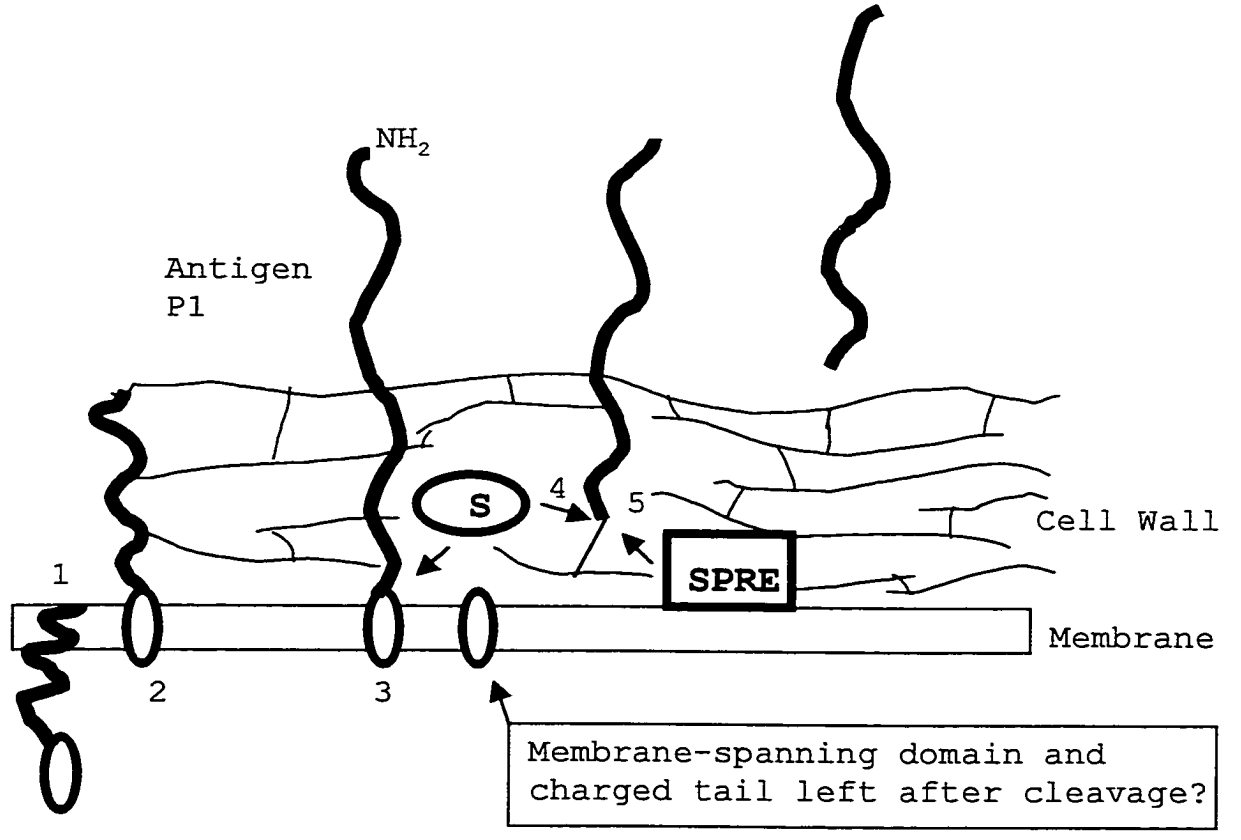
NH2
Antigen
P1
S
4
5
Cell Wall
SPRE
1
Membrane
2
3
Membrane-spanning domain and
charged tail left after cleavage?

of glycosidic and peptide bonds. Polymerization of the peptidoglycan unit catalyzed by transglycosylases allows chain elongation. Transglycosylases may be bifunctional enzymes which are also able to form peptide bonds. These bifunctional enzymes, known as penicillin binding proteins (PBPs), have been identified in numerous bacteria and are essential for growth (63, 65). In addition to catalyzing the formation of the glycosidic bond the high molecular weight PBPs also cross link glycan chains in a transpeptidation reaction (63, 65). Transpeptidation proceeds following proteolytic cleavage of the terminal D-Ala from the stem peptide of a neighbouring glycan chain with concomitant formation of a covalent bond between D-Ala of the stem peptide and the L-Lys of the cross bridge peptide (7). By crosslinking glycan chains the nascent glycan chain is drawn up into the existing cell wall above. While crosslinking is necessary for the maturation of the cell wall, not all stem peptides participate in crosslinking. The degree of crosslinking varies among bacterial species. Those stem peptides not crosslinked are trimmed by low molecular weight PBPs functioning as carboxypeptidases.

Having a rigid cell wall that resembles an exoskeleton does place constraints on the cell. While crustaceans shed their exoskeleton, bacteria cannot. Instead the bacterial cell wall must grow as the cell does. To accomplish this, bacterial cells possess enzymes capable of digesting the glycan and peptide fractions of the cell wall allowing the rigid structure to expand. A class of enzymes called autolysins, ubiquitous among bacteria, function in this capacity (182). Several autolytic enzymes exist and their sites of action are indicated in Figure 1A. Essentially the autolysins break down the cell wall creating acceptor sites to allow incorporation of new cell wall materials as the cell grows and divides. As their name suggest, the autolysins are also capable of lysing bacterial cells by weakening the wall. Autolytic activity can be affected by the ionic environment, secreted proteases and an energized membrane (35, 94, 95). There are also suggestions that autolysins may be regulated by the conformational state of peptidoglycan. Autolysins may recognise stressed peptidoglycan at the site of cell

division and areas of cell growth where expansion stretches the wall to its limit (102, 106). The remaining question is the temporal activity of the autolysins and peptidoglycan synthases (transglycosylases and transpeptidases): if peptidoglycan autolysis occurs first, followed by incorporation of new peptidoglycan, there is a period of time when the cell may be vulnerable to osmotic pressure. Inside to outside growth of the bacterial cell wall could circumvent this dilemma (105). In this case, new peptidoglycan chains formed at the bacterial membrane are incorporated into the existing stress bearing layer of peptidoglycan above in a "make-before-break" strategy. In this model, peptidoglycan in the centre of the wall provides support for the cell and is replaced by peptidoglycan from below as the cell grows. The outermost layers of peptidoglycan would then be broken down facilitating growth. The process is hypothesised to be catalysed by a multienzyme complex that moves along existing peptidoglycan and copies it in a manner similar to DNA polymearse (82).

Anchorage of P1 to the cell surface.

Antigen P1 is one of many proteins of gram-positive bacteria anchored to the cell surface via its carboxyl terminus. Other similarly anchored surface proteins include protein A of *S. aureus*, M protein of group A streptococci, and internalin of *Listeria* (152). To mediate surface localization, proteins possess several important characteristics at the C-terminus. At the extreme C-terminal end of the protein is a short charged tail, preceded by a stretch of 15-22 predominantly hydrophobic membrane spanning residues. Just past this hydrophobic sequence towards the N-terminus is a conserved hexapeptide motif, LPXTGX. N-terminal to the LPXTGX is a cell wall spanning region comprised mainly of charged and polar residues consisting of glycine and proline at regular intervals (57, 177).

Each of the C-terminal structures is critical for the correct sorting of the protein to the

cell surface. Deletion of only the charged tail alone abrogates surface localisation as does deletion of the charged tail and the membrane spanning domain (83, 178). The two domains likely function to anchor the protein at the membrane allowing subsequent covalent linkage to the cell wall (Fig. 1B). Data regarding the nature of covalent linkage of the protein to the cell wall was obtained by studying the linkage of protein A to the staphylococcal cell wall (144, 153, 178, 204, 206). Once in position at the cell membrane, the protein becomes the substrate of the enzyme sortase, a 206 amino acid protein encoded by the gene *srtA* identified in *S. aureus* (144). The enzyme appears to be a sulfhydryl-containing enzyme, with analogues in other gram-positive bacteria including *Enterococcous faecalis*, *B. subtilis* and *S. mutans*. Sortase catalyzes a two-step transpeptidation reaction (144, 206). In the first step the enzyme cleaves the membrane-bound protein between the threonine and glycine in the LPXTGX motif to form a thioester linkage between the carboxyl of threonine and the enzyme sulfhydrol. A free amino group within the pentaglycine cross-bridge may then act as a neclophile to resolve the acyl enzyme intermediate (205, 206). The final result of the reaction is the production of an amide bond between the threonine of the surface protein and a free amino group found on the cross linking peptide of the cell wall. In *S. mutans*, the threonine would be linked to a lysine in the cross-bridge (Fig. 1A). The reaction catalyzed by sortase does not require the presence of a mature cell wall. The transpeptidation reaction can occur in the presence of cell wall precursors, as the reaction has been demonstrated in protoplasts (205). In the protoplast, the reaction would leave the surface protein linked to a cell wall precursor that has not been incorporated into the peptidoglycan matrix .

The importance of the LPXTGX motif is apparent; however, the significance of the wall-spanning motif is uncertain. These polar amino acids have been shown to be buried or masked by the cell wall, presumably due to their intercalation in the peptidoglycan (84), and are capable of facilitating weak non-covalent association of the surface protein with the cell surface

(83). As the charged tail and the hydrophobic membrane-spanning region localized the protein in a position where sortase may catalyse its linkage to peptidoglycan, the wall-spanning motif may serve to keep the protein-cell wall precursor complex close to the cell membrane where the wall precursor could be incorporated into the existing wall by peptidioglycan synthases. Without the wall-spanning region, the protein-cell wall precursor complex might easily be lost from the cell surface prior to incorporation of the unit into the peptidoglycan.

These common characteristics of gram-positive surface proteins and the identification of sortase and its analogues in other gram-positive bacteria implies a universal mechanism for surface localization among proteins possessing the LPXTGX hexapeptide at their C-terminus (Fig. 1B). Additional support for the theory comes from experiments demonstrating the ability to surface localize P1 on the surface of *Streptococcus gordonii* and *E. faecalis* (83).

Release of bacterial surface proteins.

The cell surface has been described as plastic, in that it has a variable composition. Variations have been observed between biofilm and planktonic cells (cells in the fluid phase), cells in different growth phases and cells grown in the presence of sub-inhibitory concentrations of antibiotics. One mechanism by which cells could alter their surface characteristics is to release proteins from their cell surface. Pancholi and Fischetti (161) reported an endogenous enzyme activity, termed MACE, which liberated M protein from *S. pyogenes*. Lee (121) identified a surface protein-releasing enzyme (SPRE) which released full length P1 from the surface of *S. mutans*. While both enzymes release full length proteins from the cell surface, they are slightly different. SPRE had a lower pH optimum (6.0) and was not inhibited by calcium in comparison to MACE, which was inhibited by calcium and had a pH optimum of 7.4 (121, 161).

Figure 2. The possible functions of SPRE. 1, SPRE could cleave P1-sIgA complexes from the cell surface; 2, release P1 from the cell surface to function as immuno-decoys and 3, or cleave P1 from the surface allowing detachment of biofilm cells from a colonized surface (grey bar) conditioned with salivary proteins (black triangles).

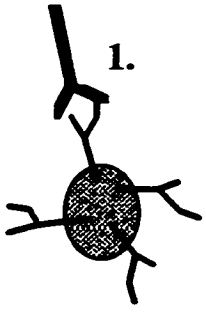

1. Shedding bound antibodies.
2. Immuno-decoy.
3. Detachment from biofilms.

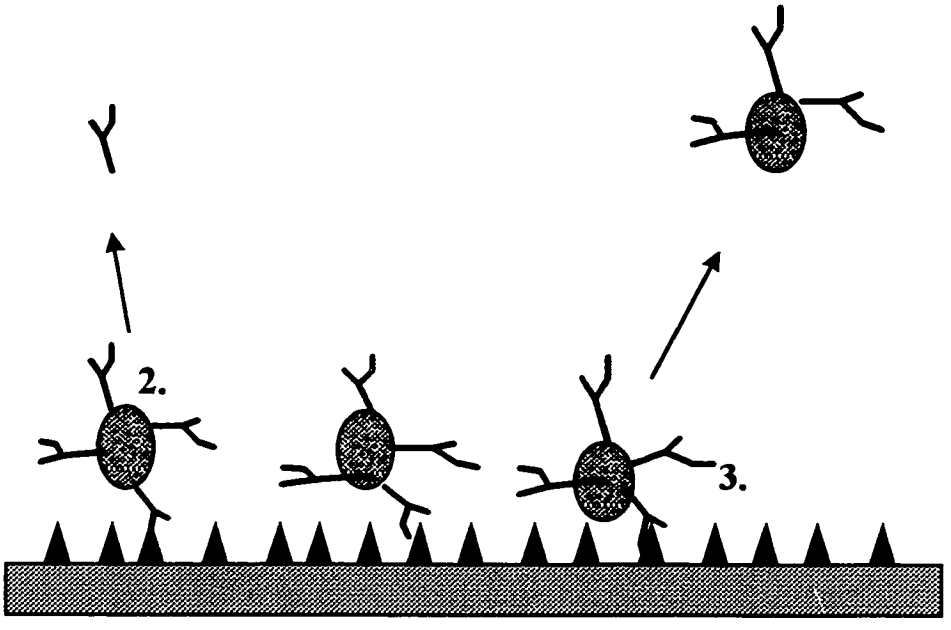

Additional studies on SPRE activity suggested potentially useful functions of the enzymatic activity (Fig. 2). In some instances the released P1 was observed to be complexed with sIgA suggesting SPRE may selectively and actively release P1-sIgA complexes to abrogate inhibitory effects of sIgA on the adhesion of *S. mutans* to SA-conditioned surfaces (120). Alternatively, P1 release by SPRE may increase the pathogenicity of *S. mutans* by releasing P1 into the saliva, thus providing a mechanism to neutralize sIgA. Active release of P1 by SPRE may also explain the reported reversibility of sucrose independent adherence as demonstrated by SPRE's ability to detach *S. mutans* cells from biofilms (123).

Unfortunately, SPRE has yet to be isolated and we can only speculate on its identity and mechanism of action (Fig. 1B). There is a possibility that SPRE is an autolysin that degrades the peptidoglycan to which proteins are attached. Many of the proteins that are anchored to the peptidoglycan are released from the surface and often found in the culture supernatants (53, 152). This release may be due to the breakdown of the cell wall during growth and cell division. While the relationship of SPRE to autolysins is not known, the fact it releases proteins anchored to the peptidoglycan suggest it likely has an enzymatic mechanism and specificity similar to autolysins.

A tightly regulated surface protein releasing enzyme may augment *S. mutans* ability to persist *in vivo* by allowing *S. mutans* to shed P1 and other antigenic surface proteins. Alternatively, if the micro-environment was depleted of nutrients or became inhospitable due to the accumulation of acid produced during the metabolism of sucrose, SPRE could facilitate detachment of the bacterium thus enabling it to re-adhere elsewhere. If isolated, the enzyme would also be a useful tool for the removal of cells from the enamel.

During the course of my research a copper transport operon which encodes a P-type ATPase and two regulatory proteins was identified. This operon appears to play a role in SPRE activity and detachment of *S. mutans* cells. Therefore, relevant background on P-type ATPases is reviewed below.

P-type ATPases and their role in heavy metal homeostasis.

Transition metals such as copper, molybdenum, and zinc are essential to life because of the catalytic and structural roles they play in proteins and other biomolecules. At the same time, these ions are very toxic to both eukaryotic and prokaryotic cells. The ions can bind to proteins and nucleic acids and may cause oxidation of lipids and proteins. Most organisms use a redundant array of cellular mechanisms to limit the toxicity of metal ions. These detoxification systems can be subdivided into reduction of metal uptake, enhanced metal exportation, and sequestration mechanisms (50).

There are a number of ion-motive ATPases which have arisen during evolution with varied structures and mechanisms of ion translocation (163). The cation translocating P-type ATPases, which derive their energy from ATP hydrolysis, are among the more common pumping mechanisms used to control the flow of ions into and out of cells and organelles. The P-type ATPases are ubiquitous; to date, 211 ATPases have been isolated from both eukaryotic and prokaryotic cells (160). Almost all of the heavy metal transporting ATPase, with the exception of CopA of *Enterococcus hirae*, are involved in pumping heavy metal ions out of the cells. In general, P-type ATPases are roughly 90-200 kDa proteins with four functional domains. These pumps are comprised of a single catalytic subunit which changes conformation upon phosphorylation of an aspartate residue in the invariant DKTGT sequence of the phosphatase domain. During the phosphorylation process, ATP is bound by its γ-phosphate via a Mg^{2+}-mediated salt bridge to the conserved sequence VGDG in the aspartyl kinase domain (180, 188). Following

phosphorylation, localized conformational changes occur as the ATPase adopts the E2 conformation allowing translocation of cations across the membrane through a conserved CPC ion transduction motif. Subsequent dephosphorylation involves the removal of the phosphate group from the aspartate residue mediated by the phosphatase domain, which contains the conserved peptide TGES, and leads to a return of the ATPase to the E1 state.

Due to their recent discovery and the difficulty associated with working with integral membrane proteins, the exact mechanism by which copper-specific P-type ATPases pump copper ions across a membrane is not known. The best studied of the heavy metal translocating ATPases are the Wilson and Menkes disease-associated proteins and the CopA and CopB of *E. hirae*. Since all the conserved domains are on the cytosolic side of the membrane, it is simplest to explain the proposed mechanism of action for the CopB, Menkes, and Wilson proteins. It is proposed that binding of copper ions to the copper-binding motif(s) causes a conformational change which exposes the buried conserved aspartic acid residue within the DKTG motif. Phosphorylation of this residue by ATP causes a conformational change which allows the opening of the transmembrane channel and hence translocation of the copper ions away from the cytosol (50). This model is fairly easy to conceptualize since the copper ions to be translocated and the copper binding domain(s) are both on the cytosolic side of the membrane. Understanding how CopA works, however, is considerably more difficult since the copper-binding domain is intracellular and the ions to be translocated are extracellular. For this reason, no clear mechanism for the activation of CopA has been proposed, but it is conceivable that it is the dissociation of copper ions from the intracellular copper-binding domain which causes the conformational change necessary for phosphorylation and hence ion translocation into the cytosol to occur.

Regulation of P-type ATPase.

In bacteria, the expression of P-type ATPase is regulated. The *E. hirae cop* operon is a well-studied operon. The operon contains four genes, *copY*, *copZ*, *copA*, and *copB* (155, 157). CopY and CopZ are two regulatory proteins, and CopA and CopB are two P-type ATPases which respectively function to import and export copper from the cell (155-157). Expression of the operon is minimal at physiological copper concentrations but induction occurs at high (>100μM) copper concentrations or after copper chelation with o-phenanthroline (10 μM) (222). Repression of the operon is mediated via binding of a CopY dimer to an inverted repeat sequence overlapping the -35 and -10 region of the promoter (192). At high copper concentrations, repression is relieved by CopZ which is believed to deliver copper to the heavy metal-binding site of CopY (42). Copper binding is believed to induce a conformational change in CopY bound to the inverted repeat sequence causing the disssociation of the CopY - DNA complex and thereby de-repressing transcription (42). The expression of the operon is also induced in low copper environments, however the mechanism of this induction is not completely clear. Induction of the operon by low copper concentration would facilitate import of copper by CopA. However, this would also result in more CopB being produced, which would pump copper out of the cell the moment it was transported in by CopA. Perhaps, there is another mechanism to control the activity of the two ATPases under this condition.

Roles of the P-type ATPases in virulence.

The primary function of the P-type ATPase is to regulate intracellular concentrations of heavy metals. However, these ATPases appear to play a role in other cellular activities including virulence.

Francis *et al.* (58, 59) showed that a *Listeria monocytogenes* strain devoid of a P-type ATPase was less virulent than the wild-type. The mutant was not impaired in intracellular growth. However, when it was used to infect mice, dramatically fewer bacteria of the mutant strain were recovered from tissues of the animal as compared to the wild-type strain (59). Unfortunately, there were no concrete explanations for the observed differences between the wild type and the mutant. Perhaps without the ATPase, the bacteria may simply have not been able to survive the extracellular phase of infection. Alternatively, without the ATPase increased intracellular copper concentrations may have altered gene expression by modifying the activity of PrfA. PrfA is a positive regulatory protein that controls expression of numerous virulence genes in *L. monocytogenes* (128). PrfA has been shown to respond to iron (15). It is possible that excess copper may also affect its activity at the promoters of virulence genes leading to the results observed in the animal experiments.

On the other hand, Lai *et al.* (113), showed that a P-type ATPase may be involved in cell swarming of *Proteus mirabilis*. These workers demonstrated that the expression of the ATPase was maximal in swarmer cells, and that cells lacking the P-type ATPase did not swarm. Examination of the genes involved in flageller biogenesis revealed their expression was reduced in the cells that did not express the ATPase (113). However, the direct link between the P-type ATPase to flagellar biosynthesis is not known.

In *Mycobacterium tuberculosis*, eleven P-type ATPase have been identified (3). It is not clear why this bacterium possesses so many different P-type ATPases. It is known that superoxide dismutase and catalase which contain copper or iron as cofactors, are important factors for intracellular survival of *M. tuberculosis*. Perhaps, an efficient ATPase activity may be necessary for the bacterium to produce these enzymes.

RESEARCH OBJECTIVE

Biofilms are ubiquitous and are of great importance in disease. In the oral cavity biofilm formation by *S. mutans* may lead to the development of dental caries. Finding a means to remove adherent bacteria from biofilms may have significant implications in medicine and in industrial processes. Previous findings from this laboratory have shown that *S. mutans* can actively detach from a hog gastric mucin-conditioned surface. The detachment was suspected to be mediated by an endogenous enzyme activity termed surface protein-releasing enzyme (SPRE).

Although the previous work provided preliminary characterization of the enzyme, the exact nature of SPRE and factors affecting its activity were still unknown. Additionally, the model biofilms used in the previous work were not relevant to the oral cavity. Hence, the prime objective of my research was to further characterize the SPRE activity, identify factors affecting its activity, and determine its role in detachment of *S. mutans* cells in a model system.

The specific goals were to (a) improve the model biofilm by mimicking conditions in the oral cavity, (b) to characterize the SPRE, and (c) to isolate a genetic locus affecting the SPRE and detachment.

The results obtained may provide better insight into how *S. mutans* can detach from surfaces. Understanding detachment processes for *S. mutans* may eventually allow us detach *S. mutans* and other bacteria with similar mechanisms of adherence from biofilms.

MATERIALS AND METHODS

Bacterial strains, media, plasmids and culture conditions.

Streptococcus mutans NG8 and JH1005 (serotype c) were grown in Todd-Hewitt broth (THB) or TYG broth (1% $Na_2HPO_4H_2O$, 1% trypticase peptone, 0.5% yeast extract, and 1% glucose, w/v) without agitation or on Todd-Hewitt agar (THA) in candle jars. In one ocassion, *S. mutans*, was also grown in the chemically defined medium (FMC) described by Terleckyg *et al.* (199). *Escherichia coli* XL-1 Blue was grown in Luria-Bertani (LB) broth. All strains were cultivated at 37°C unless harboring pTV1-OK in which case they were grown at 28°C due to the temperature sensitive origin of replication on pTV1-OK. Where required, antibiotics (Sigma Chemical Co., St. Louis, Mo., USA) were added to the media as follows: ampicillin (100 μg/mL for *E. coli*), kanamycin (50 μg/mL for *E. coli* and 400 μg/mL for *S. mutans*), erythromycin (300 μg/mL for *E. coli* and 10 μg/mL for *S. mutans*), tetracycline (10 μg/mL for *E. coli* and 15 μg/mL for *S. mutans*) and chloramphenicol (10 μg/mL for *E. coli* and 5 μg/mL for *S. mutans*). The plasmids used throughout this work are listed and described in Table 1.

Preparation of epon-hydroxyapatite rods.

Hydroxyapatite (HA) powder was prepared essentially as described by Anderson and Elliot (6). Briefly, 0.5 L of 0.246 M ammonium orthophosphate (pH 10) was added drop-wise to 2.5 L of 0.082 M calcium nitrate at 70°C, while maintaining the pH at 11 by the addition of ammonium hydroxide and stirring with a magnetic stir bar. A fluffy white precipitate formed which was allowed to settle. Excess fluid was drawn off by aspiration, and the remaining supernatant was removed after centrifugation at 2,000 x g for ten minutes at 4°C. The pellet was washed twice with 400 mL of distilled water and dried at 135°C overnight.

Table 1. Plasmids used throughout this work.

Plasmid	Relevant features	Reference
pTV1-OK	Carries Tn*917*. Temperature sensitive origin of replication	(70)
pDL276	*E. coli, S. mutans* shuttle vector. kan^R	(54)
pVA981	tet^R	(203)
pNV4	2.5 kb HindIII fragment of mutant A with 3' end of Tn917 and adjacent chromosomal DNA	This study
pWH4	*cop* promoter and upstream region, and *copY*	"
pWH4.4	pWH4 devoid of promoter and upstream sequences	
pWH4/PDL	pWH4 insert subcloned into pDL276	"
pNV5	Second 2/3 of *copB* and first 2/3 of *copZ*	"
pNV6	*cop* promoter, *copYB* and first 2/3 of *copZ*	"
pNV7	*copYBZ* operon including the promoter	"
pNV7B	Insert of pNV7 subcloned into pDL276	"
pNV7/S4	Insertion of tet^R cassette from pVA981 in place of *copYBZ*	"
pNV8	*cop* promoter	"
pPNV8	PNV8 insert cloned into pDL276	"
pZ1	*copZ* amplified using SL146 and SL150	"
pNV10	*cop* operon promoter (pPNV8), fused to *copZ*	"
pMH109	Promoterless *cat* gene, tet^R and kan^R	(87)
pHTL1	*cop* operon promoter fused to CAT gene in pMH109	(122)
pSL2	*hppG* and *spaP* genes	(122)
pHSL2/pUC	*cop* promoter CAT fusion, fragment of *spaP* for insertion into chromosome and tet^R	"

Approximately 5 g of dry HA powder was routinely produced using this method. HA powder was ground in a mortar to break up the dried chunks and was milled for 8 minutes in a Fritsch planetary Micro Mill Pulversette 7 (Laval Lab Inc., Laval, PQ, Canada). The milling process was repeated 7 times. Following milling, particle size analysis showed the HA had a mean particle size of 6 microns.

Epon-hydroxyapatite (EHA) rods (60% hydroxyapatite and 40% epon resin) were produced as described by Li and Bowden (131). Resin was first prepared by combining 1.5 g TAAB 812 resin, 0.816 g nadic methyl anhydride, 0.78 g dodecenyl succinic anhydride, and 0.05 g dimethyaminomethyl phenol 30 (Marivac Ltd., Halifax, N.S., Canada). The resin components were mixed thoroughly after which 2.63 g was placed in a mortar, and 3.89 g of HA powder was slowly mixed into the resin to produce a viscous slurry. The slurry was put into a syringe and injected into a mold comprised of tygon tubing (3 x 30 mm) fitted over the end of glass rods of equal internal diameter. The resin was cured by successive 16 h incubations at 37°C, 45°C and 60°C after which the tubing was cut away using a razor blade exposing the EHA rod. The EHA rods were wet sanded lightly prior to use. Following each use the rods were washed in 10% SDS (w/v) and rinsed with sterile water. Figure 3 shows one of the EHA rods produced according to the above procedure.

Saliva and salivary agglutinin.

Whole unstimulated saliva was routinely collected on ice from two male donors in the morning before breakfast, pooled, and clarified by centrifugation (10,000 x g, 4°C, 20 minutes). For salivary agglutinin (SA) purification, clarified saliva was stored at -70°C until needed (usually not more than two days). SA was purified from saliva either by chromatography or by adsorption to *S. mutans* cells. Chromatography was performed as described by Demuth *et al.*, (52). Fifty milliliters of clarified saliva was lyophilized and

Figure 3. Picture of an EHA rod made in the laboratory.

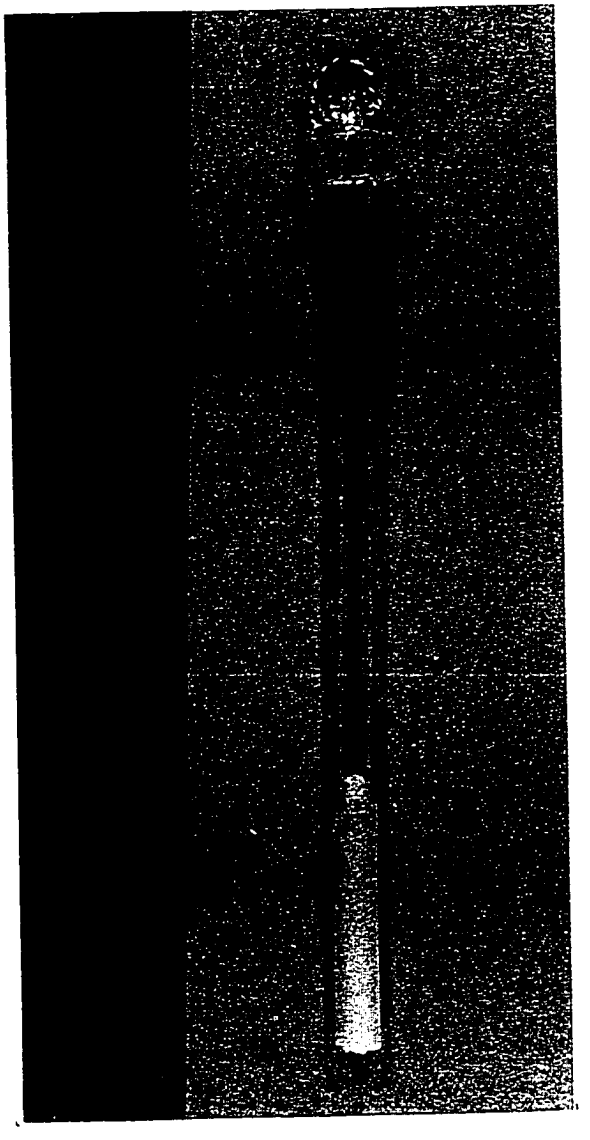

resuspended in 25 mL of 50 mM Tris (pH 8.0) and 50 mM NaCl, clarified by centrifugation, and applied to a DEAE Sepharose FF column (2.5 by 50 cm)(Pharmacia, Baie d' Urfé, Québec, Canada). The column was equilibrated with 220 mL of 50 mM Tris (pH 8.0) containing 50 mM NaCl at a flow rate of 18 mL/h, and SA was eluted with a linear gradient of NaCl (50-500 mM) in 50 mM Tris (pH 8.0). Five milliliter fractions were collected. SA was detected with an anti-SA antiserum (1/500, see below) by dot blotting 50 μL from every third fraction on a 96-well dot blotter (Bio-Rad Laboratories, Ltd, Mississauga, Ont., Canada). SA was found in fractions at the base of the NaCl gradient (65 - 175 mM NaCl). The fractions from three DEAE Sepharose FF runs were pooled, loaded onto a Sepharose 4B column (2.5 by 100 cm)(Pharmacia) and eluted with 500 mL of 50 mM Tris (pH 8.0), 50 mM NaCl and 1mM $CaCl_2$ at a flow rate of 12 mL/h. Five milliliter fractions were collected and SA was detected by dot blotting as described above. Samples from fractions containing SA were run on non-reducing sodium dodecyl sulfate-polyacrylamide (SDS-PAGE) gels. Fractions free of lower molecular weight proteins were pooled, lyophilized, resuspended in 50 mM Tris (pH 8.0) containing 50 mM NaCl, and dialyzed against the same buffer. From 150 mL of whole saliva, 7.69 mg of protein was obtained.

Alternatively, SA was also prepared by a modification of the method of Rundegren and Arnold (171) as previously described (126). Briefly, cells from 1.5 L of an overnight culture of *S. mutans* NG8 were harvested by centrifugation, washed twice with KPBS (2.7 mM KCl, 1.5 mM KH_2PO_4, 137 mM NaCl, 6.5 mM Na_2HPO_4 [pH 7.2]), and resuspended in 150 ml of KPBS. Clarified saliva (75 mL) was diluted with an equal volume of KPBS and added to the cell suspension. The cells and saliva were placed on a shaker and incubated at 37°C for 1 h. Following the incubation, the mixture was centrifuged at 2,000 x g for 15 minutes and the cell pellet was washed once with 35 mL of KPBS and then once in KPBS with 1 mM EDTA to remove absorbed SA from the cells. The cells were pelleted by centrifugation, and the SA-

containing supernatant was filtered through a 0.45 μm pore size membrane and freeze dried. The dried material was resuspended in distilled water, dialyzed against KPBS, and stored at -70°C.

The purity of the SA obtained by both methods was evaluated by non-reducing SDS-PAGE followed by silver staining. Results showed that the SA appeared as a single band of approximately 400 kDa similar to that previously described (126).

Conditioning of epon-hydroxyapatite rods with saliva and salivary agglutinin.

EHA rods were conditioned with clarified whole saliva or SA prior to the formation of *S. mutans* monolayers. We found that EHA rods were more suitable for our experiments than the conventional HA beads because these rods could be washed free of carry-over proteins and cells more quickly than the HA beads. To condition EHA rods with whole saliva, freshly collected saliva was diluted in resting cell buffer (RCB, for recipe see appendix A) and sterilized by successive filtration through a 0.45 μm and a 0.2 μm membranes. Dilution of saliva was necessary due to the lack of large quantities of whole saliva and the difficulty in filter-sterilizing viscous saliva. Sixty milliliters of the filter-sterilized saliva was pre-warmed to 37°C, placed in a 150 mL beaker and covered with a sheet of aluminum foil. Eight holes were punched in the aluminum foil to facilitate lowering 8 EHA rods into the beaker, exposing 1.6 cm^2 per rod to the solution for 15 minutes at 37°C. A magnetic stir bar provided gentle mixing. To determine the composition and quantity of salivary proteins adhering to EHA, individual EHA rods were removed from the solution, rinsed with 300 μL of fresh RCB by dispensing the RCB from the top of the rod and allowing it to flow down over the entire surface. This process

removed any carry-over and weakly adherent proteins from the rods. Adherent proteins were recovered from the rods by successively vortexing each of the eight rods vigorously for 1 minute in a glass tube (12 x 75 mm) containing 1 mL of distilled water. The method quantitatively removed the proteins as no additional proteins were recovered by boiling the vortexed rods in 0.1 % SDS (w/v) for 10 minutes. The amount of adherent proteins was quantified using the method of Bradford (17), with bovine serum IgG as the standard. The recovered proteins were also examined by SDS-PAGE. Attempts were also made to identify specific proteins among those recovered from the rods. The presence of SA, IgG and secretory IgA (sIgA) was determined by enzyme-linked immunosorbent assay (ELISA), and amylases were detected by the reducing sugar assay of Nelson- Somogyi (8), using 1% (w/v) starch as the substrate.

Control rods were conditioned in a solution of bovine serum albumin of similar protein concentration to that of the clarified 1/10 diluted filter sterilized saliva or in RCB alone.

In the conditioning of EHA rods with SA, each EHA rod was placed in 1.2 mL of SA solution in a glass tube to expose 1.6 cm^2 of the rod. The volume used in these experiments was reduced in order to conserve the limited amount of the purified SA. The concentrations of SA used is indicated in respective experiments. After 15 minutes at 37°C, SA was recovered from the rods by vortexing as above. Recovered proteins were quantified and western immunoblotting was performed to assure adherent protein was SA.

Biofilm formation and detachment of biofilm cells.

S. mutans cells (100 mL) in early exponential phase of growth (OD_{600} = 0.3) were harvested by centrifugation, washed once with cold RCB, and dechained by rapid passage through a 27 gauge needle (120). The dechained cells were diluted with RCB to 2 x 10^8

CFU/ml (ca. $OD_{600} = 0.2$). Following this treatment, *S. mutans* cells were found to have a constant viable cell count and optical density at 600 nm for 2 h and hence were considered to be resting (viable but not dividing; (123)). Prior to biofilm formation, saliva- or SA-conditioned EHA rods were blocked with 1% BSA (w/v) in RCB for 1 h at 37°C. For biofilm formation conditioned, BSA blocked rods were lowered into 60 mL of cell suspension exposing 1.6 cm^2 of the surface and incubated at 37°C. After incubation, EHA rods were removed from the cell suspension, each rod was rinsed with 300 μL of RCB to eliminate carry-over planktonic cells, and adherent cells were removed by vortexing rods in in 1 mL of RCB. To monitor biofilm formation, two EHA rods were removed from the cell suspension at increasing time points over the course of the experiment, and the adherent cells on each rod were quantified and averaged.

In detachment studies, each rod was removed from the cell suspension, rinsed with RCB and gently placed in 2.0 mL of RCB at pH 6.0. This pH value was used because it was the optimum pH for SPRE (121). The rod was incubated at 37°C for 30 or 60 minutes without agitation. Results from pilot experiments showed that the detachment rate was linear up to 60 minutes of incubation and that the effect of pH on the viability of cells was negligible within this length of time. After incubation, the rod was gently removed from the solution, leaving behind the detached cells, and gently rinsed with 300 μL of RCB. The rod was then placed in a second glass tube containing 2 mL of fresh RCB and vortexed to dislodge the remaining adherent cells. Viable cell counts for the two cell populations were determined. The sum of the adherent and detached cells provided the total number of cells on the rod. The quotient of the detached cells and the total number of cells gave the percentage of cells detaching from the EHA rod.

Surface protein-releasing assay.

Endogenous SPRE activity was assayed using a surface protein-releasing assay as previously described (121). Briefly, cells were grown to an optical density of 0.4 @ 600 nm, harvested by centrifugation, washed twice with phosphate buffered saline (PBS, 8.7 mM Na_2HPO_4, 1.2 mM NaH_2PO_4, 0.15 M NaCl) and resuspended to a cell density equal to 10^{10} CFU per mL in 0.1 M sodium phosphate buffer, pH 6.0. The cells, 0.2 mL, were incubated for 90 minutes at 37°C, pelleted by centrifugation and the supernatant was analyzed by SDS-PAGE to visualize the released surface proteins. P1 was detected among released proteins using western blotting and ELISA.

Preparation of the Surface Protein-Releasing Enzyme.

A crude preparation of the SPRE was prepared from cell membranes of *S. mutans* as initially described by Vadeboncoeur and Gauthier (211) and modified by Lee *et al.* (123). Membranes were isolated from *S. mutans* 834, an isogenic P1 knock-out mutant of NG8 as to prevent the introduction of P1 into the system. Briefly, 2 L of *S. mutans* 834 were grown to an optical density of approximately 0.45 @ 600 nm, harvested by centrifugation at 10,000 x g for 15 minutes and washed once with KPBS and subsequently with PEMPP (10 mM KPO_4 [pH 7.5], 1 mM EDTA, 14 mM β-mercaptoethanol, 0.1 mM phenylmethylsulfonyl fluoride, 0.1 μM pepstatin A). The cells were frozen at -70°C for 45 minutes and then ground at room temperature for 20 minutes in a pre-chilled mortar in the presence of alumina type A5 (3 g of alumina/g of cells wet weight). Alumina was removed by washing the lysate twice with 12 mL of cold PEMPP. The lysates were centrifuged at 5,000 x g for 10 minutes between washes. Supernatants from the two centrifugations were collected, pooled and re-centrifuged at 20,000 x g for 20 minutes to sediment the cell walls. The supernatant was further centrifuged at

200,000 x g for 16 h at 4°C (Beckman Cent Rotor SW-40). The pellet containing the cell membranes was resuspended in PEMPP containing 0.5 M KCl and centrifuged at 4°C for 5 h at 200,000 x g. The supernatant obtained was used as the crude SPRE.

Production of a poly-clonal rabbit anti-salivary agglutinin antibody.

Two New Zealand white rabbits were each given subcutaneous injections of 35 μg of SA in Freund's incomplete adjuvant. Three weeks later, each animal was boosted with half the amount of the same antigen in adjuvant by the same route. Six days later the animals were sacrificed and sera were obtained. The titer of the antisera was determined by ELISA (described below). The antibody was determined to be monospecific by western blotting.

ELISA.

For the determination of anti-SA titer, two-fold serially diluted rabbit sera were added to 96-well polystyrene microtiter plates which had been previously primed with 100 ng SA diluted in ELISA coating buffer (12 mM Na_2CO_3, 35 mM $NaHCO_3$, 4 mM $MgCl_2 \cdot 6H_2O$, pH 9.8) for 60 minutes at 37°C, and blocked with 200 μl of 1% gelatin (w/v) in PBST (8.7 mM Na_2HPO_4, 1.2 mM NaH_2PO_4, 0.15 M NaCl, 4 mM $MgCl_2 \cdot 6H_2O$ and 1 ml Tween 20 / L) for 60 minutes at 37°C. Following incubation with the rabbit sera for 1 h at 37°C, the wells were washed 4 x with PBST, and 100 μL of an alkaline phosphatase-conjugated goat anti-rabbit IgG antibody (1/30,000, Sigma) was applied. Following four washes with PBST, Sigma 104 (1 mg/mL) (Sigma) diluted in alkaline phosphatase buffer (100 mM NaCl, 5 mM $MgCl_2$, 100 mM Tris, pH 9.5) was added to the wells and the A_{405} was measured using a BioRad Plate reader (Model #3550). The antibody titres, expressed as the reciprocal of the dilution giving a A_{405} reading 0.03 above the same dilution of the pre-immune

sera, were 64,000 and 32,000 for rabbit one and two, respectively.

Additional ELISA procedures were performed essentially as described above. For the detection of sIgA present among salivary proteins recovered from EHA rods, microtiter plates were primed with 100 μL of a mouse anti-human IgA monoclonal antibody (α-chain specific, 1/1000, Sigma) diluted in ELISA coating buffer and incubated for 1 h at 37°C, blocked with 1% BSA and washed with PBST. Protein samples (90 μL) recovered from the rods were added to the plates for 60 minutes. Wells were subsequently washed with PBST and sIgA was detected using an alkaline phosphatase conjugated goat anti-human sIgA antibody (1/3000, Sigma).

IgG was detected by direct coating of protein samples on the plates followed by reaction with an alkaline phosphatase-conjugated rabbit anti-human IgG antibody (γ-chain specific, 1/3000, Bio/Can Scientific, Mississauga, Ont., Canada).

In whole-cell ELISA for the screening of Tn*917* mutants, cultures grown in sterile 96-well plates were harvested by centrifugation (850 x g, 7 minutes, 4°C, Beckman, Model TJ-6). The cells were washed once in PBS and resuspended in 100 μL of PBS. The A_{655} of the cell suspensions were measured with the Bio-Rad plate reader, the cell suspensions were adjusted to the same cell density ($A_{655} = 0.05$) with PBS and 100 μL triplicates aliquoted to fresh microplates. The cells were fixed to the plates with 2.5% glutaraldehyde (w/v) for 60 minutes at room temperature. Antigen P1 on the cell surface was detected with the monoclonal anti-P1 antibody 4-10A (1/7000; (10)) and the alkaline phosphatase-conjugated rabbit anti-mouse IgG (1/3000, Sigma). Potential clones (A_{405} readings 0.05 higher than parent JH1005) were grown up in 5 mL cultures and re-tested.

SDS-PAGE and Western blotting.

Analysis of proteins on 7.5% SDS-PAGE gels was conducted as described by Laemmli (112). In the case of non-reducing SDS-PAGE, proteins were boiled in sample buffer without β-mercaptoethanol prior to separation on the gel. Western blotting was performed as described by Towbin (207). Briefly, proteins were transferred to nitro-cellulose membranes (Millipore Corp. Bedford, MA., USA) at 200 mA for 1 h at 4°C, blocked with 1% gelatin (w/v) in PBST for 1 h at room temperature, incubated with the primary antibody in PBST for at least 1 h at room temperature, washed four times (10 minutes each) in PBST, incubated with alkaline phosphatase-conjugated goat anti-rabbit IgG (1/30,000, Sigma), and washed 4 x (ten minutes each) in PBST. Bands were visualized using nitro blue tetrazolium and 5-bromo-4-chloro-3-indoyl phosphate (Sigma).

Scanning electron microscopy.

Following biofilm formation, EHA rods were fixed with 2 mL of freshly prepared 2.5% glutaraldehyde in RCB for at least 2 h at 4°C and washed 3 x in 0.1 M sodium cacodylate buffer (pH 7.3). The rods were then stained in 1% OsO_4 (v/v) for 2 h and washed twice with distilled water, dehydrated through a graded series of acetone washes (50-100%), critical point dried with liquid CO_2 and finally sputter coated with gold. The surface was examined with a Bausch and Lomb ARL Nanolab 2000 electron microscope.

DNA isolation.

Plasmids were isolated from *E. coli* by an alkaline lysis method. Briefly, cells from 1.5 mL of an overnight culture were harvested by centrifugation, and resuspended in 186 μL of H_2O and 100 μL of GTE (50 mM glucose, 25 mM Tris, pH 8.0, 10 mM EDTA).

Cells were lysed by the addition of 10 μL of 10% SDS (w/v) and 4 μL of 10 M NaOH. The solution was neutralized by adding 150 μL of KAc (3 M potassium acetate, 2 M acetic acid) and then incubated on ice for ten minutes. The tubes were centrifuged and the supernatant was collected and treated with 2 μL of RNase (10 mg/mL) at 37°C for 30 minutes. This was extracted once with chloroform and precipitated with 95% ethanol. The pellet was washed with 70% ethanol and resuspended in TE buffer (20 mM Tris buffer, pH 8, containing 1 mM EDTA).

To isolate chromosomal DNA from *S. mutans*, 10 mL of an overnight culture was harvested by centrifugation, washed once in GTE, resuspended in 300 μL GTE and incubated with 10 kU lysozyme (Boeringher Manheim, Laval, PQ) and 1 kU mutanolysin (Sigma) at 37°C for 1 to 2 h. The cells were then lysed with 2% SDS at room temperature for 10 minutes. The cell lysates were extracted once with phenol, followed by phenol:chloroform (1:1, v/v), and chloroform. RNA was removed by RNase treatment and DNA was precipitated by ethanol and redissolved in TE buffer.

Isolation of RNA.

RNA was isolated from *S. mutans* using a modified method of Lunsford (135). Briefly, 20 mL of an *S. mutans* overnight culture was added to 200 mL of prewarmed THB and grown to early exponential phase (OD_{600} of 0.25). Glycine (5%, w/v) was added to the culture which was further incubated for 90 minutes at 37°C. The cultures were then split into two 100 mL aliquots: Cu^{2+} ($CuSO_4$) was added to the first aliquot at a sub inhibitory concentration (1 mM), the second aliquot remained untreated serving as the non-induced control. Both groups were incubated for a further 20 minutes at 37°C. Cells were harvested by centrifugation, washed with PBS and resuspended in 1 mL of PBS

containing 30% raffinose (w/v) and 1 kU of mutanolysin. After incubation at 37°C for 15 minutes, the cells were harvested by centrifugation, solublized in 700 μL of TRIZOL reagent (GIBCO/BRL Life Technologies, Inc., Burlington, Ont., Canada), and vortexed. After incubation on ice for 5 minutes, the mixture was extracted with chloroform. RNA was precipitated from the aqueous layer with one volume of isoamyl alcohol and washed with 70% ethanol. The pellet was resuspended in 200 μL of diethyl pyrocarbonate (DEPC)-treated water and 20 units of RNase-free DNase (Promega Corp., Madison, Wi., USA) were added. The RNA was further cleaned by extraction with phenol-chloroform, followed by chloroform and precipitated with two volumes of 95% ethanol. The RNA was dissolved in 200 μL DEPC-treated water and stored at -70°C.

Southern, Northern and RNA dot blotting.

DNA was routinely separated on 0.8% agarose gels (174). RNA (20 μg) was separated on formaldehyde agarose gels prepared as described by Kroczck and Siebert (110). Briefly, a 1% gel was prepared by dissolving 0.5 g of agarose in 36.7 mL of sterile DEPC-treated water and 5 mL of 10 x MOPS/EDTA (50 mM MOPS, 10 mM EDTA, pH 7.0). The gel was cooled and 8.3 mL of formaldehyde was added and the gel was quickly poured. The gel was pre-electrophoresed for 30 minutes in 1 x MOPS/EDTA at 60 V prior to sample loading.

Electrophoresed nucleic acids were transferred from the gels to nylon membranes (Biodyne A, GIBCO/BRL) using a Vacu-Blot apparatus as per the manufacture's instructions (Amersham Pharmaca Biotech, Baie d' Urfé, Québec, Canada). For RNA dot blotting, a 96-well dot blotter (Bio-Rad) was used. Following the transfer, nucleic acids were cross-linked to the nylon membranes (Biodyne A, GIBCO/BRL) by incubation at 80°C for 2 h

Blots were incubated in a hybridization oven at 42°C for 2 h in glass tubes containing 20 mL of pre-hybridization solution (50% formamide, 0.0625 M sodium phosphate buffer, pH 7.2, 10 mM NaCl, 1 mM EDTA, 7% SDS). Following prehybridization, blots were placed nucleic acid side down onto 500 µL of hybridization solution (denatured DNA probe diluted 1:20 in pre-hybridization solution) on a siliconized glass plate prewarmed to 42°C. The glass plate was wrapped with plastic wrap and incubated for at least 16 h at 42°C. Following hybridization the membranes were washed 4 x for 15 minutes each in 5 x SSC and 0.5 % SDS (w/v) at 65°C, and 2 x for 20 minutes each in 0.1 x SSC and 1% SDS (w/v) at 50°C. SSC was prepared by diluting a twenty times stock solution (3 M NaCl, 0.3 M sodium citrate dihydrate, pH 7.0). For non-radioactive probes, signal was visualized by exposure to X-Ray film (Kodak XOmat AR), following detection with a Photogene Nucleic acid detection system Version 2.0 (GIBCO/BRL). With α^{32}P-dCTP labeled probes, hybridization was visualized by exposure to X-Ray film (Kodak XOmat AR), following washing.

Colony Blot Hybridization.

Colony blot hybridizations were performed as described by Sambrook *et al.* (174). Sterile nylon membranes (Biodyne A, GIBCO/BRL) were over laid on LB agar plates and colonies were replica plated on the nylon membranes and to a master plate. The plates were incubated overnight at 37°C and colonies on the nylon filters were lysed by successively transferring the filters across four sheets of Whatman 3MM paper impregnated with 10 % SDS (w/v) for 3 minutes, denaturing solution (0.5 N NaOH, 1.5 M NaCl) for 5 minutes, neutralizing solution (1.5 M NaCl, 0.5 M Tris, pH 7.4) for 5 minutes, and 2 x SSC for 5 minutes. The filters were dried at room temperature for 30

minutes and nucleic acids were fixed to the nylon membrane by incubation at 80°C for 2 h. In preparation for hybridization, the filters were placed in prewash solution (5 x SSC, 0.5% SDS, 1 mM EDTA pH 8.0) at 65°C and the cellular debris was gently scraped from the surface with Kimwipes soaked with prewash solution. Hybridization was performed as described by Southern (189).

Synthesis of DNA probes.

Probes for hybridizations were synthesized according to use. For non-radioactive detection, 1 μg of DNA was labeled with biotin-14-dATP using the BioNick Labeling System (GIBCO/BRL). Briefly, 5 μl of a 10 x dNTP mix (0.2 mM each of dCTP, dGTP, and dTTP; and 0.1 mM each of dATP and biotin-14-dATP) was added to the DNA. Five microliters of an enzyme mix (0.25 U DNA polymerase I and 0.0037 U DNaseI) was added (total volume 50 μL) and the labeling reaction was allowed to proceed for 1 h at 16°C. The reaction was terminated by the addition of 1.5 mM EDTA.

For radioactive detection, 50-100 ng of DNA was routinely labeled with α-^{32}P dCTP by random priming (174). The DNA was denatured by boiling and quenched on ice. The following were added to the reaction tube; 3 μL dNTP mix (0.5 mM each of dATP, dGTP, and dTTP), 2.5 μL 10 x Klenow buffer, 2 μL 1 μg/μL $(N)_6$ random primers, 2 μL of 3,000 Ci/mmole α-^{32}P dCTP, and 5 U Klenow large fragment DNA polymerase (GIBCO/BRL). The tube was incubated at room temperature for 30 minutes. Unincorporated nucleotides were separated and removed from the labeled probe using spun-column chromatography (174).

Polymerase chain reaction.

One hundred microliter polymerase chain reaction (PCR) mixtures containing 1 x *Taq* reaction buffer, 0.2 mM of each of the dNTPs, 2.5 mM $MgCl_2$, 100 pM of forward and reverse primers, 0.5 U *Taq* polymerase (GIBCO/BRL), and approximately 1 nM of template DNA were routinely prepared. PCR was performed using a Corbet Research FTS-320 thermocycler (Bio/Can Scientific., Mississauga, Ont., Canada). PCR contained 30 cycles with the following steps: denaturation at 94°C for 1 minute, annealing at 50°C for 1 minute, and extension at 72°C for 1 minute. The primers used are shown in Table 2.

Primer extension.

The reverse primer SL159 (Table 2) corresponding to nucleotide positions 813 - 830 (140 nucleotides downstream of the -35 region) of the *cop* operon was end-labeled with ($\gamma^{32}P$) ATP with T4 polynucleotide kinase (174). The full length labeled oligo was separated by electrophoresis on a 20% polyacrylamide gel and purified using a SEP-PAC Light C18 column (Waters, Milford, MA) according to the manufacturer's directions. Eighty micrograms of total RNA was added to 12 million cpm of the radiolabeled primer in a total volume of 30 µL annealing buffer (0.25 M KCl, 10 mM Tris-HCl, pH 8.3). Annealing was carried out in a thermocycler: 80°C for 5 minutes, 65°C for 5 minutes, 42°C for 10 minutes, 37°C for 20 minutes. Annealed material was precipitated with two volumes of 95% ethanol, washed with 70% ethanol, vacuum dried and resuspended in 20 µL of reverse transcriptase buffer (30 mM Tris buffer, pH 8.3, 20 mM $MgCl_2$, 10 µM dithiotreiotol, 1 mM dGTP, 0.5 mM each of dATP, dCTP and dTTP, and 15 µg/mL actinomycin D). Two hundred units of Muloney murine leukemia virus reverse transcriptase (GIBCO/BRL) was added and the reaction was incubated at 37°C for 1 h.

Table 2. PCR primers.

Primer	Sequence (5' -3')	Nucleotide number[a]	Specificity/Use
SL118	TACGGATCCTTGACGGTACATC	162-187	Forward primer, for amplifying the Erm gene on Tn*917*
SL119	TACGAATTCCTTGGAAGCTGTCAG	1527 -1545	Reverse primer, for amplifying the Erm gene on Tn*917*.
SL120	TACGGATCCATCGAAATATTGAT	3808 - 3828	Forward primer, for amplifying the 3' end of Tn*917*.
SL121	TACGAATTCTAAACCAATGTTTCAAGG	5282 -5300	Reverse primer, for amplifying the 3' end of Tn*917*.
SL147	GCATGCCAGAAGATGAGCGAATGA	790 to 774 nucleotides upstream of position 1	Forward primer, for amplifying the *cop* operon promoter.
SL148	GTCGACGCTCCTTTCATCTACATT	726 to 743	Reverse primer, for amplifying the *cop* operon promoter.
SL145	GGACCTTTGCTGGATCC	3317 to 3333	Forward primer, in *copB*. Used to clone downstream ORFs directly from JH1005 chromosome.
SL146	GTAGAATTCAAAAGCGTGCCATC	3906 to 3922	Reverse primer, downstream of *copZ*, designed from *S. mutans* UAB159 sequence, used to clone genes from the chromosome of JH1005.
SL150	GTCGACATGGAAAAAACATATCATAT	3418 to 3442	Forward primer for *copZ*, starting from ATG start codon. Used with SL146 to produce an amplicon to be fused to the cop promoter.
SL159	GCAATAATTTCACTGCTG	830 to 813	Reverse primer in *copY* used for primer extension.

[a] For primers SL118 - SL120 the numbers are for the Tn*917* (Accession # M11180). For the remaining primers the numbers correspond to those in Figure 26.

After 1 h, 1 μL of 0.5 M EDTA and 1 μL of RNase (10 mg/mL) were added and incubated for 30 minutes at 37°C. The volume was then brought up to 100 μL with water and the mixture was extracted with phenol:chloroform:isoamyl alcohol, precipitated, washed, resuspended and analyzed by electrophoresis on a denaturing polyacrylamide sequencing gel.

DNA sequencing.

DNA sequence of the cloned *cop* fragments were determined with an automated DNA sequencer (Applied Biosystem, Dalhousie University-NRC Joint Lab facilities). For the primer extension experiment, the DNA sequence of *copY* and the cop promoter was generated with a DNA sequencing kit (T7 sequenase version 2, Amersham Pharmacia Biotech) using the same primer as for the primer extension and pWH4 as the template.

Transformation of *E. coli* and *S. mutans*.

Competent *E. coli* XL1-Blue cells were prepared by treatment with $CaCl_2$. Briefly, 45 mL of LB broth was inoculated with 1 mL of an overnight culture, grown to early exponential phase (OD_{600} = 0.35), harvested by centrifugation, washed once with 50 mL of cold Tfm 1 (10 mM Tris pH 7.2, 150 mM NaCl), resuspended in 50 mL of Tfm 2 (50 mM $CaCl_2$) and incubated on ice for 45 minutes. Cells were centrifuged and resuspended in 3 mL of Tfm 3 (10 mM Tris pH 7.2, 50 mM $CaCl_2$, 10 mM $MgSO_4$) and 2 mL of 50% glycerol (v/v), aliquoted, and stored at -70°C.

For transformation, 0.2 mL of competent *E. coli* cells were added to 0.1 mL of ice cold Tfm 3 containing 40 ng of DNA. The cells and DNA were incubated on ice for 45 minutes, heat shocked for 2 minutes at 37°C, incubated at room temperature for 10 minutes, and 0.5

mL of LB broth was added. The cells were incubated at 37°C for 1 h and then plated on selective LB agar.

Natural transformation of *S. mutans* was performed by a modified method of Perry and Kuramitsu (83, 164). Four milliliters of THB containing 5% (v/v) heat-inactivated calf serum (THBS) was inoculated with 50 µL of frozen culture and grown overnight at 37°C. Fresh prewarmed THBS was then inoculated (1:40) with the overnight culture and incubated at 37°C until the cells reached an OD_{600} of approximately 0.2. An aliquot (0.75 mL) of the culture was removed to an eppendorff tube containing 0.5 - 1 µg of DNA and incubated at 37°C. After 30 minutes, 0.75 mL of fresh prewarmed THBS was added and the culture was incubated for 1.5 h at 37°C. The cells were subsequently plated on selective TH agar.

Tn*917* mutagenesis and isolation of SPRE-defective mutants.

Tn*917* mutagenesis of *S. mutans* JH1005 with pTV1-OK (Fig. 4A, 11 kb, Kan^R, Em^R) was performed as described by Gutierrez *et al.* (70). Strain JH1005 was used in this study because transposon mutants were relatively easy to obtain from this strain and a number of attempts to generate transposon mutants from strain NG8 were unsuccessful. *S. mutans* JH1005 (pTV1-OK) cultures grown overnight at 28°C in THYE broth (THB supplemented with 0.3 % [w/v] yeast extract) were diluted 1/200 into fresh THYE containing 0.04 µg/mL erythromycin. The diluted cultures were incubated at 42°C for 16 to 24 h to allow insertions of Tn*917* into the chromosome to occur. Following the incubation, potential transposon mutants were isolated on THYE agar containing 10 µg/mL erythromycin. Colonies were replica plated onto THYE agar containing either 10 µg/mL erythromycin or 300 µg/mL kanamycin. Kan^S and Em^R colonies were presumed

Figure 4. (A) Physical map of the plasmid pTV1-OK (71), (B) Map of Tn*917*, the positions of PCR primers used to generate amplicons for use as probes is indicated by arrows.

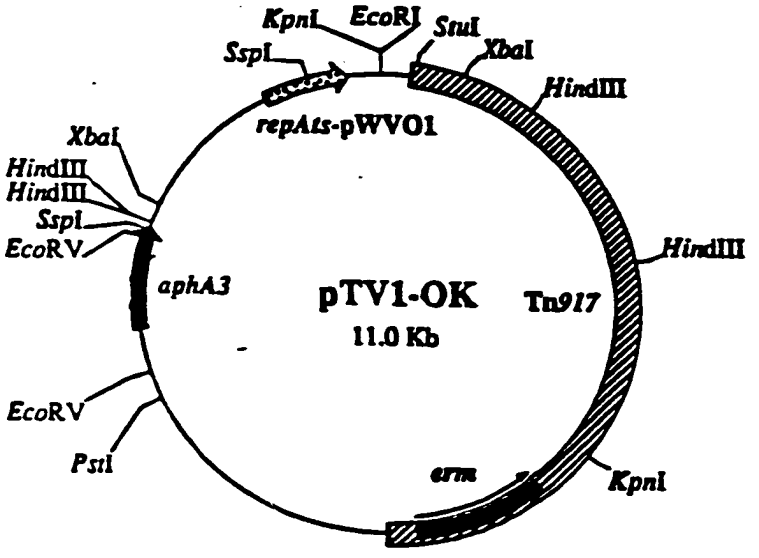
KpnI
EcoRI
StuI
SspI
XbaI
HindIII
repAts-pWV01
XbaI
HindIII
HindIII
SspI
EcoRV
aphA3
pTV1-OK
11.0 Kb
Tn917
HindIII
EcoRV
PstI
erm
KpnI

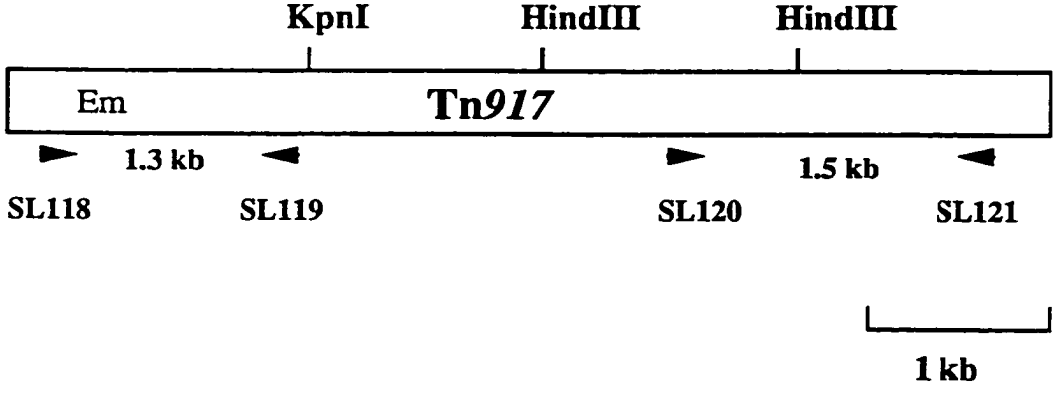
KpnI
HindIII
HindIII
Em
Tn917
1.3 kb
1.5 kb
SL118
SL119
SL120
SL121
1 kb

to have lost the plasmid backbone and were used for the screening of potential SPRE-defective mutants by whole-cell ELISA as described above.

Mapping of the Tn*917* insertion site in *S. mutans* mutant A.

Chromosomal DNA from the Tn*917* mutant A was restricted to completion by *Hind*III and separated on a 0.7% agarose gel. DNA fragments of 2 to 3 kb were recovered from the gel by electroelution (174), and cloned into *E. coli* XL1-blue using the vector pBluescript (Stratagene, La Jolla, Ca). Transformants were screened by colony hybridization (see above), using a (^{32}P)-labeled probe prepared by random priming of a 1.5 kb amplicon of the 3' end of Tn*917* (Fig. 4B). The amplicon was generated by PCR using the primers SL120 and SL121 (Table 2) and the conditions described above. The plasmid from a positive clone, NV4, was sequenced using primers to pBluescript (Applied Biosystem, Dalhousie University-NRC Joint Lab facilities). The sequences were compared to that of Tn*917* (Genbank accession # M11180).

Cloning of the *cop* operon from *S. mutans*.

Southern blot analysis of *Hind*III-digested *S. mutans* JH1005 chromosomal DNA using a probe prepared from the 2.5 kb *Hind*III insert on pNV4 yielded a signal of approximately 3 kb. To clone this 3 kb fragment, DNA fragments of 2 to 5 kb were recovered from an agarose gel, ligated into *Hind*III-digested and dephosphorylated pBluescript, and transformed into *E. coli* XL1-blue. Transformants obtained were screened by colony hybridization using the same 2.5 kb *Hind*III insert from pNV4 as a probe. A positive clone (NVD20) was obtained. DNA sequencing showed that the DNA in clone NVD20 did not contain the entire gene. Therefore, a partial library consisting of

3 to 6 kb *Hind*III fragments of partially digested *S. mutans* JH1005 chromosomal DNA, which were isolated by a sucrose density gradient (10-40%, (174)), was prepared using pUC18 as the vector. From screening the library by colony blotting using the 2.5 kb insert of pNVD20 as a probe, a positive clone (WH4) was found to carry the same 2.5 kb *Hind*III insert of pNV20 and an additional 1.5 kb *Hind*III fragment. Using the 1.5 kb *Hind*III fragment as the probe, a 1.4 kb *Hinc*II fragment was identified by Southern blotting and this fragment was cloned into *Sma*I restricted and dephosphorylated pUC18 (Amersham Pharmacia Biotech, Inc.) to obtain clone NV5. From a homology search of the database of the partial genome sequence of *S. mutans* UAB159 (www.genome.ou.edu) using our sequence as an query, a positive match within a 7.5 kb DNA fragment was identified. The sequence data from strain UAB159 was used to design the forward PCR primer SL145 and the reverse primer SL146 for amplification by PCR of a 500 bp amplicon carrying the last portion of the *cop* operon. The amplicon was blunt end cloned into *Sma*I-restricted and dephosphorylated pUC18 to obtain the plasmid pNV46.

The entire *cop* operon was reconstructed from the cloned DNA fragments. A 2.5 kb *Pst*I - *Xba*I fragment from pWH4 containing upstream sequences, the promoter, *copY* and part of *copB* was cloned into pNV5 which had been cut with the same enzymes. The resulting plasmid, pNV6 carried on it all but the last half of *copZ*. The second half of *copZ* contained within a 0.5 kb *Bam*HI - *Eco*RI fragment was isolated from pNV46 and ligated into pNV6 cut with the same enzymes. The new plasmid, pNV7, consisted of 450 bp of sequence upstream of *copY*, the 2.9 kb operon, and 280 bp of sequence downstream of the stop codon of *copZ*.

Construction of a *cop* operon knock-out mutant.

pNV7 was restricted with *Hinc*II to drop out the three ORF's comprising the *cop* operon. A 4 kb *Hinc*II fragment containing the tetracycline resistance gene from pVA981 (203) was ligated to the remainder of pNV7. The resulting construct, pNV7/S4, carried 454 bp of sequences upstream of *copY* and 377 bp of sequence downstream of *copZ*. pNV7/S4 was linearized with *Sca*I and used to transform *S. mutans* JH1005. Transformants were selected on THA containing tetracycline. One transformant, S4, was chosen for further study. Chromosomal insertion of the tetracycline cassette and loss of the operon sequences in S4 were verified by Southern blotting with two different probes. The first was specific for the 2 kb *Sst*I - *Xba*I fragment pWH4 encompassing *copY* and *copB*, and the second probe was produced by labeling pVA981, from which the tetracycline resistance gene was derived.

Construction of plasmids for complementation of *cop* knock-out mutant S4 and Tn*917* mutant A.

A plasmid with the entire *cop* operon was constructed by subcloning the *Sph*I - *Eco*RI fragment from pNV7 into the *E. coli-Streptococcus* shuttle vector pDL276 (54), yielding pNV7B (Fig. 5).

A plasmid carrying *copY* was constructed by taking the *Sph*I (on the multiple cloning site of pUC18) - *Xba*I fragment from pWH4 and ligating into similarly digested pDL276 (54) to produce pWH4/PDL (Fig. 6).

Figure 5. Outline of the construction of pNV7B. A shuttle vector carrying the entire *cop* operon.

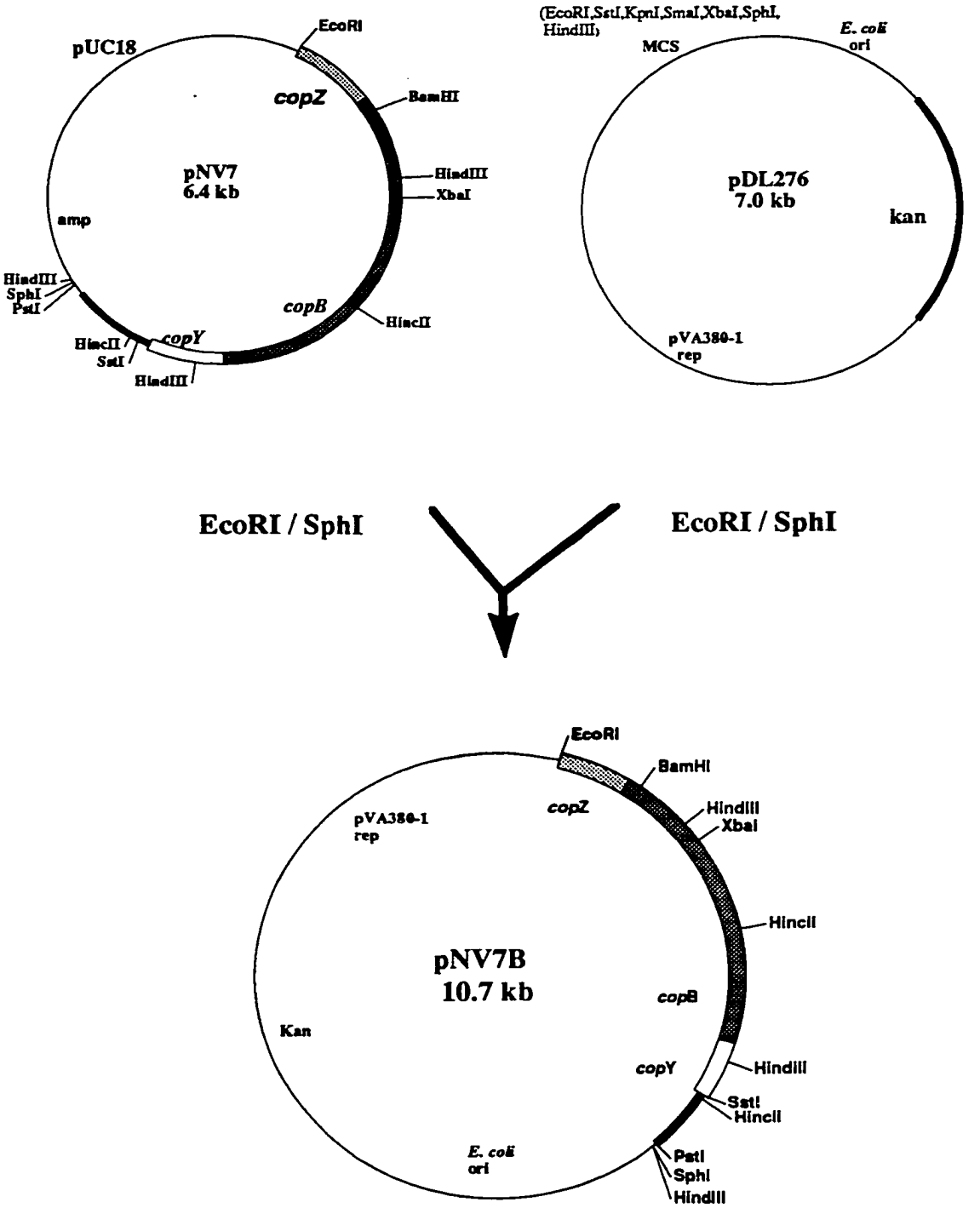
pUC18
EcoRI
copZ
BamHI
pNV7
6.4 kb
HindIII
XbaI
amp
HindIII
SphI
PstI
copB
HincII
HincII
SstI
copY
HindIII
(EcoRI,SstI,KpnI,SmaI,XbaI,SphI,
HindIII)
MCS
E. coli
ori
pDL276
7.0 kb
kan
pVA380-1
rep
EcoRI / SphI
EcoRI / SphI
EcoRI
BamHI
copZ
HindIII
XbaI
pVA380-1
rep
HincII
pNV7B
10.7 kb
copB
Kan
copY
HindIII
SstI
HincII
E. coli
ori
PstI
SphI
HindIII

Figure 6. Outline of the construction of pWH4/PDL. A shuttle vector carrying the *copY* gene.

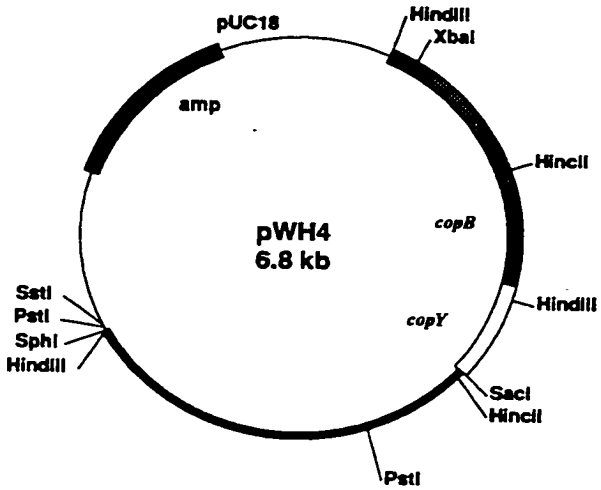
pUC18
HindIII
XbaI
amp
HincII
pWH4
6.8 kb
copB
copY
HindIII
SacI
HincII
PstI
SstI
PstI
SphI
HindIII

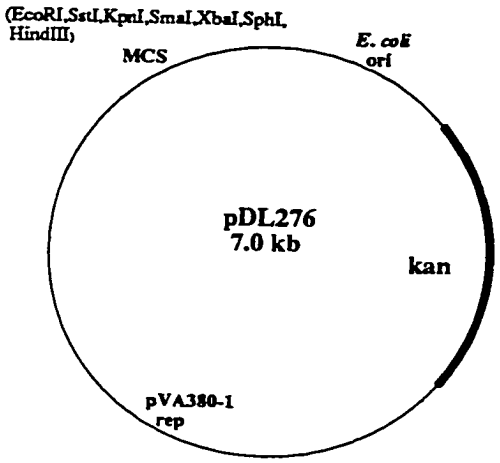
(EcoRI,SstI,KpnI,SmaI,XbaI,SphI,
HindIII)
MCS
E. coli
ori
pDL276
7.0 kb
kan
pVA380-1
rep

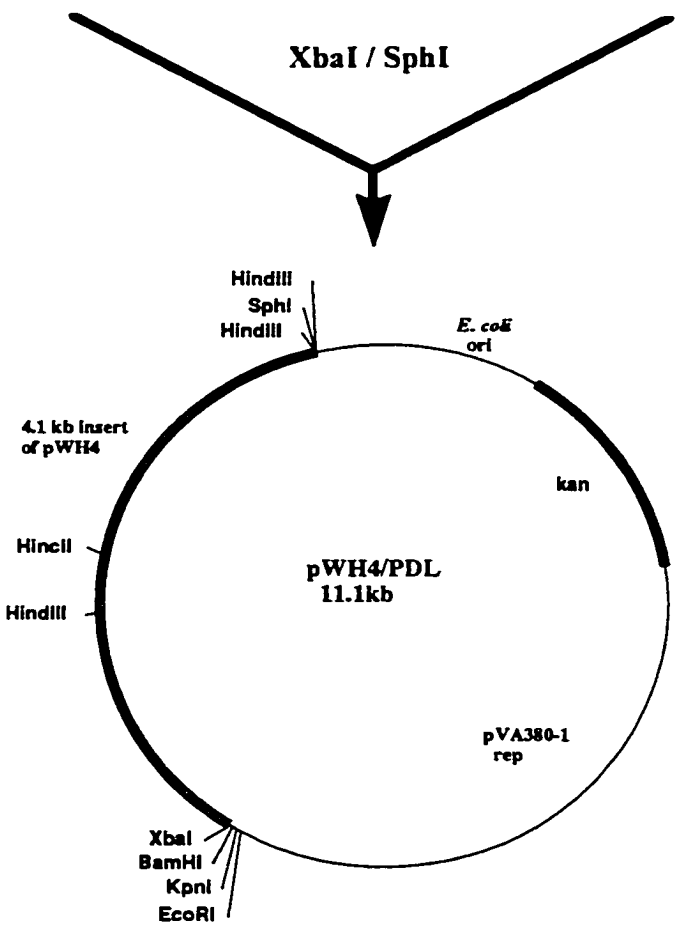
XbaI / SphI
HindIII
SphI
HindIII
E. coli
ori
4.1 kb insert
of pWH4
kan
HincII
pWH4/PDL
11.1kb
HindIII
pVA380-1
rep
XbaI
BamHI
KpnI
EcoRI

Construction of a recombinant plasmid carrying *copZ* was a multistep process (Fig. 7). In the first step, the *cop* operon promoter was amplified using the forward primer SL147, and the reverse primer, SL148, (Table 2) and ligated into *Sma*I-digested bacterial alkaline phosphatase treated pUC18 (Amersham Pharmacia Biotech, Inc.) to make pNV8. The promoter was then excised from pNV8 with *Bam*HI and *Eco*RI and subcloned into pDL276 producing pPNV8. Secondly, *copZ* was amplified using the forward primer SL150, and the reverse primer, SL146 (Table 2). The amplicon was then ligated into *Eco*RV-digested and dephosphorylated pBluescript producing pZ1. Finally, pZ1 was cut with *Sal*I, blunt ended with Klenow (GIBCO/BRL), and digested with *Eco*RI. *copZ* was then cloned into pPNV8, previously digested with *Kpn*I, blunt ended with the Klenow fragment and digested with *Eco*RI to make pNV10.

Fusion of the *cop* operon promoter with a reporter CAT gene.

The plasmid pNV8 carrying the *cop* operon promoter was digested with *Kpn*I, blunt ended with Klenow and digested with *Xba*I to yield a 1.7 kb fragment carrying the promoter. This 1.7 kb fragment was ligated into the *Sma*I and *Xba*I site of pMH109 (87). This ligation placed the promoter immediately upstream of the promoter-less chloramphenicol acetyltransferase (CAT) gene. The ligated plasmid (pHTL1, Fig. 8) was transformed into *E. coli* and expression of the CAT gene was confirmed by selection with chloramphenicol.

The plasmid pHSL2 (Fig. 8) was constructed by first digesting pHTL1 with *Hind*III, blunt ending with Klenow and digesting with *Xba*I. The 4 kb fragment of pHTL1

Figure 7. Construction of pNV10. A plasmid shuttle vector expressing *copZ*.

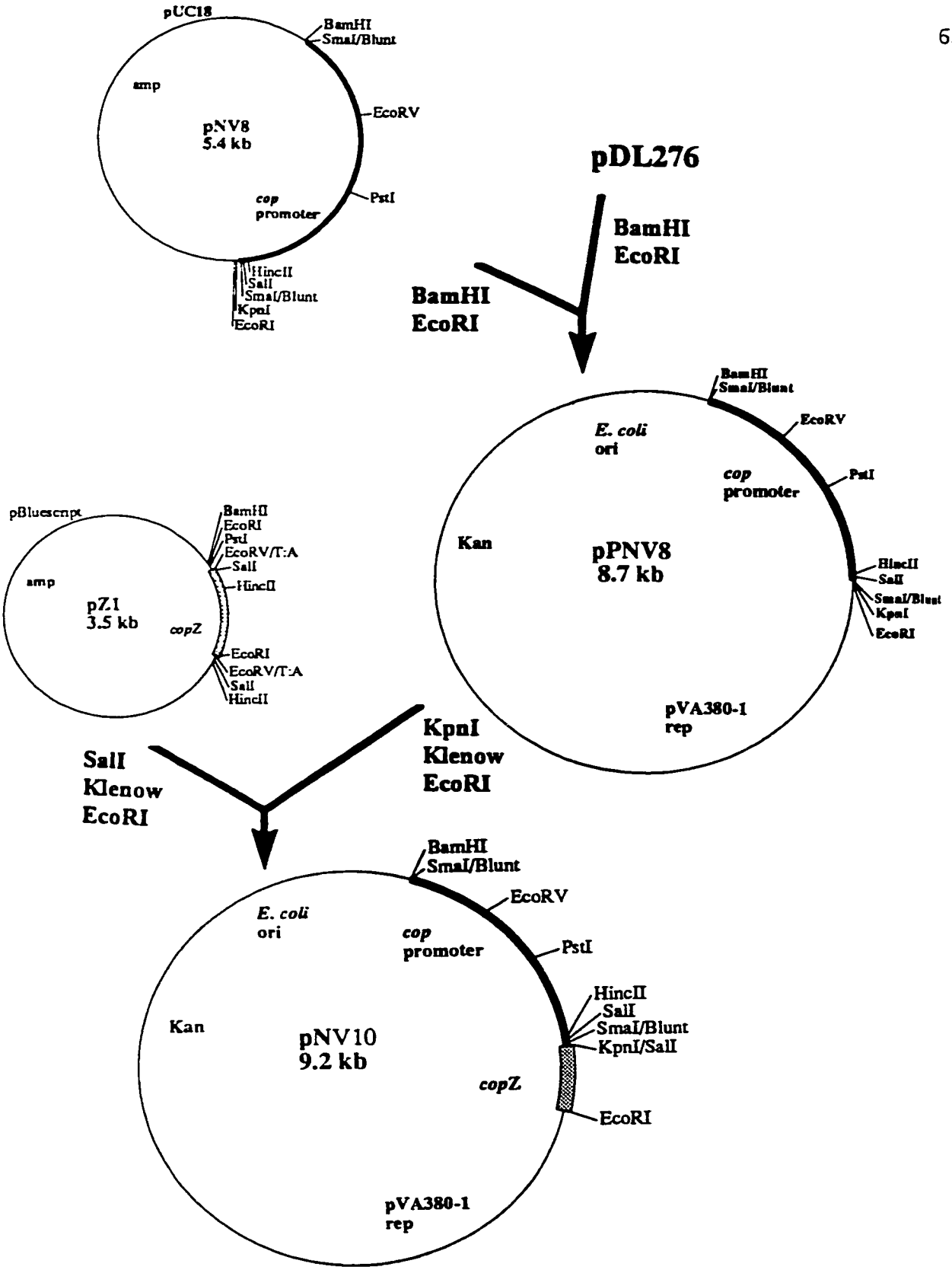
pUC18
BamHI
SmaI/Blunt
amp
pNV8
5.4 kb
EcoRV
cop
promoter
PstI
HincII
SalI
SmaI/Blunt
KpnI
EcoRI
pDL276
BamHI
EcoRI
BamHI
EcoRI
BamHI
SmaI/Blunt
EcoRV
E. coli
ori
cop
promoter
PstI
Kan
pPNV8
8.7 kb
HincII
SalI
SmaI/Blunt
KpnI
EcoRI
pVA380-1
rep
pBluescript
BamHI
EcoRI
PstI
EcoRV/T:A
SalI
HincII
amp
pZ1
3.5 kb
copZ
EcoRI
EcoRV/T:A
SalI
HincII
SalI
Klenow
EcoRI
KpnI
Klenow
EcoRI
BamHI
SmaI/Blunt
EcoRV
E. coli
ori
cop
promoter
PstI
HincII
SalI
SmaI/Blunt
KpnI/SalI
Kan
pNV10
9.2 kb
copZ
EcoRI
pVA380-1
rep

Figure 8. Construction of a *cop* operon promoter - CAT gene fusion.

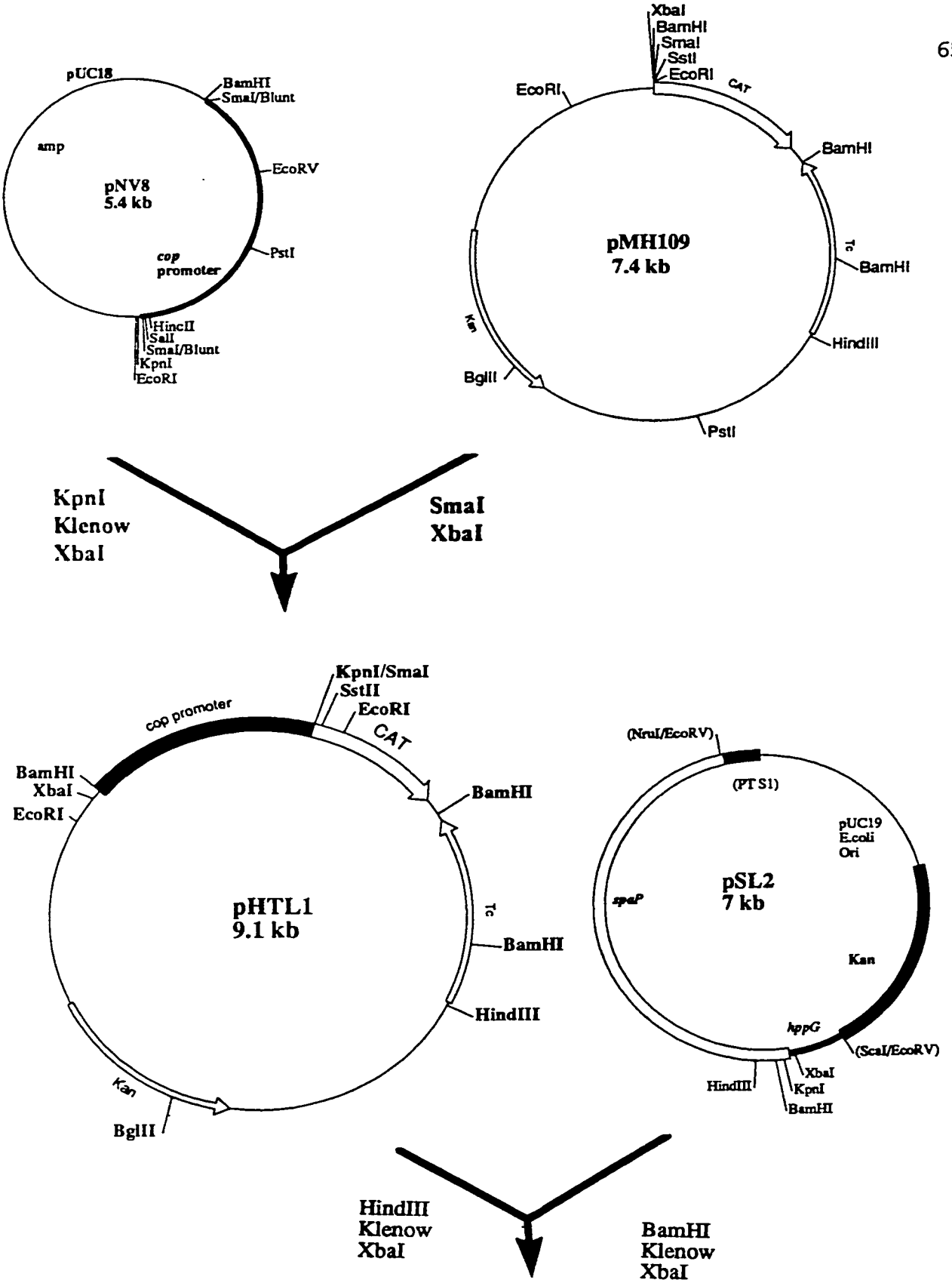
pUC18
BamHI
SmaI/Blunt
amp
EcoRV
pNV8
5.4 kb
cop
promoter
PstI
HincII
SalI
SmaI/Blunt
KpnI
EcoRI
XbaI
BamHI
SmaI
SstI
EcoRI
EcoRI
CAT
BamHI
pMH109
7.4 kb
Tc
BamHI
Kan
HindIII
BglII
PstI
KpnI
Klenow
XbaI
SmaI
XbaI
KpnI/SmaI
SstII
EcoRI
cop promoter
CAT
BamHI
BamHI
XbaI
EcoRI
pHTL1
9.1 kb
Tc
BamHI
HindIII
Kan
BglII
(NruI/EcoRV)
(PTS1)
pUC19
E.coli
Ori
pSL2
7 kb
spaP
Kan
hppG
(ScaI/EcoRV)
HindIII
XbaI
KpnI
BamHI
HindIII
Klenow
XbaI
BamHI
Klenow
XbaI

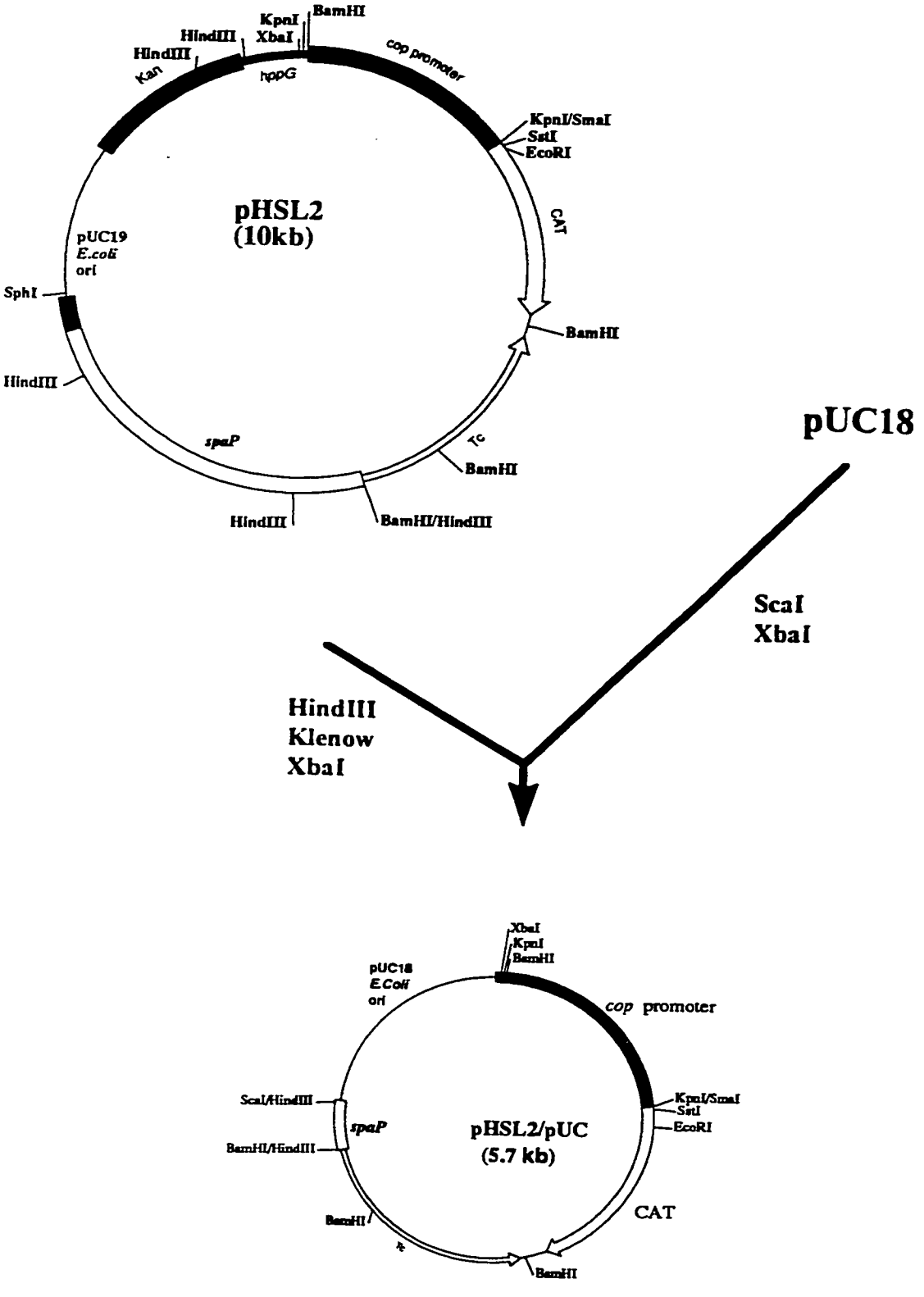
pHSL2
(10kb)
KpnI
XbaI
BamHI
HindIII
HindIII
Kan
hppG
cop promoter
KpnI/SmaI
SstI
EcoRI
CAT
BamHI
pUC19
E.coli
ori
SphI
HindIII
spaP
Tc
BamHI
HindIII
BamHI/HindIII
pUC18
ScaI
XbaI
HindIII
Klenow
XbaI
XbaI
KpnI
BamHI
pUC18
E.Coli
ori
cop promoter
ScaI/HindIII
spaP
BamHI/HindIII
pHSL2/pUC
(5.7 kb)
KpnI/SmaI
SstI
EcoRI
CAT
BamHI
Ap
BamHI

was isolated and ligated to a 6.5 kb fragment of pSL2 generated by digestion with *Bam*HI (followed by Klenow treatment) and *Xba*I. pSL2 was a plasmid constructed in our laboratory which contained a 0.4kb DNA fragment coding for a non-essential oligopeptide transport gene (*hppG*) originated from *Streptococcus gordonii* DL1 (92). pSL2 also carried a 1.5 kb of the *spaP* gene which codes for the major surface protein antigen P1 from *S. mutans* NG5 (101). The presence of the *hppG* and *spaP* fragment would facilitate the integration of pSL2 into the streptococcal chromosome via homologous recombination. Finally, pHSL2/pUC (Fig. 8) was produced by digesting pHSL2 with *Hind*III, blunt ending the overhang with the Klenow enzyme followed by digestion with *Xba*I yielding a 4 kb fragment encompassing the promoter/CAT fusion and a fragment of the *spaP*. The 4kb fragment was ligated to the 1.7 kb *Sca*I-*Xba*I fragment of pUC18 which provided an origin of replication.

Introduction of pHSL2/pUC into the *S. mutans cop* operon knock-out mutant S4.

pHSL2/pUC was naturally transformed into *S. mutans* S4. Chloramphenicol resistant transformants were selected on THA. Colonies appearing after 24 h were picked and used to inoculate TH broth containing chloramphenicol. One of the transformants obtained, S4/CAT, was then used as the recipient for the plasmids pNV7B, pWH4/PDL, and pNV10. These plasmids carried the entire *cop* operon, *copY*, and *copZ* respectively. The growth of S4/CAT and complemented strains in the presence of chloramphenicol or copper was determined.

Determination of minimal inhibitory concentration (MIC) to heavy metal ions.

S. mutans were grown overnight in THB and diluted in fresh THB to a concentration of approximately 10^6 CFU/mL. Aliquots (0.5 mL) of the cultures were then added to aliquots (0.5 mL) of THB containing two-fold dilutions of metal ions to be tested. The tubes were then incubated at 37°C for 20 to 24 h and scored visually for growth. The tube containing the lowest concentration of the metal ions still able to inhibit growth was recorded as the MIC.

Effect of Cu^{2+} on growth of *S. mutans*.

Fresh TYG was dispensed into sterile cuvettes and inoculated (1:10) with overnight cultures grown in the same medium. THB was not suitable in this growth study because the higher concentrations of $CuSO_4$ required to inhibit growth were found to interfere with optical density measurements. The cultures were placed in a 37°C water bath and growth was monitored by measuring the optical density (OD_{600nm}) at hourly intervals.

Cellular autolysis and osmotic fragility assays.

Cellular autolysis and osmotic fragility assays were performed as described by Massidda *et al.* (141). Ten milliliters of THB were inoculated (1:25) with an overnight culture and cells were grown to exponential ($0D_{600nm}$ = 0.65) or stationary ($OD_{600\ nm}$ = 1.15) phase of growth. Cells were harvested by centrifugation, washed twice with distilled water and once with 10 mM sodium phosphate buffer, pH 6, and resuspended in 5 mL of

the same buffer. The cells were dechained by rapid passage through a 27 gauge needle, centrifuged and resuspended to the same density (OD_{600nm} = 1) with 10 mM sodium phosphate buffer, pH 6.0. The OD_{600nm} of 1 mL aliquots was measured and recorded as 100%. The aliquots were subsequently incubated at 37°C and removed at intervals to monitor the OD_{600nm}.

For the osmotic fragility assay, stationary and exponential phase cells were centrifuged and washed once in the protoplast buffer (10 mM sodium phosphate, pH 7.2 and 30% raffinose). Cells were then dechained by rapid passage through a 27 gauge needle and adjusted to the same cell density (OD_{600nm} = 1) and incubated in the protoplast buffer (1.5 mL) containing 1 kU of mutanolysin per milliliter at 37°C. Starting at time 0 (immediately after mutanolysin addition) and at intervals thereafter, 20 μL aliquots of the cell suspension were rapidly diluted in 1 mL of 10 mM sodium phosphate buffer pH 7.2 and the optical density was measured. The OD_{600nm} of a diluted sample at time 0 was taken as 100%.

Statistical analysis.

The significance of the difference between samples was determined by ANOVA at a 95% level of confidence.

RESULTS

Formation of a model *S. mutans* biofilm using epon-hydroxyapatite rods and salivary proteins.

Production of smooth cylindrical EHA rods (Fig. 3) provided a surface for biofilm formation. The surface was well suited for our experiments due to its calcium phosphate composition. Subsequent conditioning of the rods with salivary proteins provided a surface mimicking the enamel following acquisition of the acquired enamel pellicle. Since the rods were "lab-made", the initial experiments were to define the parameters for their conditioning with salivary proteins. Biofilm formation on the conditioned surface was subsequently characterized.

The parameters of conditioning EHA rods with salivary proteins.

The binding capacity of the EHA rods was determined by conditioning EHA rods with bovine serum albumin (BSA), and vortexing the rods to recover adherent protein which could be quantitated. The amount of BSA recovered from rods by vortexing following conditioning with 10 and 0.83 mg/mL of BSA was 4.3 and 3.6 $\mu g/cm^2$ respectively (Table 3). The minute difference in the recovery of proteins from rods exposed to solutions whose protein content differed by one order of magnitude suggested that the binding capacity of EHA is very small (4 $\mu g/cm^2$), in comparison to the total protein in the system. The lack of large quantities of saliva and the difficulty in filter sterilizing viscous undiluted saliva required that saliva be diluted prior to use in conditioning EHA rods. Three dilutions of saliva (1/5, 1/10, and 1/15) were made. Upon conditioning EHA rods with 1/5, 1/10, or 1/15 dilutions of saliva (0.28, 0.14 and 0.09 mg of protein /mL), 3.2, 2.1, and 1.5 $\mu g/cm^2$ of protein was found on the respective rods

Table 3. Differential conditioning of EHA rods with bovine serum albumin or whole unfiltered clarified saliva.

	Concentration (mg/ml)	Dilution (concentration, mg/ml) [a]	Protein recovered from rods ($\mu g/cm^2$)
Bovine Serum Albumin	10	- (10)	4.30 ± 0.4
		1/12 (0.83)	3.63 ± 0.6
Unfiltered Saliva	1.40 ± 0.16	1/5 (0.28)	3.22 ± 0.07
		1/10 (0.14)	2.08 ± 0.20
		1/15 (0.09)	1.46 ± 0.28

[a] Concentration of the diluted sample was estimated by dividing the concentration of the undiluted sample by the dilution factor.

(Table 3). Although saliva diluted 1/5 allowed the highest protein-coating on EHA, it was still too viscous to be efficiently filtered. Saliva diluted 1/10 could be easily filter-sterilized and allowed protein–coating to reach half the binding capacity of EHA. Therefore, 1/10 diluted saliva was chosen for use in subsequent experiments.

To ensure that filtration did not drastically alter the composition of saliva, qualitative and quantitative comparisons of filtered and unfiltered saliva were made. SDS-PAGE analysis showed that the filtered and unfiltered saliva exhibited similar protein profiles with the same relative intensities for all the protein bands except the 45 kDa band (Fig. 9, lanes 2 and 4). Total proteins present in 1/10 diluted unfiltered saliva and filtered saliva were 0.21 ± 0.05 and 0.17 ± 0.07 mg/mL, respectively (Table 4). These results suggest that filtration reduced the total protein content in saliva but did not significantly alter the composition.

When EHA rods were conditioned with filtered and unfiltered saliva, 1.5 $\mu g/cm^2$ and 2.3 $\mu g/cm^2$ of protein, respectively, was found to adhere to the rods (Table 4). SDS-PAGE analysis of proteins recovered from filtered and unfiltered saliva-conditioned EHA rods showed similar protein profiles (Fig. 9, lanes 3 and 5). Among the proteins adhering to filtered saliva-conditioned EHA, sIgA (26.4 ng/cm^2), and SA (126.5 ng/cm^2) were detected by ELISA. Amylases were also detected by the reducing sugar assays.

To examine the stability of the conditioning film on EHA, two sets of rods were conditioned with the same batch of filtered saliva for 15 minutes. The adherent proteins from one set of rods were immediately recovered and quantified (2.7 $\mu g/cm^2$). The second set of rods was incubated in RCB buffer lacking exogenous protein for 1 hour prior to recovery of adherent protein. The 60 minute incubation in RCB buffer resulted in a slight decrease in protein recovered from rods (2.2 $\mu g/cm^2$).

Figure 9. A silver-stained SDS-PAGE gel showing the proteins present in saliva and proteins recovered from EHA. Saliva was collected, clarified, diluted and filtered where required. Eight EHA rods were then immersed in either filtered or unfiltered saliva for 15 minutes. Adherent proteins were recovered by successively vortex rods in 1 mL of distilled water. Four hundred microliters of 1/10 diluted filtered or unfiltered saliva and the proteins recovered from EHA rods conditioned in the solutions were precipitated in 10% trichloroacetic acid (TCA, w/v), suspended in 20 μL of non-reducing sample buffer, boiled and loaded onto a 7.5% SDS-PAGE gel. Lanes: **1.** Protein marker, **2.** Unfiltered saliva, **3.** Proteins recovered from rods conditioned in unfiltered saliva, **4.** Filtered saliva, **5.** Proteins recovered from rods conditioned in filtered saliva.

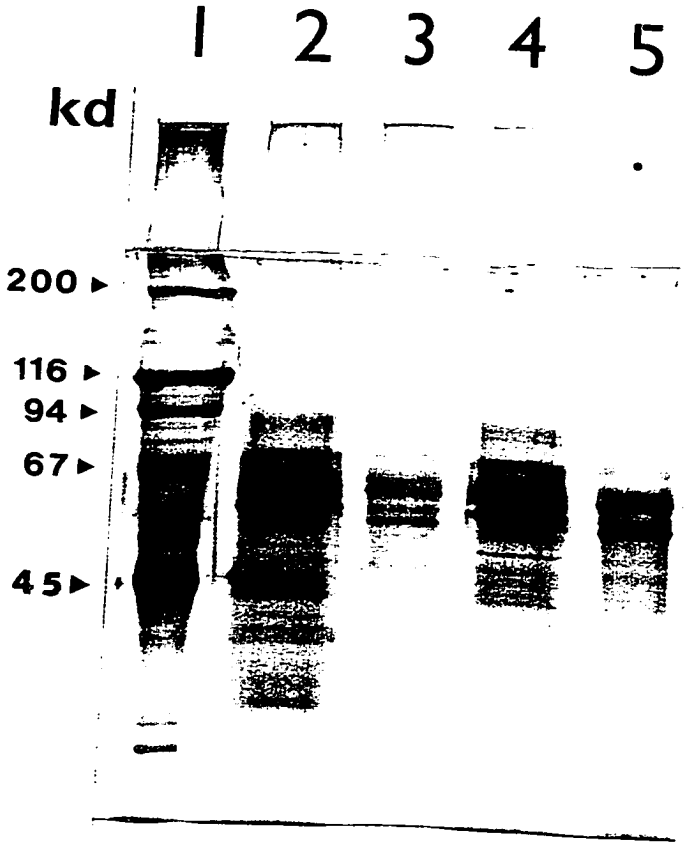
1
2
3
4
5
kd
200
116
94
67
45

Table 4. Amount of proteins recovered from EHA rods after coating with 1/10 diluted unfiltered or filtered-clarified saliva.

	Salivary protein (mg/ml)	Protein recovered from rods ($\mu g/cm^2$)
Unfiltered saliva	0.21 ± 0.05	2.28 ± 0.25
Filtered saliva	017 ± 0.07	1.47 ± 0.45

The data presented is the average of three experiments done on separate days with freshly collected saliva.

When EHA rods were conditioned with purified SA (80 μg/mL), 1.3 ± 0.2 μg/cm^2 protein was recovered from the EHA rods. Protein adhering to EHA was confirmed to be SA by its reactivity with the monospecific polyclonal anti-SA antibody in western blots (Fig. 10). The immuno-reactive band was estimated to be in the range of 400 kDa.

Biofilm formation on EHA conditioned with salivary proteins.

After establishing that salivary proteins and SA could adhere to EHA surfaces, the adherence of *S. mutans* NG8 cells was investigated on saliva- or SA-conditioned rods as well as on control rods conditioned with BSA or RCB (bare rods). As shown in Figure 11, *S. mutans* cells quickly adhered to the rods and the number of accumulated cells reached a plateau after 20 minutes. After 75 minutes, the total number of *S. mutans* cells accumulated on bare rods, BSA-, saliva-, or SA-conditioned rods were 6.23 [± 0.31] x 10^5, 2.31 [± 0.31] x 10^5, 1.60 [± 0.07] x 10^5, and 3.28 [± 0.97] x 10^5 CFU/cm^2, respectively. The kinetics and degree of adherence to the bare rods was surprising and may be due to nonspecific interactions between bacterial surface proteins and the bare surface of the EHA.

The results clearly indicate that after 60 minutes of incubation, a relatively stable *S. mutans* biofilm was formed on EHA and this time point was used for all subsequent biofilm experiments. Scanning electron microscopy showed that biofilms formed on the saliva-conditioned EHA rods provided a sparse monolayer coverage of the surface (Fig. 12). Similar biofilms were observed on BSA- and RCB-conditioned EHA rods (not shown). These biofilms are similar to those previously reported (123, 130).

The role of antigen P1 in biofilm formation on SA-conditioned EHA rods was investigated by comparing adherence of *S. mutans* NG8 and its isogenic P1-negative mutant

Figure 10. Western immunoblot of SA recovered from EHA rods following conditioning for 15 minutes in RCB containing 1 μg/mL SA. SA was recovered from the rods by vortexing. Five hundred microliters of proteins recovered from eight conditioned EHA rods (Lane 1) and 500 μL of the 1 μg/mL SA solution used to condition the rods (Lane 2) were precipitated in 10% TCA (w/v). Protein was resuspended in 1 x non-reducing sample buffer, run on a 7.5% SDS-PAGE gel, transferred to nitrocellulose and probed with a polyclonal rabbit anti-SA antibody (1/500, see Materials and Methods).

1 2

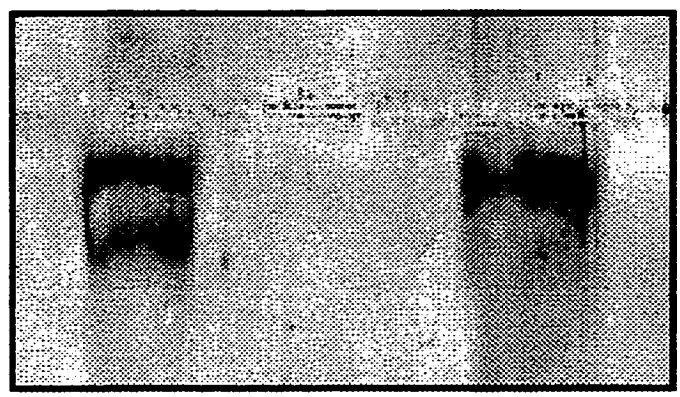

Figure 11. The accumulation of *S. mutans* NG8 on EHA. EHA was conditioned with clarified whole saliva (Δ, 0.17 mg/ml), SA (●, 1 μg/mL), BSA (■, 0.18 mg/mL), or RCB buffer (♦).

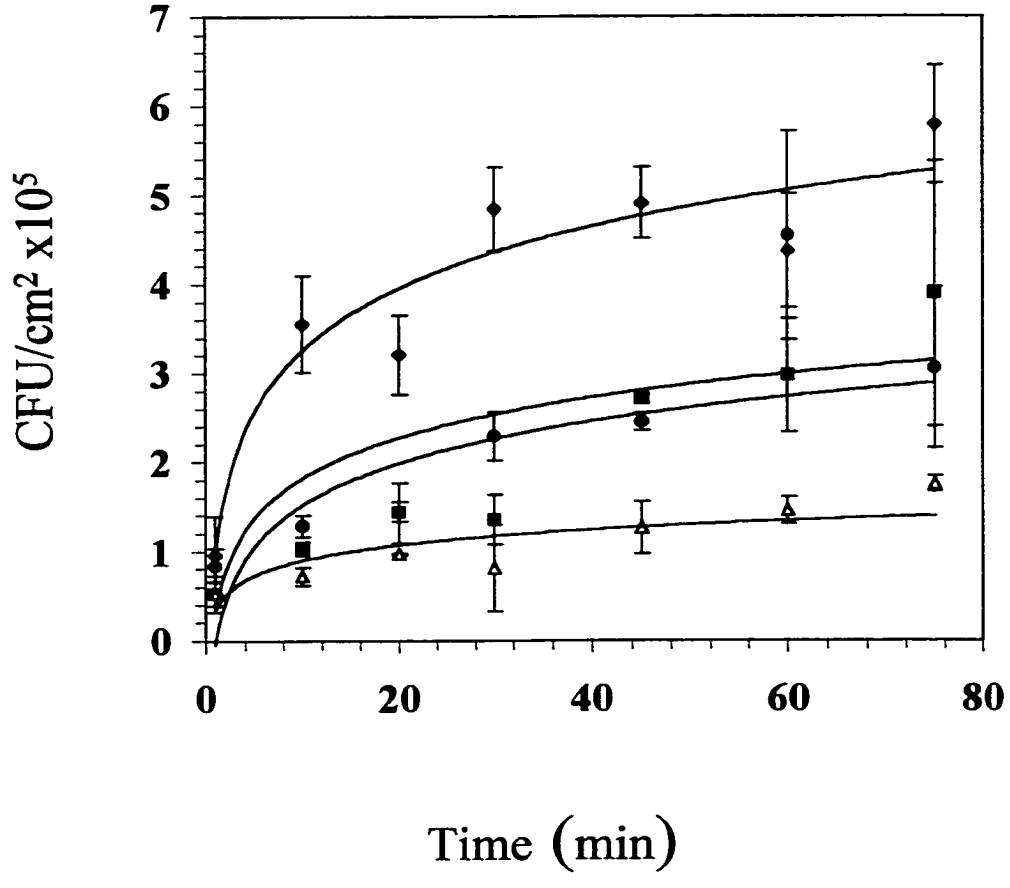
CFU/cm² x10⁵
0
1
2
3
4
5
6
7
0
20
40
60
80
Time (min)

Figure 12. Scanning electron micrograph of *S. mutans* biofilms formed on saliva conditioned rods.


15KV X1 98K 25 03UM 0001 -ARL-
15KV X4 96K 02 01UM

834 (126) to EHA rods conditioned in RCB with increasing concentrations of SA. At low SA concentrations (1 - 10 μg/mL) there were negligible differences in the ability of the two strains to adhere to the SA-conditioned rods (Fig. 13). Increasing the concentration of SA (20 - 80 μg/mL) used to condition the rods resulted in an increased adherence of NG8, but not 834, to SA-conditioned EHA rods.

Our model system provided a surface to examine biofilm formation. The adherence of *S. mutans* to the surface diminished following conditioning of the EHA with protein. The greatest decrease in adherence was observed following conditioning of EHA with saliva. This decrease suggested that while saliva possesses proteins capable of mediating specific interactions with bacteria resulting in irreversible adherence, saliva may also play a protective role by limiting non-specific bacterial adherence to enamel. By conditioning EHA with SA we provided a specific system for adherence (SA-P1 interaction) of *S. mutans* to the EHA that would be useful in detachment experiments.

Detachment of adherent *S. mutans* NG8 from the model biofilms.

Detachment mediated by endogenous enzymatic activity.

Detachment experiments were initially performed with biofilms formed on saliva-conditioned EHA rods. Detachment was assayed as a function of pH and temperature. Following biofilm formation, individual rods were placed in culture tubes containing 2 mL of RCB adjusted to pH's ranging from 4.5 - 7.5 for 30 minutes. Detachment from biofilms took on a characteristic bell shape curve with a maximum detachment at pH 5.5 -6.0 (Fig. 14A). The effect of the pH of the medium on the viability of cells during this incubation was found to

Figure 13. Effect of SA concentration on the accumulation of *S. mutans* NG8 (■) and its P1 deficient mutant 834 (□) on EHA rods. EHA rods were conditioned for 15 minutes in the SA solutions and biofilms were formed. Results shown are the average of two rods ± SD.

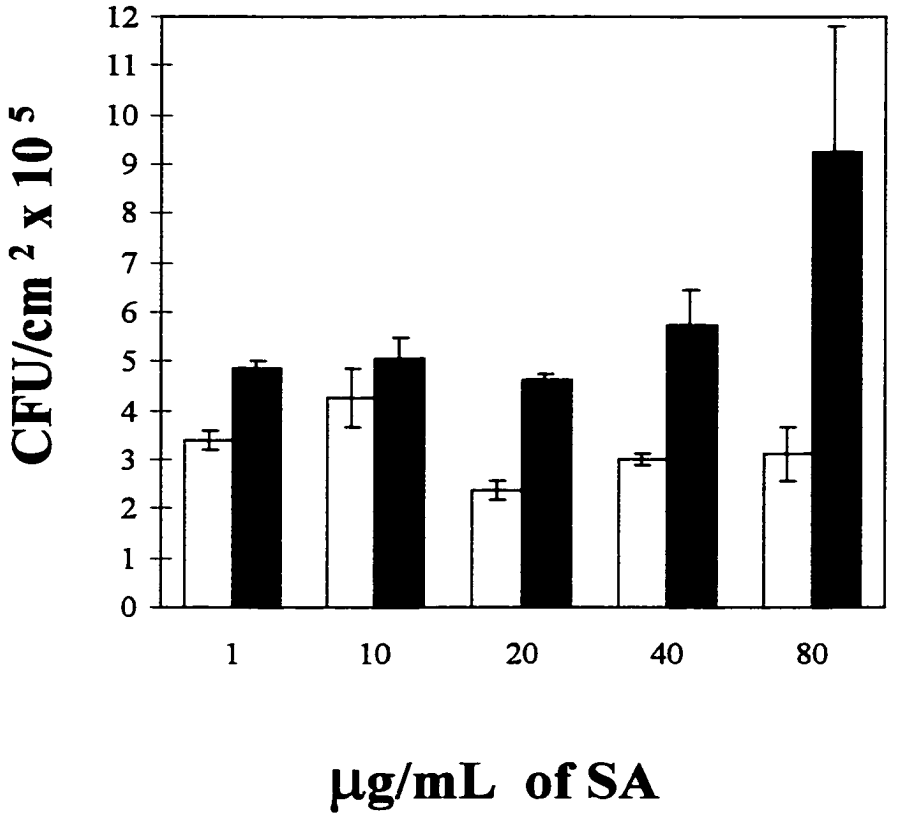
CFU/cm 2 x 10 5
12
11
10
9
8
7
6
5
4
3
2
1
0
1
10
20
40
80
µg/mL of SA

Figure 14. Effects of pH at 37°C (A) or temperature at pH 6.0 (B) on the detachment of *S. mutans* NG8 from saliva-conditioned EHA. Results shown are the average of two rods ± SD.

A

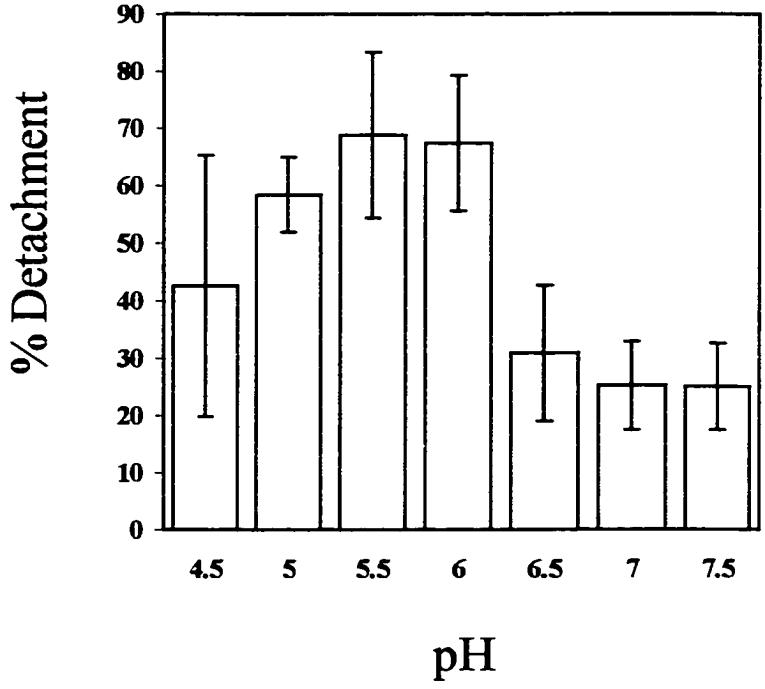
% Detachment
90
80
70
60
50
40
30
20
10
0
4.5
5
5.5
6
6.5
7
7.5
pH

B

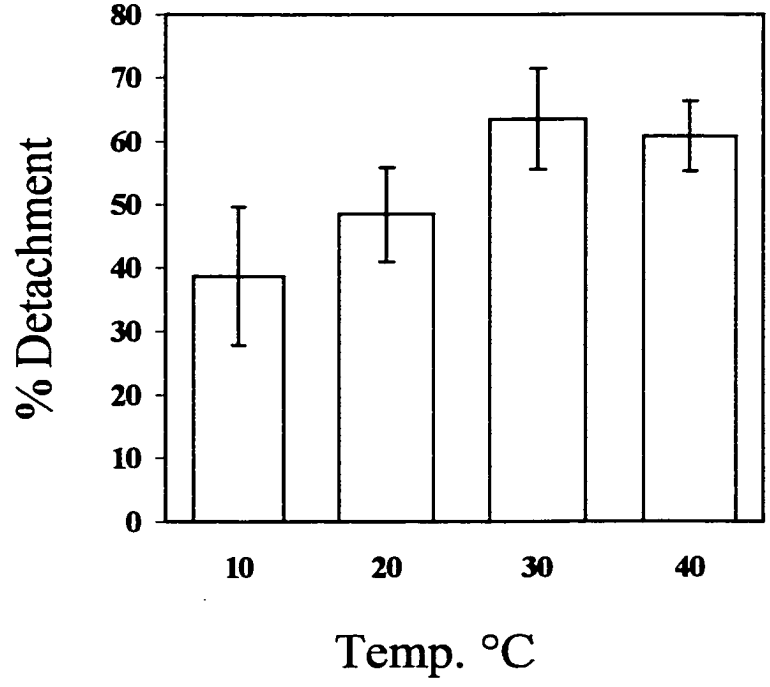
% Detachment
80
70
60
50
40
30
20
10
0
10
20
30
40
Temp. °C

be negligible. At pH 6.0, detachment of cells from biofilms was also found to be temperature-dependent (Fig. 14B). The influence of temperature and pH on detachment suggests that detachment may be an active enzyme-mediated process (121).

Detachment mediated by an exogenous SPRE enzyme preparation.

To further support the notion of enzymatic detachment, SPRE was prepared from the mutant 834 and used to detach *S. mutans* cells adhering to SA-conditioned EHA surfaces. Mutant 834 was used as the source of SPRE simply to eliminate the addition of exogenous P1 to the system. The extent of detachment responded to increasing quantities of the crude SPRE preparation in a dose-dependent fashion (Fig. 15A). Incrementally increasing the amount of SPRE added from 10 to 88 μg/mL resulted in an increase in the detachment of biofilm cells. The addition of more than 88 μg/mL SPRE did not result in significant increases in the detachment of cells from biofilms. The detachment activity of the SPRE preparation could be inactivated by pretreatment of the SPRE with pronase followed by boiling (20 minutes). Boiling was necessary to inactivate the pronase whose protease activity may have induced detach of biofilm cells. As shown in Figure 15B, live enzyme induced a detachment which was significantly higher than that induced by pronase-treated SPRE, BSA, and the buffer control ($p<0.05$). The detachment induced by the pronase-treated SPRE was not significantly different from the BSA and buffer controls ($p >0.2$). Inability of BSA, buffer control, or the pronase treated enzyme to induce detachment ruled out the possibility that detachment resulted from the addition of protein or salt derived from the SPRE preparation added to the RCB during the detachment experiments.

The above results strongly suggest that detachment is an active enzyme mediated process warranting further investigation.

Figure 15. Detachment of *S. mutans* NG8 cells adhered to SA-conditioned EHA as a function of exogenously supplied SPRE (A). Detachment of adherent *S. mutans* NG8 cells in the presence of active SPRE (Enzyme, 200 μg/mL), pronase-inactivated SPRE (1 mg/mL pronase, 37°C, 1 h), BSA (200 μg/mL), or buffer control (PEMPP) (B).

A

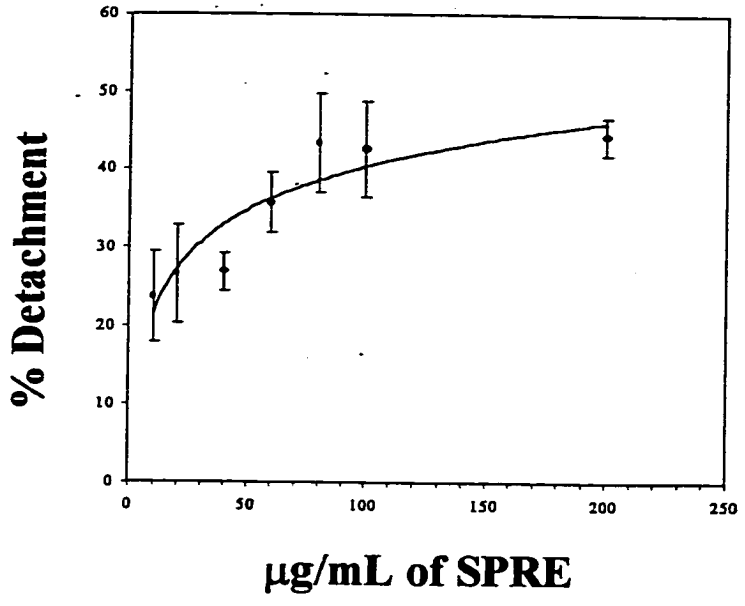
% Detachment
60
50
40
30
20
10
0
0
50
100
150
200
250
µg/mL of SPRE

B

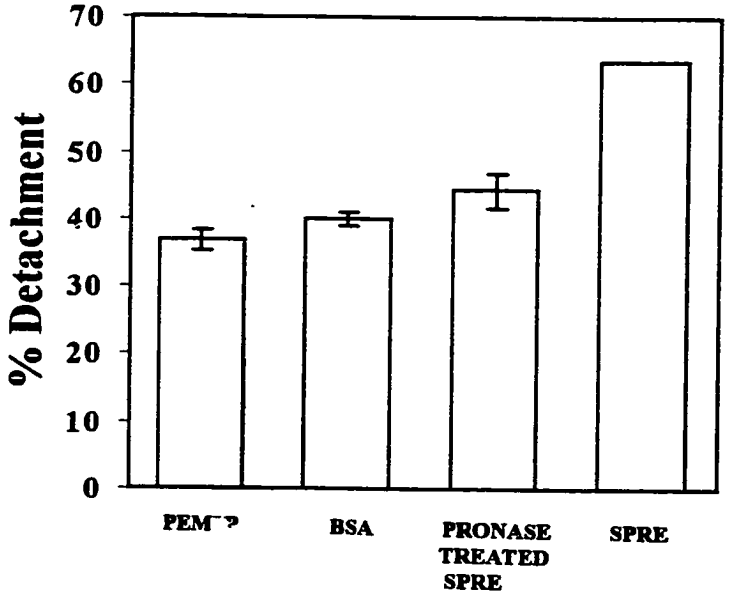
% Detachment
70
60
50
40
30
20
10
0
PEM
BSA
PRONASE TREATED SPRE
SPRE

Isolation of "detachment - defective" mutants by Tn*917* mutagenesis.

Isolation and preliminary characterization of mutant A and E.

To further confirm that detachment was enzyme-mediated and to isolate genes affecting or controlling detachment, putative SPRE-defective mutants were generated by Tn*917* mutagenesis. Transposon mutants were produced by delivering Tn*917* into *S. mutans* JH1005 on pTV1-OK. *S. mutans* JH1005, not strain NG8, was used due to the low transposition frequencies observed in *S. mutans* NG8. Following transposition, 3600 colonies were patched to THYE plates containing Kan or Em, from which 1039 Kan^S Em^R colonies were obtained. These Kan^S Em^R mutants were screened for an increase in cell-associated P1 by whole-cell ELISA. The assumption is that a higher amount of P1 on cells is an indication of a deficiency in SPRE and, therefore, detachment-defective. Two mutants, A and E, that gave consistently higher A_{405} readings (0.1) than the parent strain JH1005 were identified.

The effect of the transposon insertions on the growth of the mutants was found to be very slight (Fig. 16). The only apparent difference was a slightly increased (30 minutes) lag phase for mutant A and E.

Southern hybridization using Tn*917* as the probe demonstrated the insertion of Tn*917* into the chromosome of mutants A and E (Fig. 17). The probe hybridized to a single *Eco*RI fragment of 8.5 and 7.4 kb from DNA of mutant A and E, respectively, but it did not hybridize with the JH1005 DNA. The probe also hybridized to 2.5 kb and 7.4 kb *Hin*dIII fragments from mutants A and E DNA, respectively, in addition to a common 1.2 kb band. This common 1.2 kb fragment appeared to be the same 1.2 kb internal *Hin*dIII fragment in Tn*917* (Fig. 4). These results suggest that mutants A and E each carries a single and distinct Tn*917* insertion within the chromosome.

Figure 16. Growth of *S. mutans* JH1005 (▲), mutant A (◆), and mutant E (■) in Todd-Hewitt broth. Overnight cultures were used to inoculate prewarmed THB (1:25) and growth was monitored by measuring the OD_{600nm} at hourly intervals.

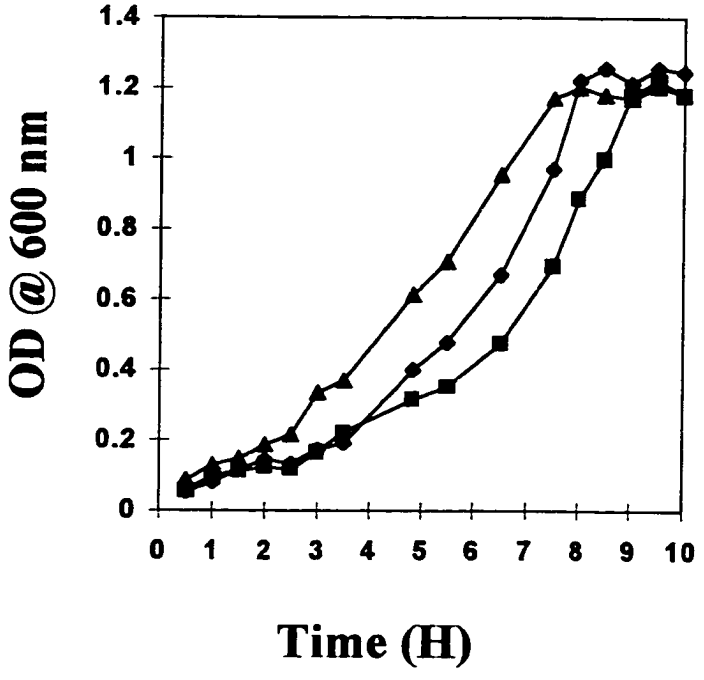
OD @ 600 nm
1.4
1.2
1
0.8
0.6
0.4
0.2
0
0 1 2 3 4 5 6 7 8 9 10
Time (H)

Figure 17. Southern blot analysis of chromosomal DNA from *S. mutans* JH1005 (lane 3), mutant A (lane 1), and mutant E (lane 2). C: *Kpn*I digest of pTV1-OK. E: 5 μg of *Eco*RI digested DNA. H: 5 μg of *Hind*III digested DNA. The probe was ^{32}P-labeled DNA obtained by random priming of the 4 Kb *Kpn*I fragment of pTV1-OK containing Tn*917* (Fig. 2).

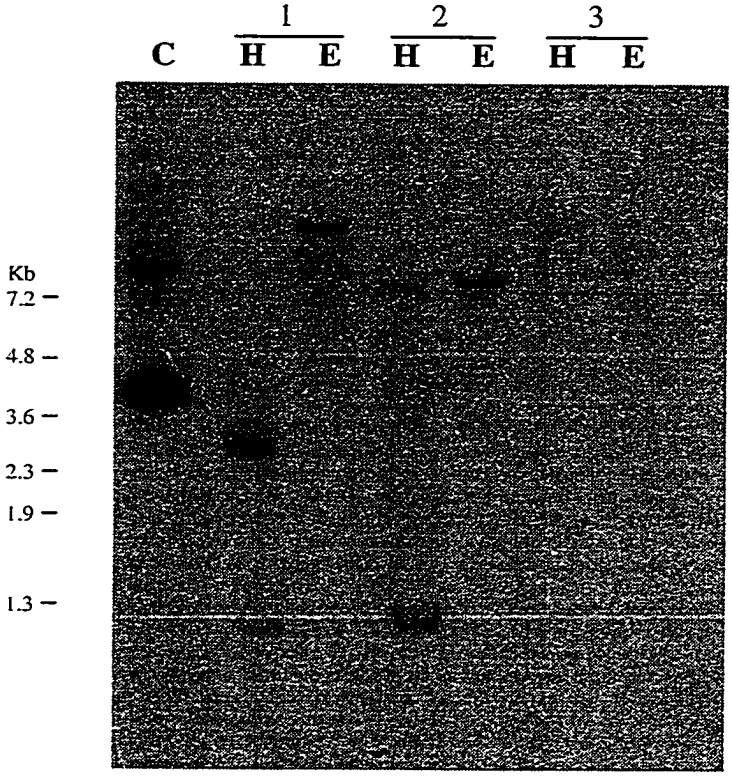
1
2
3
C
H
E
H
E
H
E
Kb
7.2
4.8
3.6
2.3
1.9
1.3

When the mutants were analyzed for their ability to release surface proteins, they were found to release comparable amounts of low molecular weight proteins, but much fewer high molecular weight proteins than the wild type (Fig. 18A). Western blotting showed that P1 was released by the wild type, but was released to a much lesser extent or at undetectable levels by mutant E and mutant A, respectively (Fig. 18B). Figure 18C showed that the mutanolysin extracts prepared from mutants A and E contained an immuno-reactive band of approximately 185 kDa indicating that P1 was produced in its full length form by the mutants. The P1 band was slightly less intense in the mutant A extract than in the mutant E and wild type extracts. This observation may be explained by the incomplete action of mutanolysin on mutant A cells.

Impaired detachment ability of mutant A and E.

To determine if decreased release of surface proteins translated into decreased detachment of cells from surfaces, detachment of wild type JH1005, mutant A, and mutant E from SA-conditioned EHA (80 μg/mL) was quantified (Fig. 19). While there was no difference in the number of cells accumulated on the surface (ca. 3.5×10^5 CFU/cm^2), a difference in the degree of detachment between the mutants and JH1005 was noted. After 60 minutes incubation at pH 6, mutant A gave a 20.9 ± 2.9 % detachment which is significantly lower than that by JH1005 (36.5 ± 2.5 %) and mutant E (30.5 ± 5.5%) ($p=0.05$). The difference in % detachment between JH1005 and mutant E was not statistically significant ($p>0.2$).

SPRE from mutant A and JH1005 was prepared and used to detach adherent *S. mutans* NG8 cells from SA-conditioned EHA rods (Fig. 20). Mutant A SPRE induced a 37.8 ± 0.2% detachment which was significantly lower than the 50.9 ± 4.9% detachment induced by the JH1005 SPRE ($p<0.05$) and is similar to the detachment induced by

Figure 18. SDS-PAGE and western immunoblotting of proteins released from *S. mutans* JH1005, mutants A and E. Panel A: a silver stained SDS-PAGE gel (7.5%) of the proteins obtained by the surface -protein releasing assay. Each lane consists of 15 μl from the 200 μl released proteins. Panel B: a western blot of the same proteins as in panel A using a rabbit polyclonal anti-P1 antibody (1/2000; Lee, (121)). Panel C: a western blot of mutanolysin extracts (83) from the cells using the same anti-P1 antibody. Lanes 1, mutant A; 2, mutant E; and 3, JH1005.

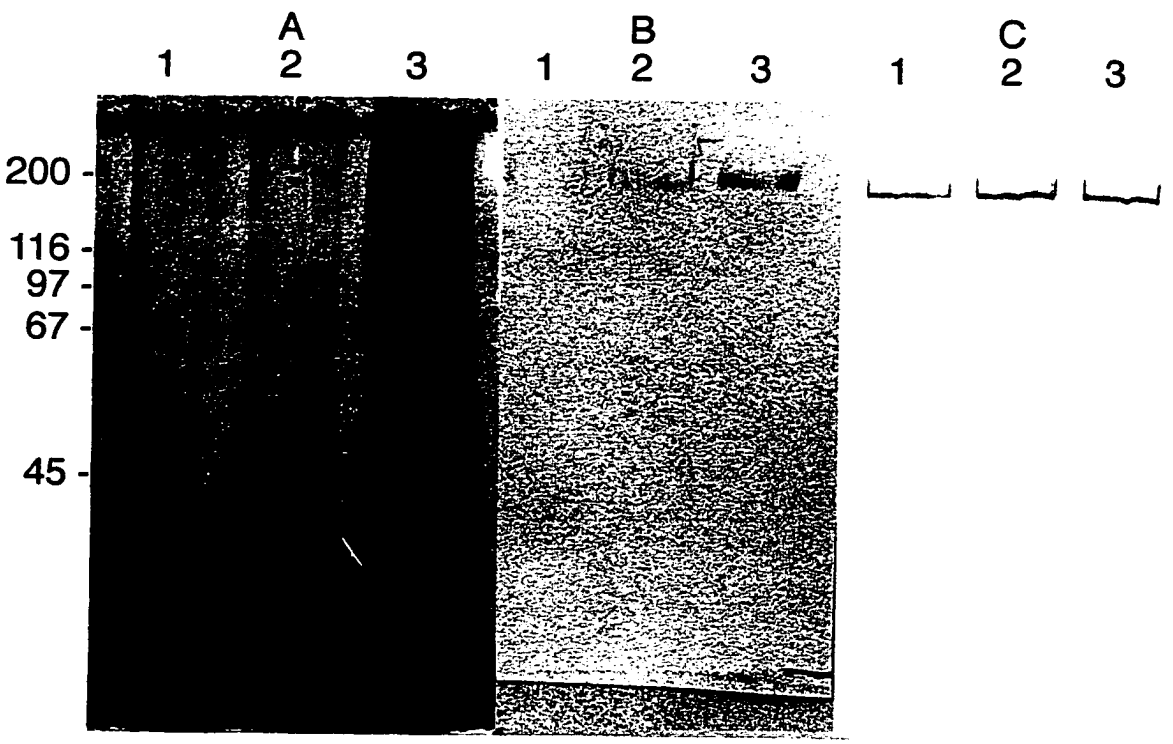
A
B
C
1
2
3
1
2
3
1
2
3
200
116
97
67
45

Figure 19. Detachment of *S. mutans* JH1005, mutant A, and mutant E from biofilms formed on SA-conditioned (80 μg/mL) EHA rods. Cells were allowed to detach for 60 minutes in RCB at pH 6.0, in the absence exogenously supplied SPRE.

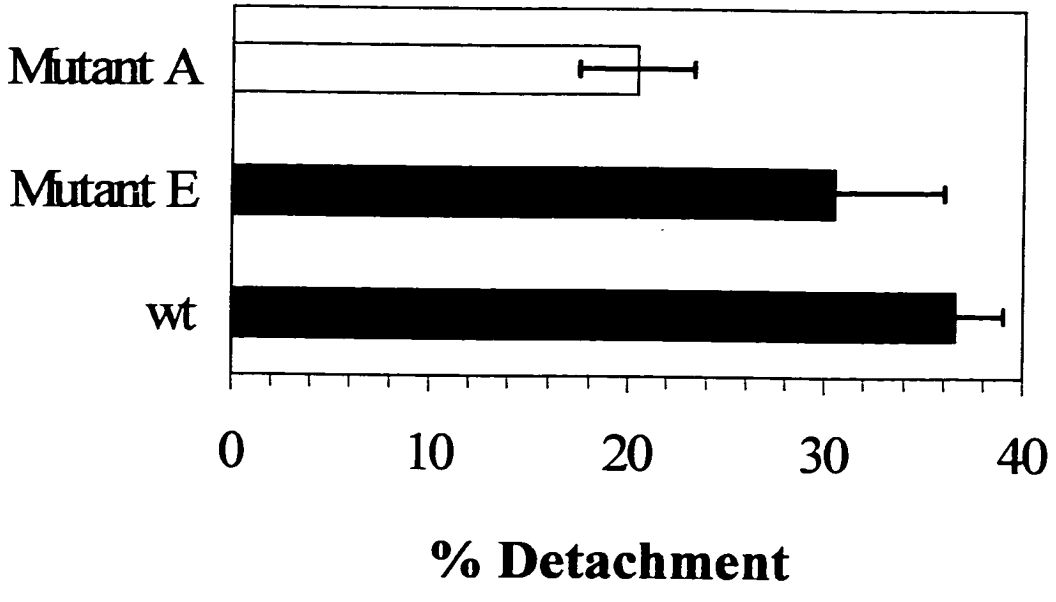
Mutant A
Mutant E
wt
0
10
20
30
40
% Detachment

Figure 20. Detachment of *S. mutans* NG8 from biofilms with exogenously supplied SPRE. Biofilms were formed on SA-conditioned (80 μg/mL) EHA rods. Following biofilm formation, crude SPRE preparation (200 μg/mL) from mutant A, the wild type JH1005, or PEMPP (buffer control) was applied to biofilms. Detachment was allowed to proceed for 60 minutes in RCB at pH 6.0.

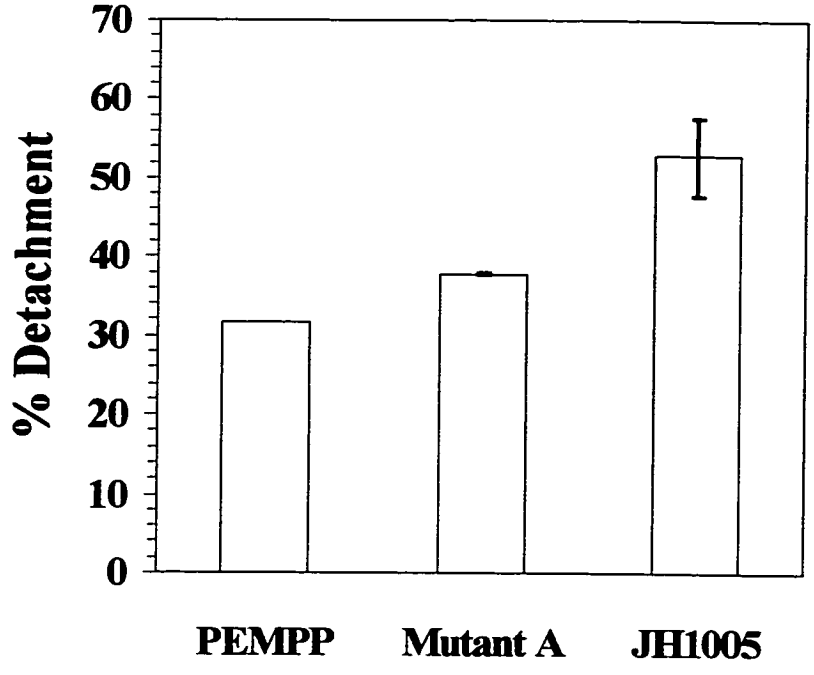
70
60
50
40
30
20
10
0
% Detachment
PEMPP
Mutant A
JH1005

PEMPP, the buffer control (SPRE was extracted from the membranes of mutant A and the wild type using PEMPP).

Collectively, the decreased release of surface proteins and the impaired detachment of mutant A suggest that transposon inserted into a locus required for SPRE activity.

Genetic characterization of the putative "SPRE - negative" mutant A.

Identification of the Tn*917* insertion site.

Phenotypic data demonstrated mutant A may be "SPRE - negative," further characterization of mutant A would require identification of the genetic locus disrupted by Tn*917*. Results from an aforementioned Southern blot (Fig. 17) of mutant A chromosomal DNA probed with a radiolabeled fragment of pTV1-OK highlighted two *Hind*III bands of approximately 2.5 and 1.2 kb. The latter is an internal Tn*917* *Hind*III fragment, while the 2.5 kb band is likely comprised of transposon and chromosomal sequences. Hence, mutant A DNA was digested with *Hind*III and DNA fragments of about 2.5 kb were recovered from an agarose gel and cloned into *E. coli* XL-1 Blue using pBluescript as the vector. Transformants (330 clones) were screened by colony hybridization using a 1.5 kb probe specific to the 3' end of Tn*917* (Fig. 4). Eleven positive colonies were identified. Of these, nine positives were verified to contain a 3.0 kb *Hind*III insert which hybridized to the 1.5 kb probe of the 3' end of Tn*917* following Southern hybridization. One positive clone (NV4) was chosen for further analysis. The plasmid pNV4 harboured by this clone had a 2.9 kb insert comprised of 1 kb of Tn*917* sequence followed by a 1.9 kb of chromosomal DNA (Fig. 21). The insert was sequenced and the transposon insertion junction between the 3' end of Tn*917* and the chromosomal

Figure 21. Physical map of pNV4, the plasmid containing a fragment of chromosomal DNA from *S. mutans* mutant A containing Tn*917* and chromosomal DNA sequence.

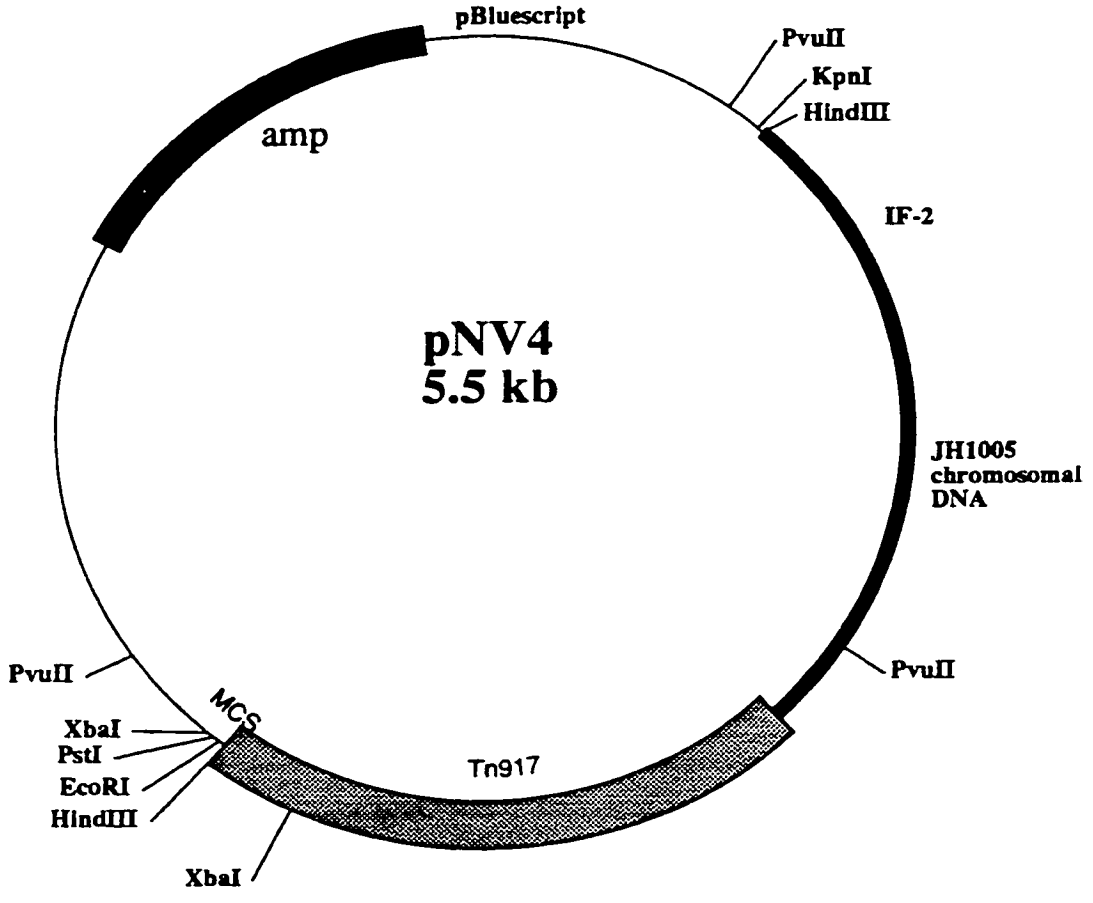
pBluescript
PvuII
KpnI
HindIII
amp
IF-2
pNV4
5.5 kb
JH1005
chromosomal
DNA
PvuII
PvuII
MCS
XbaI
PstI
EcoRI
HindIII
Tn917
XbaI

DNA was identified (see below, Fig. 28). No open reading frames (ORFs) were identified on the chromosomal DNA immediately adjacent to the 3' end of the Tn*917*; however, an ORF with homology to translational initiation factor two (IF-2) was found at the distal end of the chromosomal DNA (Fig. 21). Subsequent cloning and sequencing of the locus from the wild type JH1005 (see below), revealed the transposon had inserted into an AT rich region just upstream of the -35 region of an open reading frame later identified as *copY*, a negative regulator of the *cop* operon (Fig. 28).

Cloning of the *cop* operon adjacent to the Tn*917* insertion site.

To identify the 1.9 kb mutant A DNA in the wild-type JH1005 chromosome, pNV4 was labeled and used as a probe in Southern hybridization. The blotting demonstrated the probe hybridized to a 11 kb *Bam*HI fragment, an approximately 12 kb *Eco*RI, a 2.5 kb *Hin*dIII fragment, and a 7.5 kb *Xba*I fragment from the respective digests of JH1005 DNA (Fig. 22). Since the *Hind*III fragment was smaller in size and should be easier to clone than the other fragments, a partial-library was constructed with 2 - 5 kb *Hind*III fragments. Two putative colonies (NVD20 and F9) were identified following screening of the partial-library by colony hybridization. Southern blotting verified these two clones carried an insert of 2.5 kb (Fig. 23). Clone NVD20 was chosen for further study. DNA sequencing revealed the insert on pNVD20 was identical to that on pNV4 and it possessed an additional 400 bp DNA. A promoter and a truncated open reading frame were identified in this 400 bp sequence.

The remainder of this ORF and downstream genes, which formed the *cop* operon, were subsequently cloned in three overlapping fragments. Screening a partial library prepared from 3 to 6 kb partial *Hind*III fragments of JH1005 chromosomal DNA yielded a positive clone (WH4). The plasmid harbored by WH4 contained a 4 kb insert

Figure 22. Identification of DNA fragments adjacent to the Tn*917* insertion site by Southern hybridization. *S. mutans* JH1005 chromosomal DNA was digested with *Bam*HI (lane 2), *Eco*RI (lane 3), *Hind*III (lane 4) or *Xba*I (lane 5) and probed with the insert of pNV4 which was ^{32}P-labeled DNA by random priming. Lane 1, *Hind*III digested pNV4.

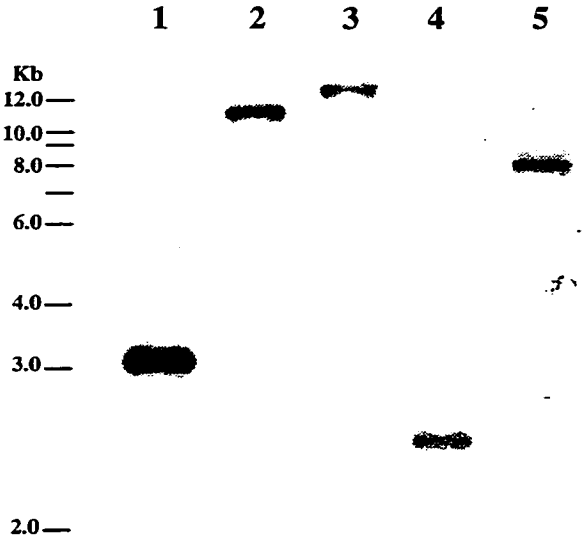
1
2
3
4
5
Kb
12.0
10.0
8.0
6.0
4.0
3.0
2.0

Figure 23. Southern hybridization of plasmid DNA from clones NVD20 (lane 1) and F9 (lane 2). DNA was digested with *Hind*III and *Sac*I and probed with the ^{32}P-labeled insert of pNV4. Lane 3, *Hind*III, *Sca*I digest of pNV4.

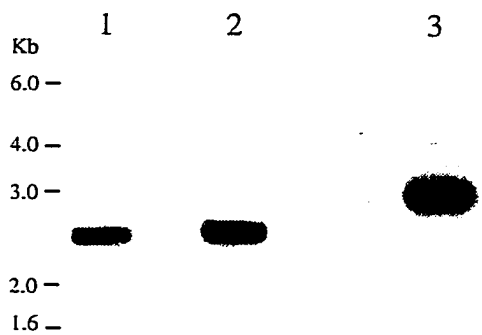
1
2
3
Kb
6.0
4.0
3.0
2.0
1.6

carrying the same 2.5 kb *Hin*dIII insert of pNVD20 as evidenced by Southern blotting and an additional 1.5 kb *Hin*dIII DNA fragment (Fig. 24). Sequencing the insert on pWH4 identified the remainder of the truncated ORF of pNVD20 and part of a second ORF. Probing *Hinc*II digested chromosomal DNA with the 1.5 kb *Hin*dIII fragment identified two bands at 1.3 and 1.4 kb (Fig. 25). The 1.3 kb band was an internal fragment within pWH4 while the 1.4 kb band contained an additional 0.6 kb of chromosomal DNA. The 1.4 kb fragment was cloned in pUC18 yielding pNV5. Sequencing the insert on pNV5 provided the remainder of the second ORF of pWH4 and the beginning of a third. The final fragment of chromosomal DNA comprising the operon was identified by searching the partial genome sequence of *S. mutans* UAB159. The sequence facilitated the design of PCR primers to amplify and clone the final fragment of *S. mutans* JH1005 chromosomal DNA to make the plasmid pNV46, as outlined in the Materials and Methods. In addition to the sequence overlapping pNV5, the amplicon encoded the second half of the third ORF followed by a factor-independent terminator.

The genetic organization of the entire *cop* operon and a map of the overlapping fragments cloned into the various plasmids are depicted in Figure 26. The overlapping nature of the clones allowed the operon to be reconstructed easily on a single plasmid pNV7 (Fig. 27).

Analysis of the nucleotide and amino acid sequence of the *cop* operon.

From the DNA sequence of the inserts carried by pNVD20, pWH4, pNV5, and pNV46, three putative ORFs encoding proteins of 147, 743, and 66 amino acids were identified (Fig. 28). The sequence contained a single promoter, which was found upstream of the first ORF, each ORF was preceded by a Shine-Dalgarno sequence, and a factor-independent terminator was located approximately 100 bp downstream of the stop

Figure 24. An agarose gel (A) and a Southern blot of *Hind*III digested pWH4 (B). Lane M, 1 kb ladder; lane 1, pWH4. The blot was probed with a 0.8 kb *Pst*I fragment of the insert of pNV4 which was ^{32}P-labeled by random priming.

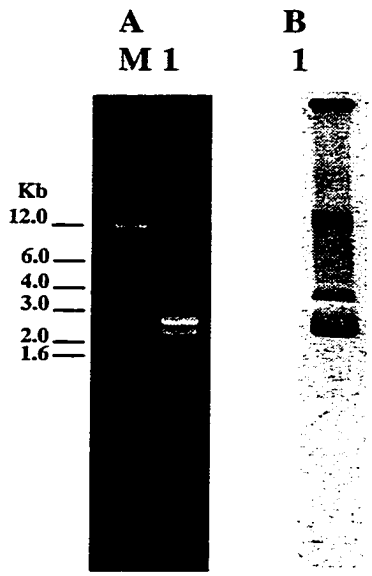
A
M 1
B
1
Kb
12.0
6.0
4.0
3.0
2.0
1.6

Figure 25. Southern blotting of *S. mutans* JH1005 to identify the final ORF of the *cop* operon. Lane 1, *Hind*III digested pWH4.4; Lane 2, 5 μg of *S. mutans* JH1005 chromosomal DNA digested with *Hinc*II probed with biotin-labeled pWH4 (Bio-Nick labeling kit, GIBCO/BRL).

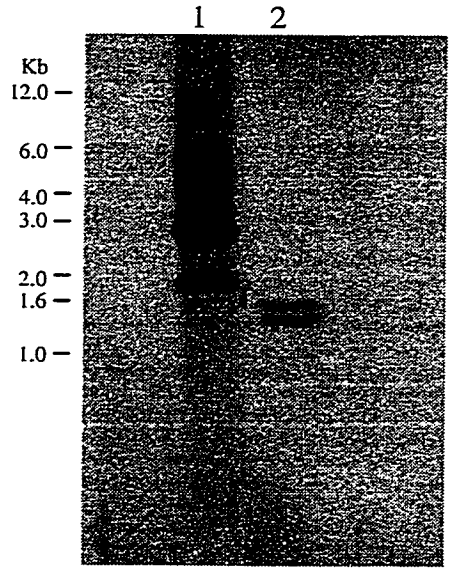
1
2
Kb
12.0
6.0
4.0
3.0
2.0
1.6
1.0

Figure 26. The genetic organization of the *S. mutans* JH1005 *cop* operon, the three open reading frames *copYBZ* are indicated. The positions of relevant restriction sites are shown; (B) *Bam*HI, (E) *Eco*RI, (H) *Hind*III, (Hc) *Hinc*II, (P) *Pst*I, and (X) *Xba*I. Below the operon are drawings depicting the cloned *cop* fragments carried by the different plasmids constructed in this study.

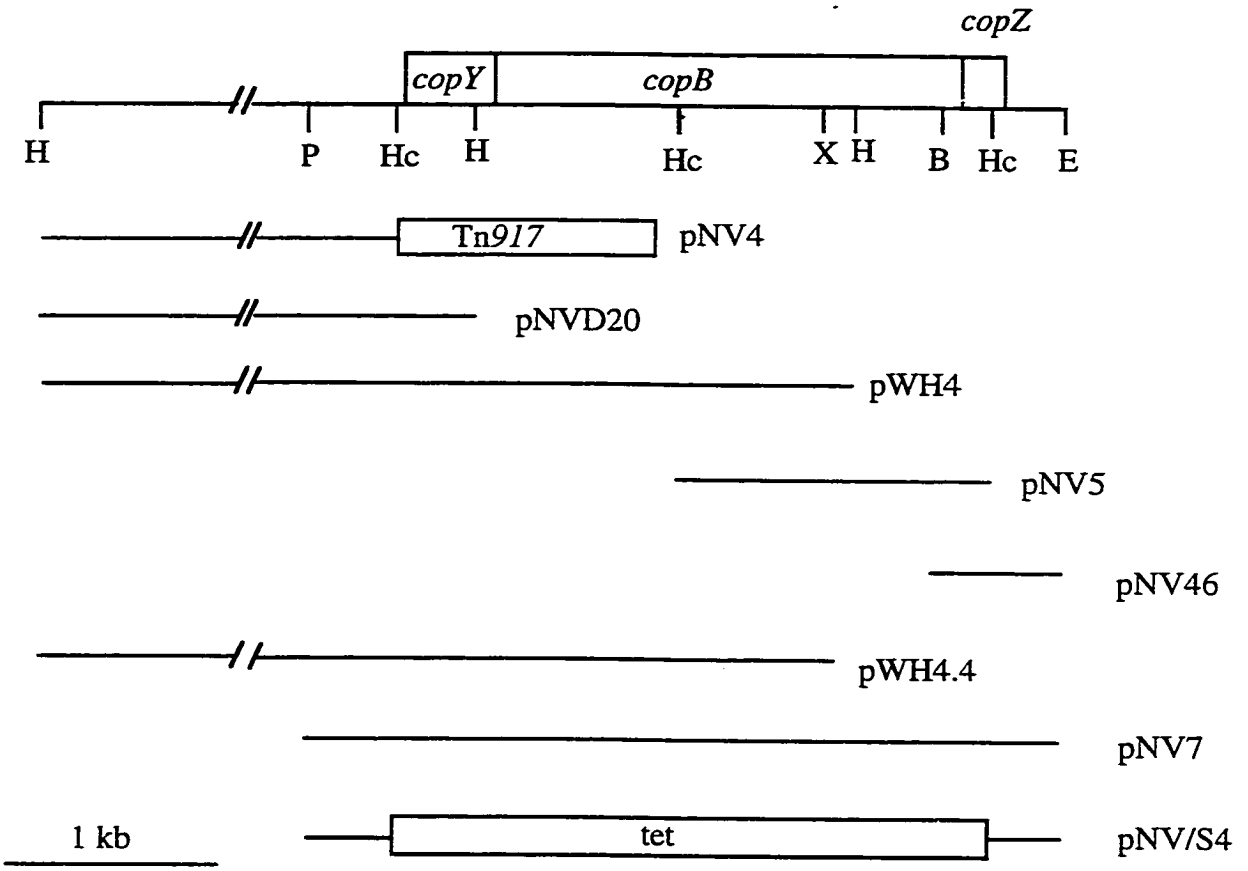
copZ
copY
copB
H
P
Hc
H
Hc
X
H
B
Hc
E
Tn917
pNV4
pNVD20
pWH4
pNV5
pNV46
pWH4.4
pNV7
1 kb
tet
pNV/S4

Figure 27. Flowchart outlining the reconstruction of the entire *cop* operon. The entire *cop* operon was reconstructed from the cloned DNA fragments. A 2.5 kb *Pst*I - *Xba*I fragment from pWH4 containing upstream sequences, the promoter, *copY* and part of *copB* was cloned into pNV5 which had been cut with the same enzymes. The resultant plasmid, pNV6, carried on it all but the last half of *copZ*. The second half of *copZ* contained within a 0.5 kb *Bam*HI - *Eco*RI fragment was isolated from pNV46 and ligated into pNV6 cut with the same enzymes. The new plasmid, pNV7, consisted of 450 bp of sequence upstream of *copY*, the 2.9 kb operon and 280 bp of sequence downstream of the stop codon of *copZ*.

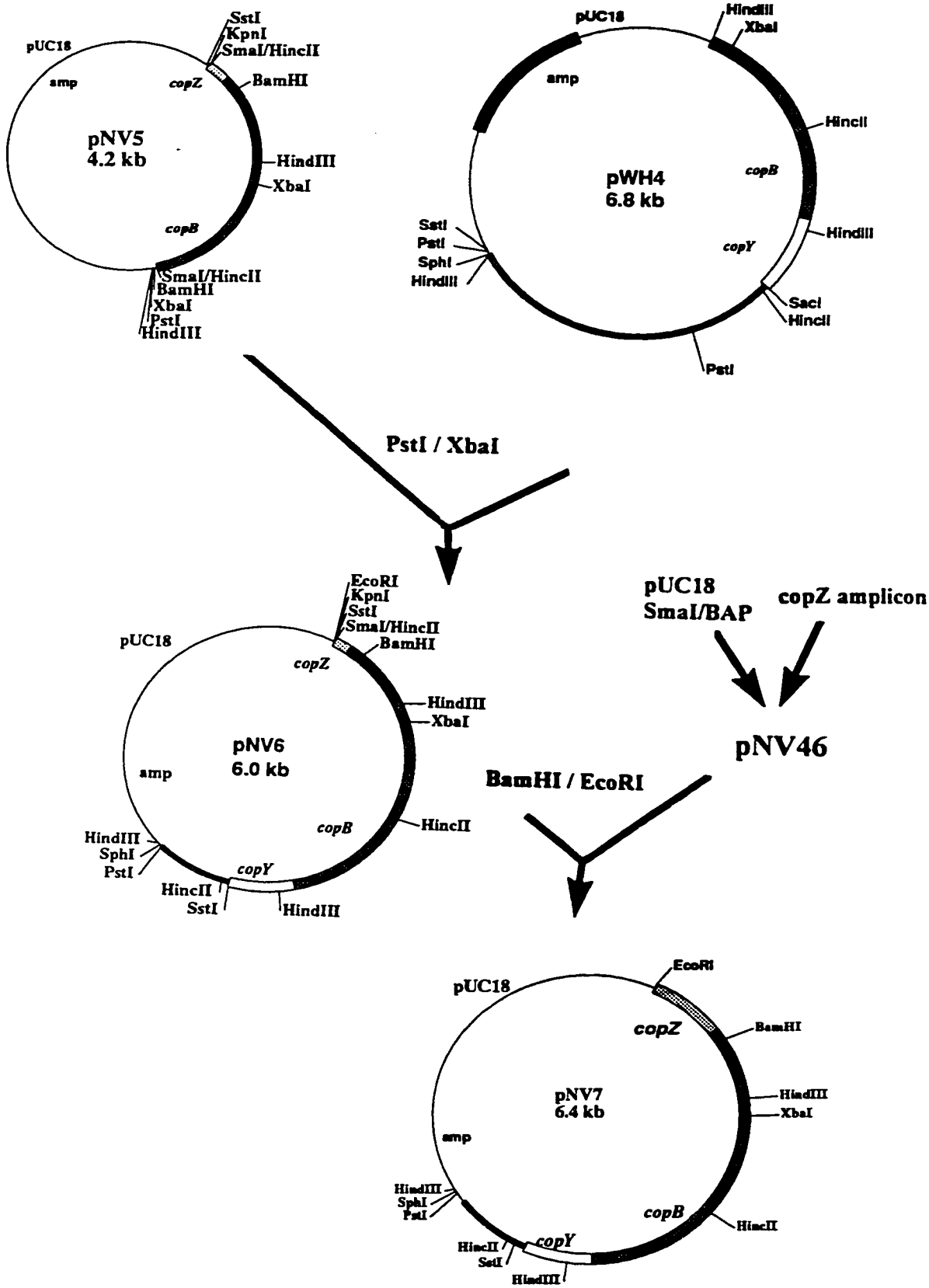
pUC18
SstI
KpnI
SmaI/HincII
amp
copZ
BamHI
pNV5
4.2 kb
HindIII
XbaI
copB
SmaI/HincII
BamHI
XbaI
PstI
HindIII
pUC18
HindIII
XbaI
amp
HincII
pWH4
6.8 kb
copB
HindIII
copY
SacI
HincII
PstI
SstI
PstI
SphI
HindIII
PstI / XbaI
pUC18
SmaI/BAP
copZ amplicon
pNV46
EcoRI
KpnI
SstI
SmaI/HincII
BamHI
pUC18
copZ
HindIII
XbaI
pNV6
6.0 kb
amp
copB
HincII
HindIII
SphI
PstI
copY
HincII
SstI
HindIII
BamHI / EcoRI
EcoRI
pUC18
copZ
BamHI
HindIII
XbaI
pNV7
6.4 kb
amp
copB
HincII
HindIII
SphI
PstI
copY
HincII
SstI
HindIII

Figure 28. DNA and the deduced amino acid sequence of the *cop* operon and the open reading frames, respectively. In the nucleotide sequence the position of the transposon insertion is indicated by a vertical arrow head, the inverted repeats are represented by the horizontal arrows above and below the sequence the -35, -10 region, the Shine-Dalgarno (SD) sequences and the terminator are in bold face. In the amino acid sequence the conserved functionally important residues are in bold face. The eight predicted transmembrane helicies (TM) are labeled and underlined.

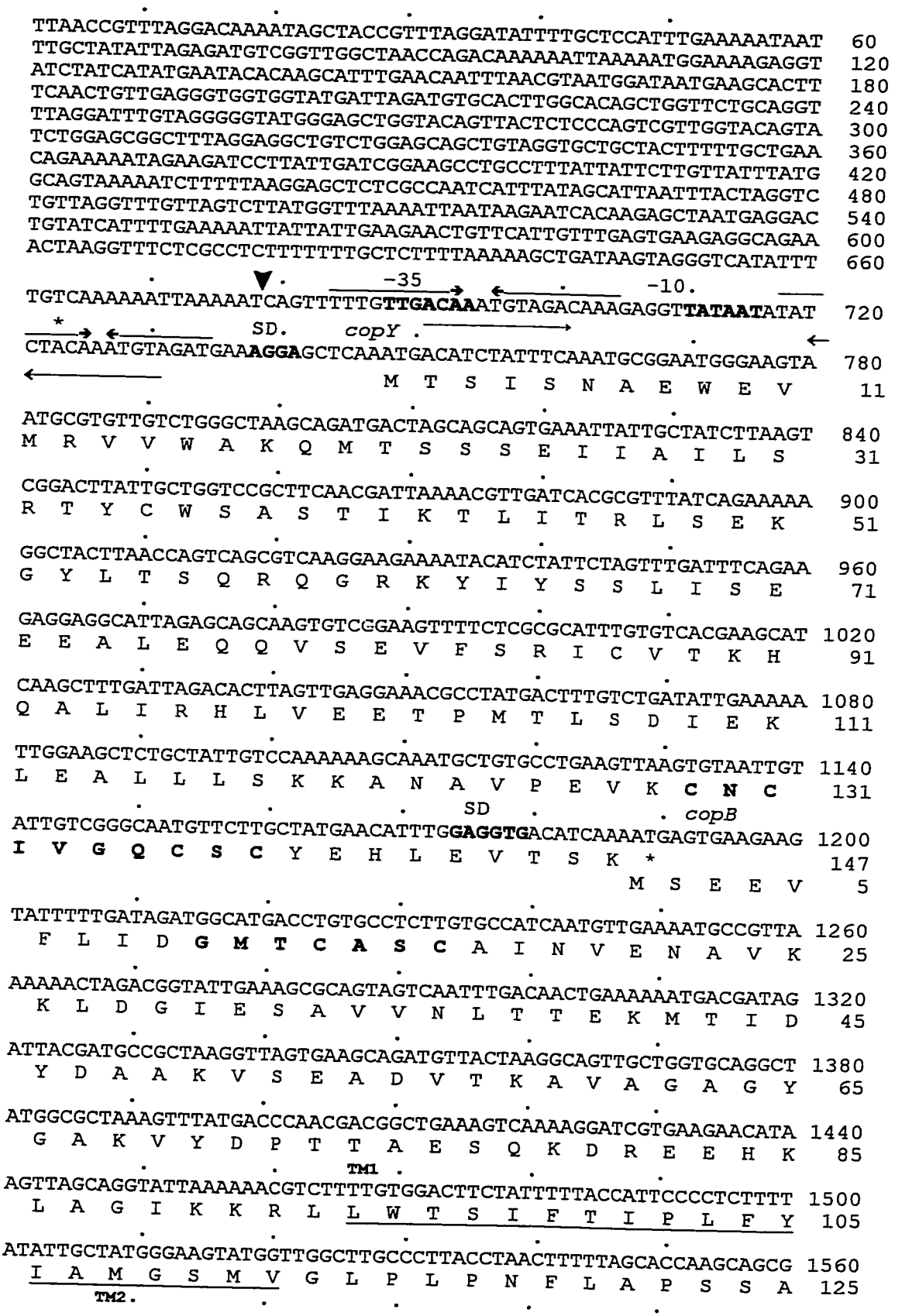
-35
-10.
SD.
copY
SD
copB
TM1
TM2.

```
CTCCGCTCACTTATGCGATGGTTTTGCTTCTTTTGACAATTCCGGTTATCGTGTTAAGTT 1620
  P  L  T  Y  A  M  V  L  L  L  L  T  I  P  V  I  V  L  S  W  145

                                                        TM3
GGAGCTTCTATGACAATGGTTTTAGATCGCTTTTTAAAGGTCATCCTAATATGGACTCAT 1680
  S  F  Y  D  N  G  F  R  S  L  F  K  G  H  P  N  M  D  S  L  165

TAGTGTCCTTAGCAACAACAGCGGCGTTTCTTTACAGTCTTTATGGAACTTACCATGTTT 1740
  V  S  L  A  T  T  A  A  F  L  Y  S  L  Y  G  T  Y  H  V  Y  185

                TM4.
ACTTGGGACATACACATCATGCTCACCATCTCTATTATGAATCGGTAGCTGTTATTTTAA 1800
  L  G  H  T  H  H  A  H  H  L  Y  Y  E  S  V  A  V  I  L  T  205

CTCTCATTACTTTAGGGAAATACTTTGAAACCCTATCGAAAGGTCGAACCTCAGATGCGA 1860
  L  I  T  L  G  K  Y  F  E  T  L  S  K  G  R  T  S  D  A  I  225

TAAAAAAATTAATGCATTTGTCTGCTAAAGAGGCTACTCTGATACGTGATGGCGAGGAGA 1920
  K  K  L  M  H  L  S  A  K  E  A  T  L  I  R  D  G  E  E  I  245

TTAAGGTTCCTATTGAGCAAGTGCAAATCAGAGATCAAATTTTAGTCAAACCCGGTGAAA 1980
  K  V  P  I  E  Q  V  Q  I  R  D  Q  I  L  V  K  P  G  E  K  265

AAATACCTGTGGATGGTCGAGTCCTGTCAGGGCATTCTGCTATTGATGAATCCATGTTAA 2040
  I  P  V  D  G  R  V  L  S  G  H  S  A  I  D  E  S  M  L  T  285

CAGGAGAATCTATTCCTATTGAAAAAATGGCGGATAGCCCTGTTTATGCCGGGTCAATCA 2100
  G  E  S  I  P  I  E  K  M  A  D  S  P  V  Y  A  G  S  I  N  305

ATGGTCAGGGAAGTCTGACTTTTGAGGCTGAAAAAGTTGGCAATGAAACCTTGCTTTCAC 2160
  G  Q  G  S  L  T  F  E  A  E  K  V  G  N  E  T  L  L  S  Q  325

AAATTATTAAATTGGTTGAGAACGCTCAGCAAACTAAGGCACCCATTGCCAAGATTGCTG 2220
  I  I  K  L  V  E  N  A  Q  Q  T  K  A  P  I  A  K  I  A  D  345

      TM5
ATAAGGTATCTGCTGTCTTTGTACCTGTTATTATAACGATTGCTATTTTGACTGGTCTCT 2280
  K  V  S  A  V  F  V  P  V  I  I  T  I  A  I  L  T  G  L  F  365

                                TM6.
TCTGGTATTTTGTCATGGGACAAGACTTTACCTTTTCAATGACAATCAGTGTCGCTGTTC 2340
  W  Y  F  V  M  G  Q  D  F  T  F  S  M  T  I  S  V  A  V  L  385

TTGTCATTGCCTGCCCTTGTGCTTTGGGTCTTGCAACGCCAACGGCTATTATGGTTGGTA 2400
  V  I  A  C  P  C  A  L  G  L  A  T  P  T  A  I  M  V  G  T  405

CAGGTCGTGCTGCTGAAAATGGAATCCTTTATAAACGTGGTGATGTCTTGGAATTGGCAC 2460
  G  R  A  A  E  N  G  I  L  Y  K  R  G  D  V  L  E  L  A  H  425

ATCAGATTAATACTATTGTTTTCGATAAAACAGGCACTATTACTCAAGGTAAACCAGAAG 2520
  Q  I  N  T  I  V  F  D  K  T  G  T  I  T  Q  G  K  P  E  V  445

TTGTTCATCAATTTTCTTATCATGATCGAACTGATTTAGTGCAAGTGACAGCTGCCTTAG 2580
  V  H  Q  F  S  Y  H  D  R  T  D  L  V  Q  V  T  A  A  L  E  465

AAGCATTATCTGAACATCCCCTTAGTCAGGCCATTGTTGATTATGCTAAAAAAGAAGGGA 2640
  A  L  S  E  H  P  L  S  Q  A  I  V  D  Y  A  K  K  E  G  T  485

CTCATTTACTTGCAGTGGATGACTTTACTTCTCTAACAGGGCTAGGACTGAAAGGTTGTG 2700
  H  L  L  A  V  D  D  F  T  S  L  T  G  L  G  L  K  G  C  V  505

TTGCTGATGAAACTTTGCTTGTTGGTAATGAAAAATTGATGCGTCAAGCTAATATCTCTC 2760
  A  D  E  T  L  L  V  G  N  E  K  L  M  R  Q  A  N  I  S  L  525
```

```
TAGAACAGGCTCAAGCAGATTTTAAGGCAGCAACAGCTCAGGGACAAACACCCATTTTTG 2820
  E  Q  A  Q  A  D  F  K  A  A  T  A  Q  G  Q  T  P  I  F  V  545

TTGCCAGTGATGGTCAATTGTTAGGACTGATTACGATTGCGGACAAGGTAAAGAATGACA 2880
  A  S  D  G  Q  L  L  G  L  I  T  I  A  D  K  V  K  N  D  S  565

GTGCAGCAACAGTTAAAGCTTTACAGAATATGGGGGTTGAAGTGGCCATGCTGACGGGTG 2940
  A  A  T  V  K  A  L  Q  N  M  G  V  E  V  A  M  L  T  G  D  585

ATAATGAAGAAACTGCGCAGGCTATTGCCAAAGAAGTGGGGATTACTTTTGTTATCAGTC 3000
  N  E  E  T  A  Q  A  I  A  K  E  V  G  I  T  F  V  I  S  Q  605

AAGTTTTCTCGCAGGAAAAAACACAGGCCATTCTTGATTTGCAGGCGGAAGGCAAGAAAG 3060
  V  F  S  Q  E  K  T  Q  A  I  L  D  L  Q  A  E  G  K  K  V  625

TTGCCATGGTTGGAGACGGTATTAATGACGCTCCGGCACTTGCGACAGCAGATATTGGCA 3120
  A  M  V  G  D  G  I  N  D  A  P  A  L  A  T  A  D  I  G  I  645

TTTCCATGGGCTCTGGAACAGATATTGCCATGGAGTCCGCGGATATTGTCTTGATGAAAC 3180
  S  M  G  S  G  T  D  I  A  M  E  S  A  D  I  V  L  M  K  P  665

CTGCAATGCTTGATATTATTAAGGCACTGAAAATTAGTCGTGTTACTATTATTAATATTA 3240
  A  M  L  D  I  I  K  A  L  K  I  S  R  V  T  I  I  N  I  K  685
                    TM7
AAGAAAATCTTTTCTGGGCATTTATTTATAATGTTCTGTCAGTTCCTATTGCTATGGGAG 3300
  E  N  L  F  W  A  F  I  Y  N  V  L  S  V  P  I  A  M  G  V  705
                                TM8
TACTTTATCTCTTTGGCGGACCTTTGCTGGATCCAATGATTGCTGGTCTAGCCATGAGCT 3360
  L  Y  L  F  G  G  P  L  L  D  P  M  I  A  G  L  A  M  S  F  725
                                                        SD
TTAGCTCTGTTTCTGTTGTTCTAAATGCCCTGCGTCTTAAAGTTGTAAAATTATAAAGGA 3420
  S  S  V  S  V  V  L  N  A  L  R  L  K  V  V  K  L  *        743
          copZ
GAATTATCATGGAAAAAACATATCATATTGATGGCTTAAAATGCCAAGGCTGCGCTGACA 3480
        M  E  K  T  Y  H  I  D  G  L  K  C  Q  G  C  A  D  N   17

ATGTCACCAAACGCTTTTCAGAATTAAAGAAAGTCAATGATGTCAAAGTTGACCTTGATA 3540
  V  T  K  R  F  S  E  L  K  K  V  N  D  V  K  V  D  L  D  K   37

AAAAAGAAGTCAGGATTACAGGAAATCCAAGCAAGTGGTCTCTTAAACGAGCACTGAAAG 3600
  K  E  V  R  I  T  G  N  P  S  K  W  S  L  K  R  A  L  K  G   57

GAACCAATTATGAATTGGGAGCAGAAATTTAAGTAGGCTTCATATACCTTAAAAACTGTA 3660
  T  N  Y  E  L  G  A  E  I  *                                  66
                                                  Terminator
AAGACACAGTTATTTCATTGCATCTTATCAGATGGTCACAAAGAGGGAGAAGACTGGGAA 3720

ACCAGTTTTTTTTCTGCTGTAAAATGAATTTATAGCATTGTCATAGTTATCTGTTTCAAT 3780

TATTGTAGAATATACAGAATTATAATAACTTGCTGTGCCAGTTTCCTTGATTTGTGATAC 3840

ACTAGATAGTGGAATGTTTTAGAAAAGGTTATATGATTATGGTTAAACTGATTGCTATTG 3900

ATATGGATGCACGCTTTTGAATT  3922
```

codon of the third ORF. These features suggest that the three ORFs form an operon.

The first ORF encoded a small protein of 147 amino acids named CopY. A putative heavy metal binding motif $CXCX_4CXC$ was identified at the C-terminus of CopY. A similar motif was also present in CopY of *E. hirae* and OrfY of *Lactobacillus sake* (Fig. 29). At the N terminus of CopY two stretches of conserved sequence which shared high homology to *E. hirae* CopY, *L. sake* OrfY, *Staphylococcus aureus* BlaI, *S. aureus* MecI, and *Bacillus licheniformis* PenI were present (Fig. 29). The amino acid identity of *S. mutans* CopY to *E. hirae* CopY, OrfY of *L. sake*, *S. aureus* BlaI, *S. aureus* MecI, and *B. licheniformis* PenI was 34, 33, 21, 20 and 23%, respectively.

The second ORF encoded a 743 amino acid protein (CopB), which shared homology to a large group of evolutionarily conserved ion motive ATPases, including CopA and CopB of *E. hirae*, and CopA of *Helicobacter pylori*. Analysis of the deduced sequence of CopB revealed several features that are hallmarks to P-type ATPases. These include: (a) an N-terminal heavy metal binding motif GXXCXXC (Fig. 30A), (b) eight transmembrane regions (Fig. 28), (c) a TGES motif that forms part of the phosphatase domain which mediates phosphorylation of an aspartic acid within the DKTGT motif permitting the protein to transduce ions via a CPC motif located in a hydrophobic transmembrane region (Fig. 30B), and (d) a C-terminal VGDGINDAP motif (Fig. 30C) that is predicted to form a Mg^{2+} salt bridge with the γ-phosphate of ATP, placing the phosphate in a position where it can be transferred to the aspartic acid.

Figure 29. Sequence alignments of *S. mutans* CopY (copYSm) with other negative regulatory proteins. CopY was aligned with CopY of *E. hirae* (CopYEhirae, accession # Z46807) a negative regulator of the *cop* operon which regulates intracellular copper homeostasis, and OrfY of *Lactobacillus sake* (OrfLsk, accession # O07127) a putative negative regulator of an P-type ATPase similar to *copB* of *E. hirae*. The remaining proteins PenI and BlaI of *B. lichenformis* (penIBlichen and blaIBlic, accession numbers P06555 and B28183), *S. aureus* MecI (mecISaur, accession # P26598), and *S. aureus* BlaI (BlaISa, accession # P18415) regulate β-lactam resistance. The proteins were aligned using ClustalW. Identical residues are shaded black, conserved residues in at least 60% of the sequences are gray, and similar residues are in lower case. In the consensus line, identical residues are indicated by ! and conserved or similar residues by *. Setting the value for conserved residues at 60% prevented the shading of the metal binding motif ($CXCX_4CXC$), residues135 – 145, of CopY of *E. hirae* and *S. mutans* and OrfY of *L. sake*.

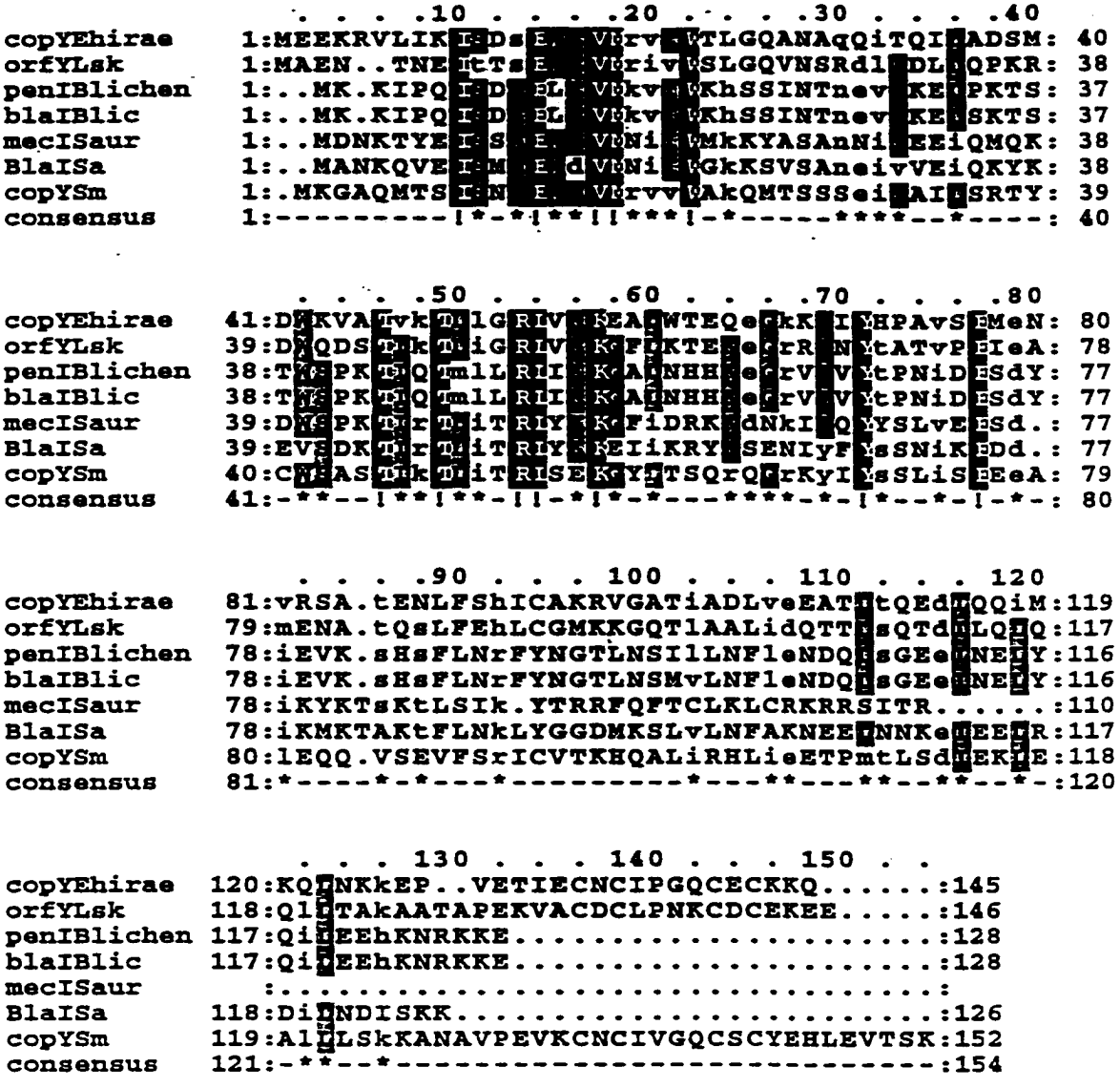
copYEhirae
orfYLsk
penIBlichen
blaIBlic
mecISaur
BlaISa
copYSm
consensus

Figure 30. Sequence alignments of the N-terminal metal binding sites (A), the phosphatase domain (B), or the ATP stabilization domain (C) of *S. mutans* CopB (SmutanCopB) to other P-type ATPases. CopA and CopB of *E. hirae* (EhiraeCopA and EhiraeCopB, accession # L13292). CopA of *H. felis* (HfelisCopA accession # O32619), and CadC of *L. sake* (LsakeCadC accession # O07127) were aligned using ClustalW. CopB was not included in the alignment of the N-terminal binding region as it possesses an alternate metal binding motif (HXXMXGM). Identical residues are shaded black, conserved residues in at least 60% of the sequences are gray, and similar residues are in lower case. In the consensus line, identical residues are indicated by !, and conserved or similar residues by *.

A

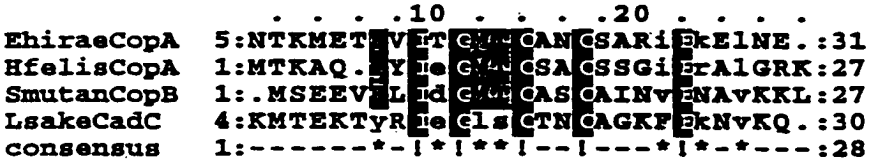

B

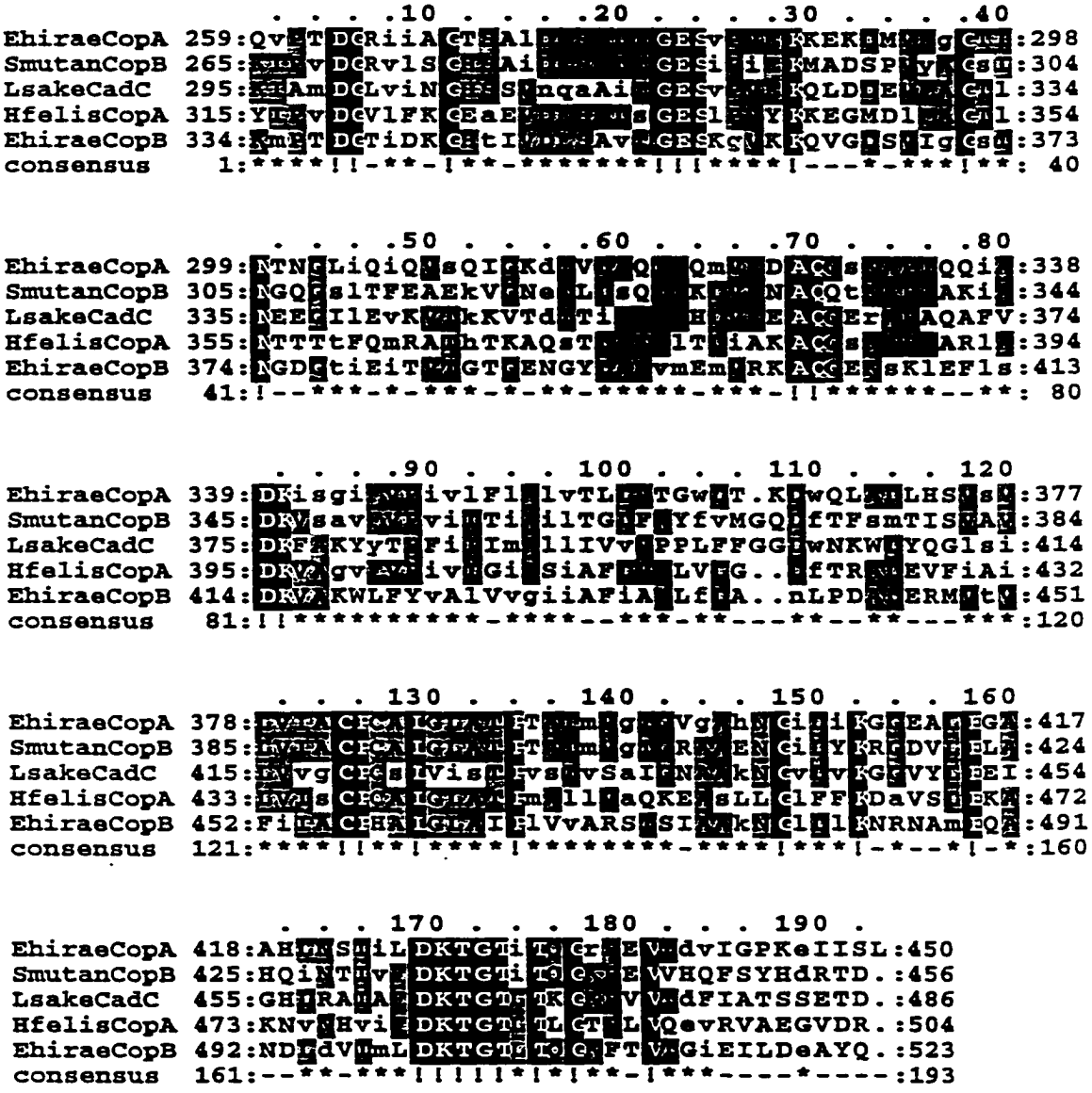

C

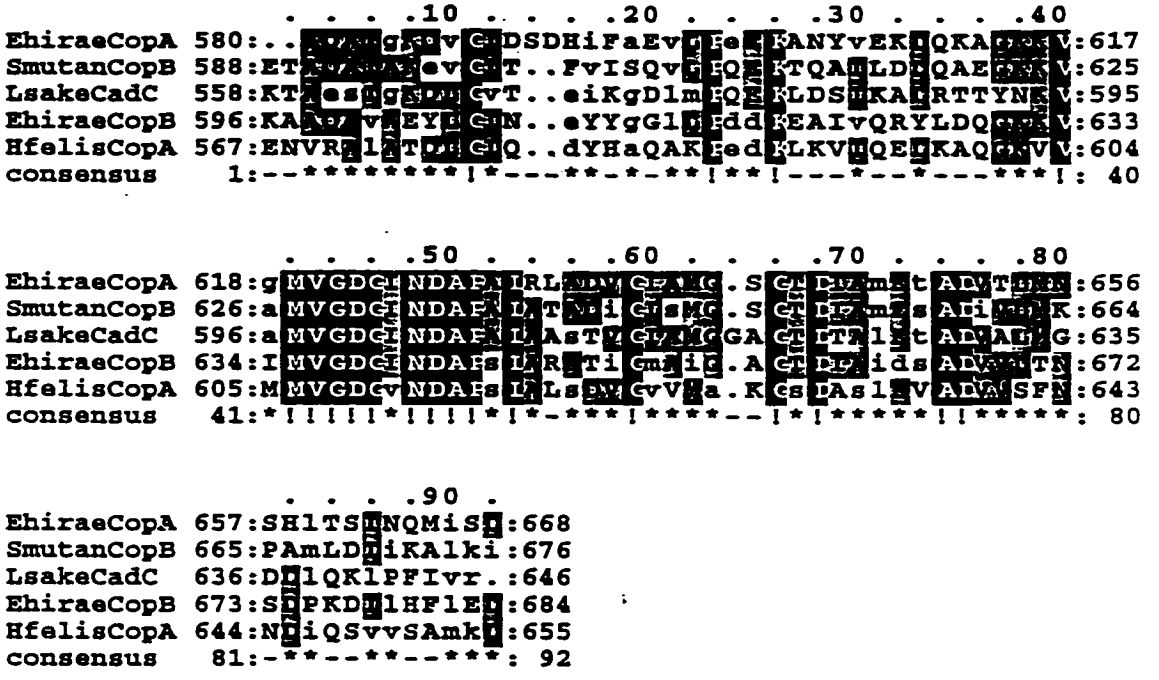
. . . .10 . . . . .20 . . . . .30 40
EhiraeCopA 580:..
SmutanCopB 588:ET
LsakeCadC 558:KT
EhiraeCopB 596:KA
HfelisCopA 567:ENVR
consensus 1:
. . . .50 . . . . .60 . . . . .70 80
EhiraeCopA 618:g
SmutanCopB 626:a
LsakeCadC 596:a
EhiraeCopB 634:I
HfelisCopA 605:M
consensus 41:
. . . .90 .
EhiraeCopA 657:SH1TS
SmutanCopB 665:PAmLD
LsakeCadC 636:D
EhiraeCopB 673:S
HfelisCopA 644:N
consensus 81:

The third ORF of the operon encoded a 67 amino acid protein (CopZ), which also contained a heavy metal binding motif, CXXC, at the N terminus. Homology searches provided matches to four known small proteins involved in copper or mercury resistance: (a) CopZ of *E. hirae* , (b) CopP of *H. pylori*, (c) CopP of *Helicobacter felis*, and (d) MerP of *Pseudomonas alcaligenes* (Fig. 31). The amino acid sequence identity of CopZ to these proteins was 17, 21, 30, and 17 %, respectively. The *S. mutans* CopZ also showed homology to another small hypothetical protein, SynCh of *Synechocystis* sp with an amino acid identity of 27 % (Fig. 31).

At the promoter-operator region of the operon was a pair of inverted repeats; the first repeat overlapped the -35 region and the second immediately followed the -10 region (Fig. 28). Similar repeats were also present at the promoter-operator region of the *E. hirae copYZAB* and *S. aureus cadAC* operons (154, 155), where they function as binding sites for the regulatory proteins CopY and CadC respectively (55, 192).

To summarize, Tn*917* had inserted itself in the chromosome of mutant A upstream of the first gene of an operon which encodes two putative regulatory proteins and a membrane protein hypothesized to transport heavy metal out of the cytoplasm. While the transposon did not disrupt the ORFs, the transposon insertion had an effect on the operon which affected SPRE activity of mutant A.

Figure 31. Sequence alignments of *S. mutans* CopZ (CopZSmutans) to other proteins. CopZ was aligned with CopP of *H. pylori* and *H. felis* (copPHpylori and copPHfelis, accession numbers Q48271 and O032620), MerP of *P. alcaligenes* (PalcMerP, accession # AAC33271), SynCh of *Synechocystis* sp (SynCh, accession # BAA17240), and CopZ of *E. hirae* (copZEhirae, accession # Z46807) using ClustalW. Identical residues are shaded black, conserved residues in at least 60% of the sequences are gray, and similar residues are in lower case. In the consensus line identical residues are indicated by !, and conserved or similar residues by *. *Helicobacter* CopP and enterococcal CopZ are metal binding proteins postulated to regulate the activity of ATPases and function as anti-repressors of the *cop* operons, respectively. MerP is a mercury binding protein aiding mercury resistance by sequestering mercury. SynCh is a hypothetical protein acting as a chaperone.

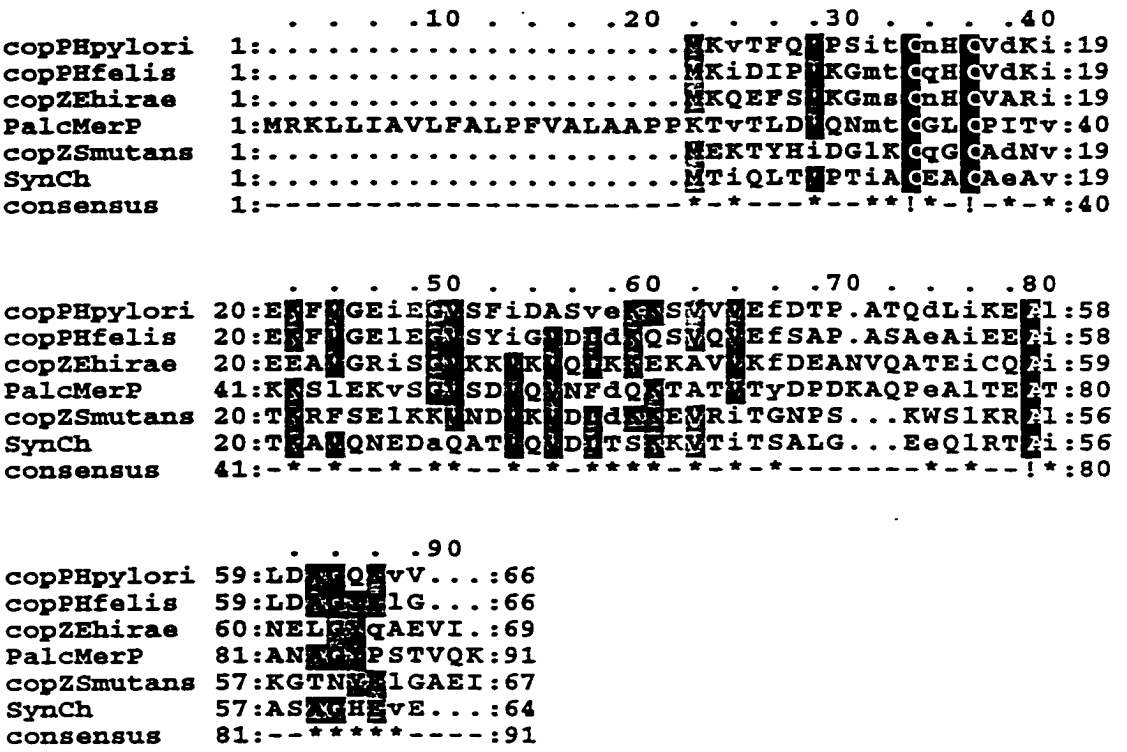
. . . . .10 . . . . .20 . . . . .30 40
copPHpylori 1:.....MKvTFQIPSitCnHCVdKi:19
copPHfelis 1:.....MKiDIPVKGmtCqHCVdKi:19
copZEhirae 1:.....MKQEFSIKGmsCnHCVARi:19
PalcMerP 1:MRKLLIAVLFALPFVALAAPPKTvTLDVQNmtCGLCPITv:40
copZSmutans 1:.....MEKTYHiDGlKCqGCAdNv:19
SynCh 1:.....MTiQLTVPTiACEACAeAv:19
consensus 1:--------------------*-*---*--**!*-!-*-*:40
. . . . .50 . . . . .60 . . . . .70 80
copPHpylori 20:EIFVGEiEGVSFiDASveKSMVVEfDTP.ATQdLiKEFl:58
copPHfelis 20:EIFVGElEGVSYiGVDTdSQSVQVEfSAP.ASAeAiEEFi:58
copZEhirae 20:EEAVGRiSGVKKVKVQIKFEKAVVKfDEANVQATEiCQFi:59
PalcMerP 41:KVSlEKvSGVSDVQVNFdQVTATVTyDPDKAQPeAlTEFT:80
copZSmutans 20:TVRFSElKKVNDVKVDVdEKEVRiTGNPS...KWSlKRFl:56
SynCh 20:TVAVQNEDaQATVQVDVTSKKVTiTSALG...EeQlRTFi:56
consensus 41:-*-*--*-**--*-*-*****-*-*-*-------*-*--!*:80
. . . .90
copPHpylori 59:LDVVQEvV...:66
copPHfelis 59:LDVGEVlG...:66
copZEhirae 60:NELGVqAEVI.:69
PalcMerP 81:ANVGVPSTVQK:91
copZSmutans 57:KGTNVKlGAEI:67
SynCh 57:ASAGHEvE...:64
consensus 81:--*****----:91

Generation of a *cop* operon knock-out mutant.

An isogenic mutant (S4) of *S. mutans* JH1005 devoid of the *cop* operon was produced by homologous recombination using the construct, pNV7/S4 (Fig. 26 and 32). Results of Southern blotting showed that chromosomal DNA from mutant S4 did not hybridize to the probe made from *copYB* DNA while the wild type DNA showed an expected 1.8 kb band with this probe (Fig. 33A). When the DNA was hybridized with a probe made from the tetracycline cassette specific to pNV7/S4, two bands of 7 kb and 2.5 kb were noted in the S4 DNA, but were absent in the wild-type DNA (Fig. 33B). These results indicate that the tetracycline-resistant transformant, S4, lacked the *cop* operon and had the tetracycline cassette in its place. The strain S4 would allow us to explore the function of the *cop* operon in SPRE activity.

Analysis of the *cop* transcript.

To aid in determining if the three genes, *copYBZ*, form an operon the size of the transcript and the transcriptional start site were determined. Northern dot-blotting using a probe made from *copYB* showed a positive signal with RNA samples from JH1005, but not from the mutant S4 RNA (Fig. 34A) further indicating that the *cop* operon was inactivated in mutant S4. Interestingly, a much stronger signal was observed with RNA prepared from Cu^{2+}-induced JH1005 cells than from non-induced cells. These observations were confirmed by Northern hybridization (Fig. 34B). In the Cu^{2+}-induced sample, three bands of 4, 3.2, and 1.3 kb were observed. Weak transcripts were detected in the non-induced sample and no transcripts were observed in the S4 RNA samples.

Figure 32. Construction of a *cop* knock-out *S. mutans* mutant. The flow chart depicts the construction of the knock-out construct pNV7/S4 used for insertional activation of the *cop* operon with a tetracycline cassette (A). *Sca*I linearized pNV7/S4 was transformed into *S. mutans* JH1005 and the chromosomal *cop* operon is envisioned to be inactivated via homologus recombination (B).

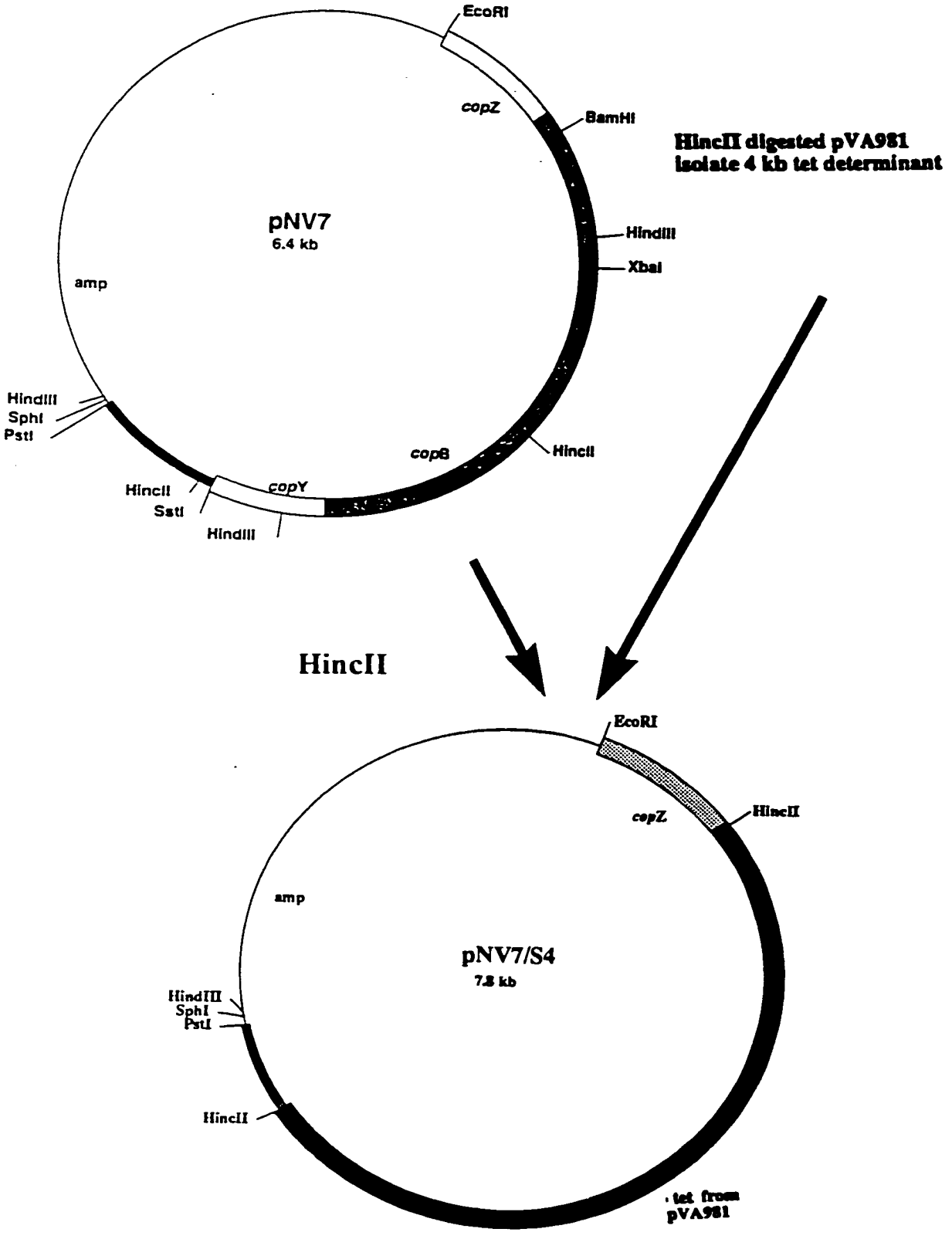
EcoRI
copZ
BamHI
HincII digested pVA981
isolate 4 kb tet determinant
pNV7
6.4 kb
HindIII
XbaI
amp
HindIII
SphI
PstI
copB
HincII
HincII
copY
SstI
HindIII
HincII
EcoRI
copZ
HincII
amp
pNV7/S4
7.8 kb
HindIII
SphI
PstI
HincII
tet from
pVA981

B.

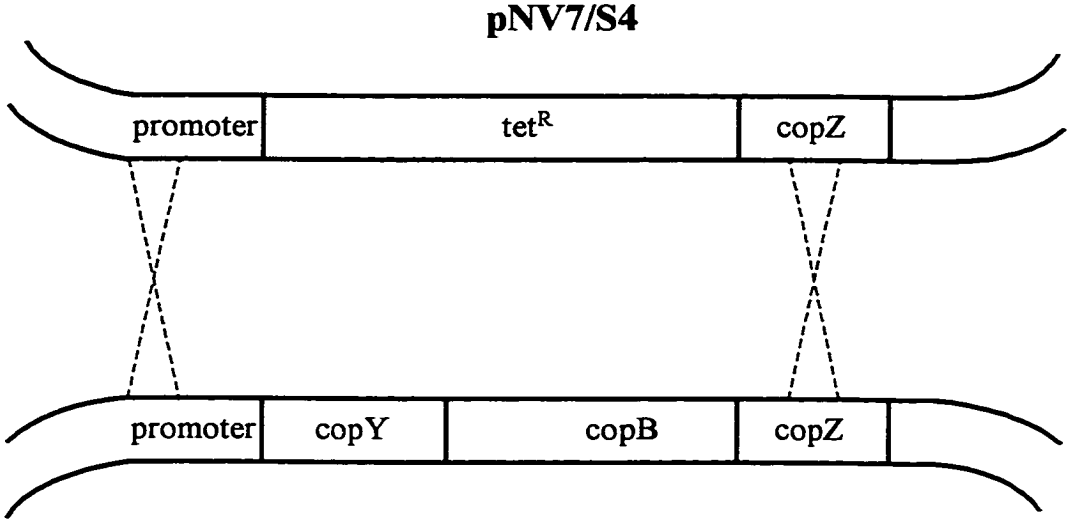
pNV7/S4
promoter
tet^R
copZ
promoter
copY
copB
copZ
S. mutans JH1005
chromosome

Figure 33. Southern hybridization verifying the lack of *cop* genes in mutant S4. *Hind*III digested JH1005 wild type (lane 1) and the mutant S4 (lane 2) chromosomal DNA (5 μg) were hybridized with probes specific for *copYB* (A) or the tetracycline cassette of pVA981 (B). Probes were prepared by labeling plasmids pWH4.4 or pVA981 using the Bio-Nick labeling kit and signals were detected by a Photogene detection system (GIBCO/BRL).

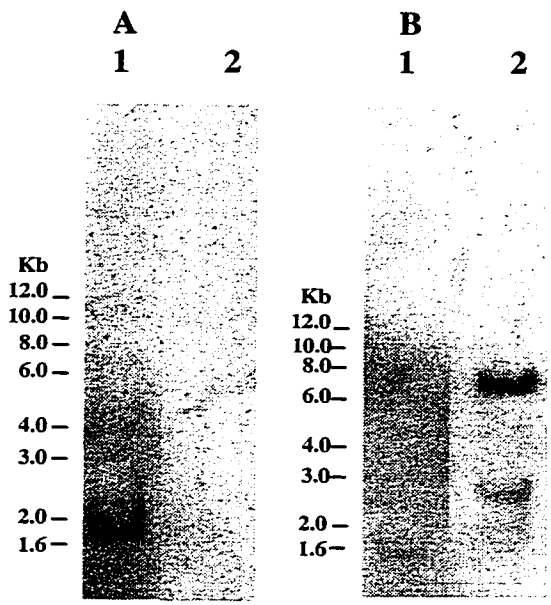
A
1
2
Kb
12.0
10.0
8.0
6.0
4.0
3.0
2.0
1.6
B
1
2
Kb
12.0
10.0
8.0
6.0
4.0
3.0
2.0
1.6

Figure 34. Analysis of the *cop* operon transcript. (A) RNA dot blotting. Total RNA from JH1005 or S4, were dot-blotted and cross-linked to a Biodyne A filter (GIBCO/BRL). The filter was probed using a probe produced by biotin labeling pWH4.4 using the Bio-Nick labeling kit (GIBCO/BRL). (B) Northern hybridization. Total RNA (20 μg) was separated on a formaldehyde agarose gel, transferred to a nylon membrane and probed as above. Lanes: 1, non-induced JH1005 RNA; 2, 1 mM Cu^{2+}-induced JH1005 RNA; 3, non-induced S4 RNA; 4, S4 1 mM Cu^{2+}-induced RNA.

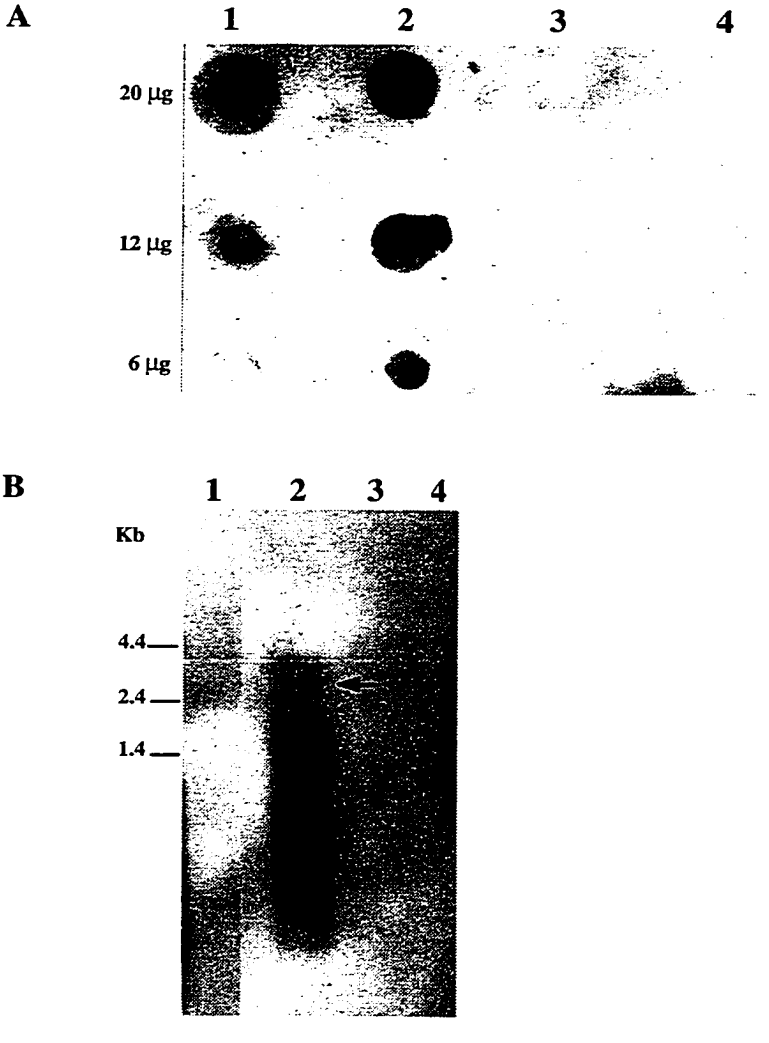
A
1
2
3
4
20 µg
12 µg
6 µg
B
1
2
3
4
Kb
4.4
2.4
1.4

The transcriptional start site of the *cop* operon was determined by primer extension using RNA prepared from the Cu^{2+}-induced wild-type cells. The first base of the transcript was identified as the thymidine located 6 nucleotides downstream of the -10 region (Fig. 35). Assuming transcription terminates at the terminator identified downstream of *copZ* (Fig. 28) the postulated size of the transcript encoding the three ORFs would be 3 kb, which corresponds to the approximately 3 kb signal observed in the Northern blot.

Role of the *cop* operon in copper resistance of *S. mutans*.

Effect of copper on growth of *S. mutans*.

The sequence similarities of the ORFs to the *E. hirae cop* operon suggested that the *cop* operon of *S. mutans* was also involved in copper transport. Hence, the effect of copper on growth of *S. mutans* wild type, S4, and mutant A was determined. The wild type cells exhibited impaired growth as the copper concentration increased and growth was inhibited at 800 μM Cu^{2+} (Fig. 36A). Interestingly the Tn*917* mutant A was able to tolerate higher Cu^{2+} concentrations than the wild type. Although growth was impaired, mutant A was able to grow better in the presence of 800 μM Cu^{2+} than JH1005 (Fig. 36B).

Complementation of mutant A with *copY* carried on plasmid pWH4/PDL resulted in growth inhibition by 400 μM Cu^{2+} (Fig. 36B, graph with open squares symbols). In comparison, growth of the *cop* knock-out mutant S4, was severely impaired by 200 μM

Figure 35. Mapping the transcriptional start site of the *cop* operon by primer extension. Eighty micrograms of total RNA isolated from Cu^{2+}-induced JH1005 cells was annealed with the primer which was end-labeled with (γ^{32})P ATP using T4 polynucleotide kinase. A reverse-transcriptase reaction was performed on the annealed sample. A Sanger sequencing reaction, using the same primer as in the primer extension assay, was also performed on the template pWH4. The reaction products (A, C, G, T) were resolved on a 7% polyacrylamide gel alongside the primer extension product (P). The DNA sequence is shown on the left and the transcriptional start site is indicated with an asterisk.

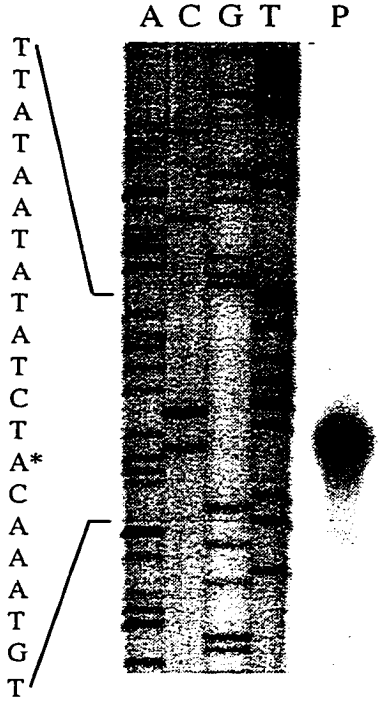
A C G T P
T
T
A
T
A
A
T
A
T
A
T
C
T
A*
C
A
A
A
T
G
T

Figure 36. Growth of *S. mutans* JH1005 (A), mutant A (B), S4 (C), and S4 complemented with the *cop* operon on pNV7B (D). Overnight cultures were inoculated 1:10 into 1.5 mL of TYG and incubated at 37°C for 1 hour. After 1 hour, Cu^{2+} was added to a final concentrations of 400 (▲), 600 (●), or 800 (■) μM of Cu^{2+}. One tube (◆) with no added copper served as a control. In panel B, (□) represents mutant A complemented with pWH4/PDL grown in 400 μM Cu^{2+}.

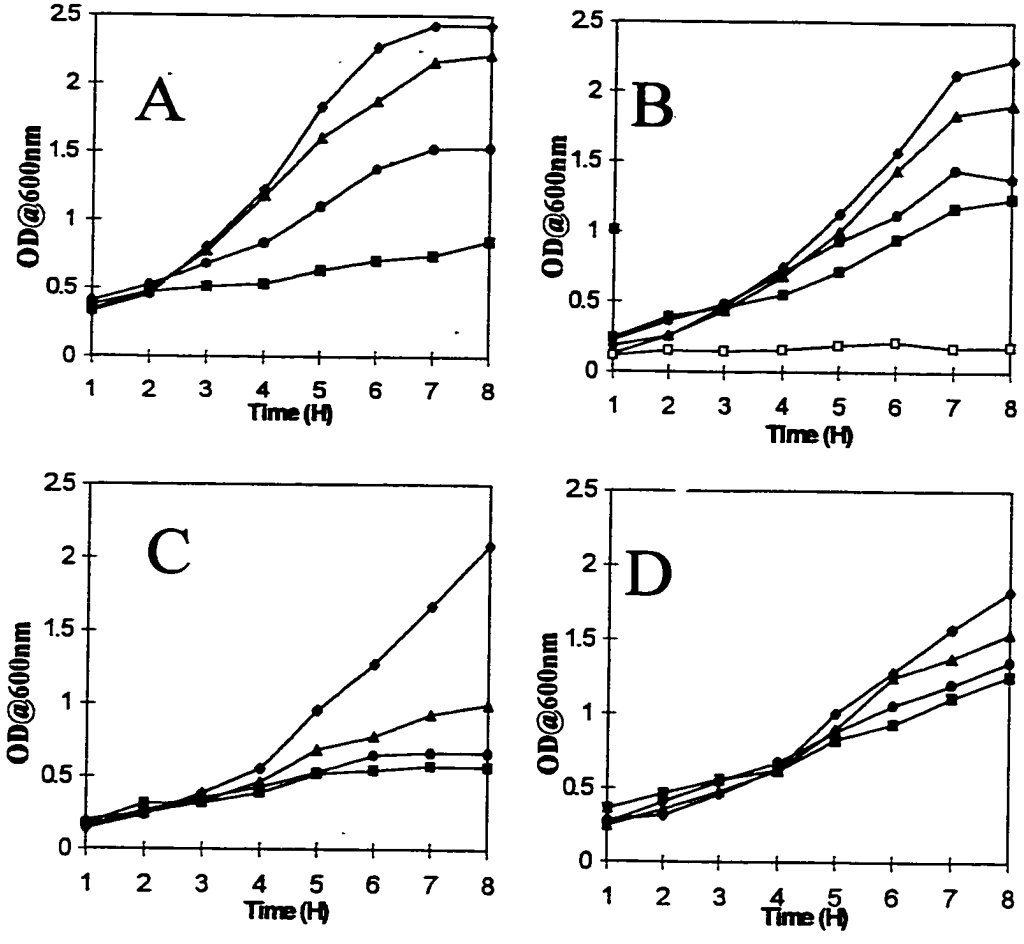
A
B
C
D
OD@600nm
Time (H)
0
0.5
1
1.5
2
2.5
1
2
3
4
5
6
7
8

Cu^{2+} and completely inhibited by 400 μM Cu^{2+} (Fig. 36C). As expected, the ability of S4 to grow in higher Cu^{2+} concentrations was restored by complementation with the *cop* operon (Fig. 36D).

MIC of copper and other divalent cations.

The observations on the effects of Cu^{2+} on growth were further confirmed by results from susceptibility studies. The MIC values of JH1005, mutant A, and *cop* knock-out mutant S4 to Cu^{2+} were 8, 9, and 2 mM, respectively. These values are higher than that in the growth studies and can be attributed to the use of a more complex medium. Complementing S4 cells with the *cop* operon restored the MIC value to wild type level. When JH1005 and mutant A were complemented with *copY* alone, the MIC values of Cu^{2+} decreased slightly to 6 and 7 mM, respectively; while a similar complementation of S4 did not change the MIC value. The sensitivity of JH1005 and the mutants to other heavy metal ions was also examined. There was no difference in MIC for JH1005 and the mutants to Ag^{2+} (175 μM), Cd^{2+} (40 μM), Cr^{2+} (> 20 mM), Zn^{2+} (5 mM), and Hg^{2+} (50 μM).

These data suggest that the *cop* operon mediates *S. mutans's* resistance to high extracellular concentrations of copper.

Regulation of the *cop* operon.

Production of a *cop* promoter-CAT fusion gene.

The results of the transcript analysis suggest that the expression of the *cop* operon is regulated by Cu^{2+} concentrations. To assist in the study of *cop* expression, a promoterless CAT gene was fused to the *cop* promoter. This fusion was accomplished with the construction of pHTL1 (Fig. 8). The promoter function was confirmed by selecting for chloramphenicol resistance following transformation of the ligated plasmid into *E. coli*. The *cop* promoter-CAT fusion gene was further subcloned into pSL2 which carried a fragment of the *spaP* gene that would allow homologous recombination with the chromosomal counter-part of *S. mutans*. The resulting plasmid pHSL2 carried a kanamycin resistance gene which would hamper attempts to complement the strain created with shuttle vectors (pDL276, kan^r) carrying the *cop* genes. Hence the plasmid pHSL2/pUC was constructed by ligating the fusion gene and a fragment of the *spaP* gene fragment into the pUC18 backbone. The plasmid pHSL2/pUC was transformed into the *S. mutans cop* knock-out mutant S4 and transformants were selected with chloramphenicol. Chloramphenicol resistant transformants were assumed to have the fusion gene integrated into the chromosome since the plasmid did not have an origin of replication that is functional in *S. mutans*. The new strain was named S4/CAT.

Expression of the *cop* promoter-CAT fusion gene.

Plasmids carrying the entire operon, *copY*, or *copZ* were transformed into S4/CAT and the ability of the strains to grow in a chemically defined medium (198) in the presence

of chloramphenicol or chloramphenicol and copper was determined. The results are shown in Table 5. All the strains grew equally well in the absence of chloramphenicol. The addition of chloramphenicol to the media did not affect the growth of S4/CAT or S4/CAT complemented with *copZ*. However, strains carrying either the entire operon or *copY* were unable to grow in the presence of chloramphenicol. Inclusion of 0.01 mM or 0.10 mM $CuSO_4$ did not have any effect on the growth of S4/CAT or S4/CAT with *copZ*. However, at 1 mM $CuSO_4$ growth of S4/CAT and S4/CAT with *copZ* was impaired, presumably by the toxicity of 1 mM $CuSO_4$. Growth of S4/CAT complemented with the entire *cop* operon was facilitated by the addition of copper to the chloramphenicol containing media. In the presence of 1mM copper growth of S4/CAT *copYBZ* was comparable to S4/CAT in the presence of 1 mM $CuSO_4$. S4/CAT complemented with *copY* showed no significant growth in the presence of copper in the chloramphenicol containing media. The results imply that the gene products of the *cop* operon control their own expression, with CopY functioning as a negative regulator, and CopB, CopZ, or CopB and CopZ functioning as anti-repressors.

Effect of the *cop* operon on detachment and cell wall related properties of *S. mutans*.

Ability of SPRE from S4 to detach biofilm cells.

To determine whether the *cop* operon has a direct role in detachment of biofilm cells, SPRE was prepared from mutant S4 and *cop*-complemented S4. The ability of the SPRE preparations to detach *S. mutans* NG8 biofilm cells formed on SA-conditioned

Table 5. Growth of *S. mutans* S4/CAT and *cop* genes complemented strains in FMC in the presence of copper and chloramphenicol. FMC is a chemically defined medium as described by Terleckji (198).

Strains[a]	No additions[b]	$[Cu^{2+}]^c$			
		0 mM	0.01 mM	0.10 mM	1 mM
S4/CAT	1.262[d]	1.191	1.242	1.203	0.562
S4/CAT *copYBZ*	1.198	0.073	0.102	0.215	0.659
S4/CAT *copY*	1.163	0.072	0.078	0.083	0.112
S4/CAT *copZ*	1.191	1.194	1.167	1.116	0.509

[a] S4/CAT is the *cop* operon knock-out assumed to have the *cop* promoter-CAT gene fusion integrated into its chromosome.
S4/CAT *copYBZ* is S4/CAT complemented with the entire *cop* operon.
S4/CAT *copY* is S4/CAT complemented with *copY*.
S4/CAT *copZ* is S4/CAT complemented with *copZ*.

[b] Chloramphenicol and copper were not included in the media.

[c] Chloramphenicol (5 μg/mL) was included in the media

[d] OD_{600nm} readings following 18h incubation at 37°C.

EHA rods was tested. The results showed that SPREs from S4, *cop*-complemented S4, and wild type JH1005 yielded 30.8 ± 2.3 %, 30.2 ± 0.6%, and 33.1 ± 0.6% detachment, respectively (Table 6). In contrast, SPRE from mutant A effected 23.6% ± 0.2% detachment which was significantly lower than that by JH1005 and *cop*-complemented S4 ($p<0.05$), and was similar to the PEMPP buffer control of 20.3 ± 0.6%. The inability of mutant A SPRE to effect detachment is consistent with results from earlier experiments (see Fig. 20).

Autolytic activity and osmotic fragility of the mutant.

Possible relationships between decreased SPRE function and cell wall-related properties were examined by cellular autolytic and osmotic fragility assays. Lysis resulting from the activity of cellular autolysins was first determined. Cells from the exponential or stationary phases of growth were suspended in 10 mM sodium phosphate buffer, pH 6.0, the optimal pH of the SPRE, and the optical density was monitored. As shown in Figure 37, the OD_{600nm} of exponential and stationary phase cell suspensions decreased by approximately 30% of the initial values after a four hour incubation. The wild-type and mutant A displayed identical rates of decrease.

The osmotic fragility of bacterial cells following treatment with mutanolysin was also examined. Cells were incubated in protoplast buffer containing mutanolysin (1 kU/mL) and incubated at 37°C. At various time intervals aliquots were removed and quickly diluted in 10 mM sodium phosphate buffer (pH 7.2) to induce cell lysis. As shown in Figure 38, both the exponential and stationary phase cells of mutant A were slightly

Table 6. Detachment of *S. mutans* NG8 cells from biofilms in the presence of SPRE prepared from various strains.

	Rod 1			Rod 2			
	Total CFU[a]	Det. CFU[b]	% Det[c]	Total CFU	Det. CFU	% Det.	Avg. % Det.
PEMPP	2.69	0.53	19.7	4.3	0.9	20.9	20.3 ± 0.6
JH1005 SPRE	4.80	1.56	32.5	5.62	1.89	33.6	33.1 ± 0.6
Mutant A SPRE	6.08	1.45	23.8	6.8	1.60	23.4	23.6 ± 0.2
S4 SPRE	7.37	2.1	28.5	6.22	2.06	33.1	30.8 ± 2.3
cop-complemented S4 SPRE	4.72	1.46	30.9	6.40	1.90	29.6	30.2 ± 0.6

a Total CFU (x 10^5 per rod) adhered to epon-hydroxyapatite rods. Prior to biofilm formation rods were conditioned with 80 μg/ml SA for 15 minutes and blocked with 1% (w/v) BSA for 1 h.

b Cells detached (x 10^5 per rod) from biofilms after 1 h incubation at pH 6.0 in the presence (200 μg/mL) or absence of exogenous SPRE.

c % detachment = (Det. CFU / Total CFU) x 100.

Figure 37. Cellular autolysis of *S. mutans* JH1005 (◆), mutant A (■). Cells were grown to: A, exponential ($0D_{600\ nm}$ = 0.65); or B, stationary ($OD_{600\ nm}$ = 1.15) phase of growth. Cells from 10 mL cultures were harvested by centrifugation, washed twice with distilled water and once with 10 mM sodium phosphate buffer, pH 6, and resuspended in 5 mL of the same buffer. The cells were dechained by rapid passage through a 27 gauge needle and the cells were resuspended to the same density (OD_{600nm} = 1) with phosphate buffer. One milliliter aliquots were incubated at 37°C. The OD_{600} at time 0 minutes was taken as 100%.

A

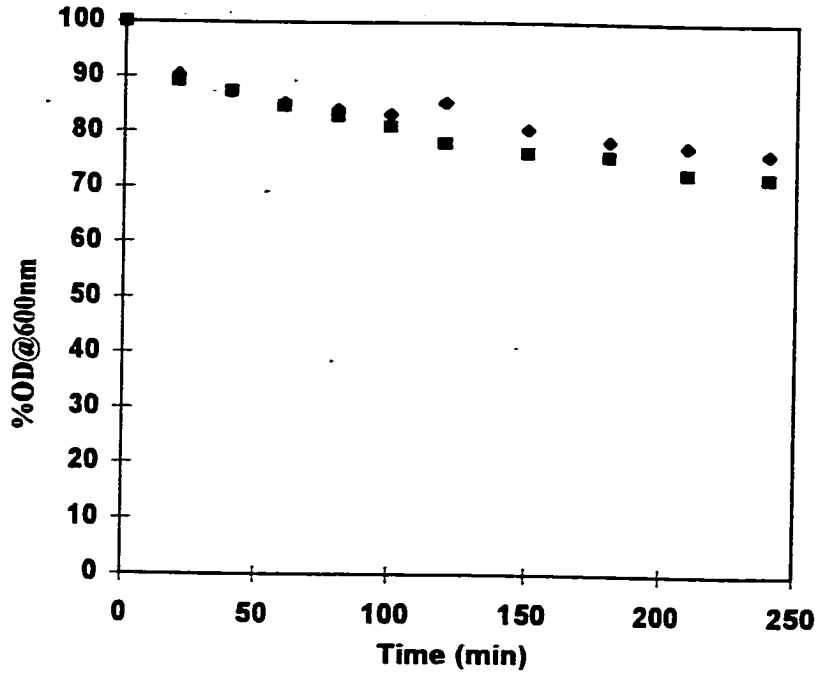
100
90
80
70
60
50
40
30
20
10
0
%OD@600nm
0
50
100
150
200
250
Time (min)

B

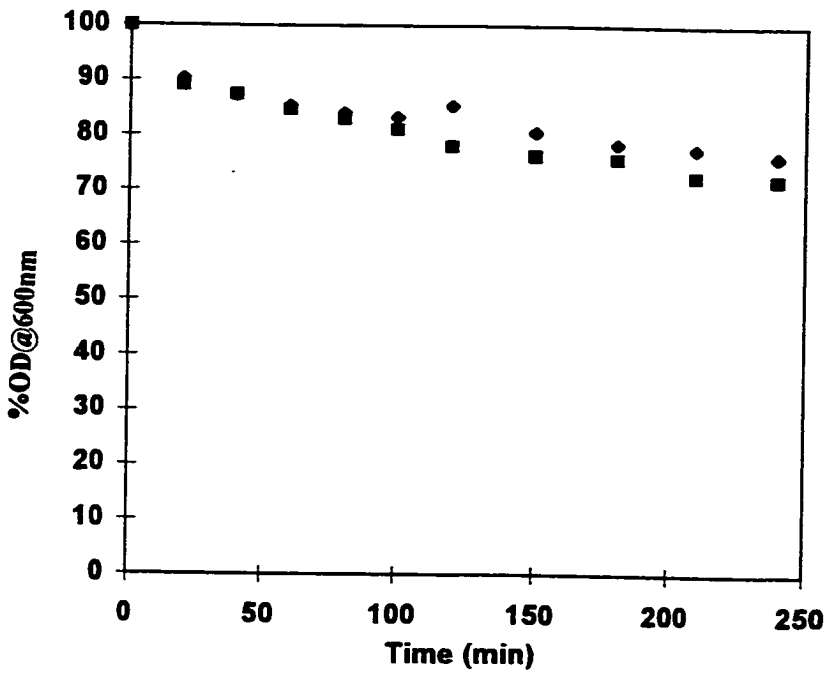
100
90
80
70
60
50
40
30
20
10
0
%OD@600nm
0
50
100
150
200
250
Time (min)

Figure 38. Osmotic fragility of mutanolysin treated *S. mutans* JH1005 (■), and mutant A (◆). Cells were grown until: A, exponential ($OD_{600\ nm}$ =0.65); or B, stationary ($OD_{600\ nm}$ = 1.15) phase of growth. Cells from 10 mL cultures were harvested by centrifugation, washed once in protoplast buffer, dechained by rapid passage through a 27 gauge needle and was adjusted to the same cell density (OD600 = 1) with protoplast buffer containing 1 kU of mutanolysin per milliliter. The cells were incubated at 37°C. At intervals, 20 μL of the cell suspension was diluted in 1 mL of 10 mM sodium phosphate buffer pH 7.2. The optical density of the time 0 sample was taken as 100%.

A

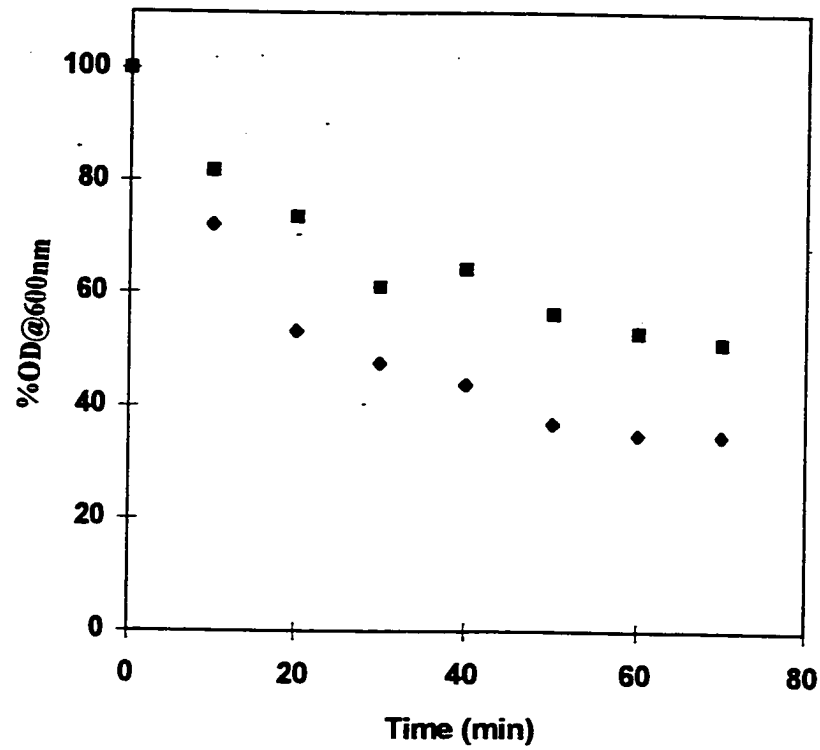
100
80
60
40
20
0
%OD@600nm
0
20
40
60
80
Time (min)

B

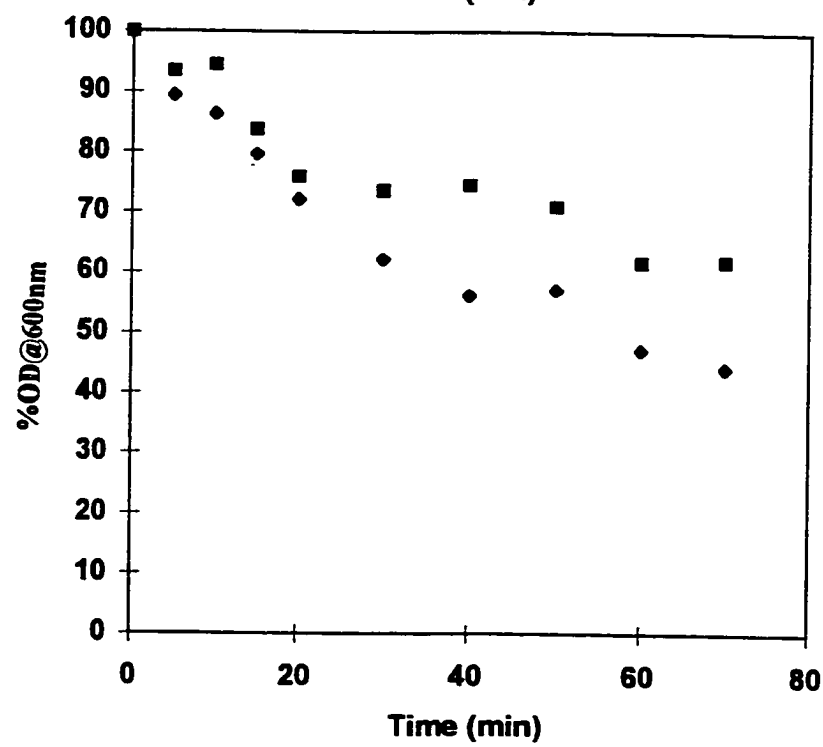
100
90
80
70
60
50
40
30
20
10
0
%OD@600nm
0
20
40
60
80
Time (min)

more osmotically fragile than JH1005. After 70 minutes of incubation with mutanolysin the OD_{600nm} of exponential phase mutant A and JH1005 decreased to 35% and 51% relative to the zero time samples. The OD_{600nm} of stationary phase mutant A and JH1005 cell dropped to 44% and 61% of the time zero samples. The data demonstrate that the transposon insertion had little affect on autolysis but the osmotic fragility was increased in mutant A. This suggests the transposon insertion affected other cellular processes in addition to the SPRE activity.

DISCUSSION

Formation of model biofilms.

Biofilm formation is a multistep process culminating in the formation of adherent microcolonies on surfaces exposed to a fluid environment. A prerequisite for biofilm formation is the availability of a substratum which may or may not be conditioned with macromolecules from the environment. Cells are then actively or passively transported to the substratum with which they can interact. The primary interaction between cells and the substratum mediates reversible adherence in which the cells are believed to be able to move in two dimensions across the surface until they detach or bind irreversibly to the substratum (213). Following irreversible adherence of the primary colonizers, the adherent population becomes more complex. Thick, multi-species biofilms may develop and cells can produce copious quantities of extracellular polysaccharides which may encapsulate the microcolony. For our experiments we have designed a model system mimicking the surface that *S. mutans* might encounter in the oral cavity. To this end, we have used EHA as the substratum which mimics the tooth enamel whose primary chemical constituents are hydroxyapatite. Since the enamel is always coated with saliva, we have also mimicked this condition by coating EHA with saliva or purified SA in biofilm formation. Hence, the model system used in this study is more relevant to the natural *in vivo* conditions than those used by others involving glass cover slips.

Conditioning of EHA rods.

Surfaces immersed in fluid environments are quickly conditioned by macromolecules

adsorbed from the fluid phase (34), and the oral cavity is of no exception. In the oral cavity saliva bathes the enamel, depositing on it a pellicle of salivary proteins referred to as the acquired enamel pellicle (AEP). Early reports on the acquisition of the AEP examined pellicles of at least two hours old (79, 166, 185). These studies demonstrated that the complexity of adherent salivary proteins increases with time. Looking into the initial protein deposition on contact lenses, Sack *et al.* (173) found that the limiting factor for the initial rate of protein deposition on the surface was the rate at which tear fluid could deliver proteins to the surface. Using transmission electron microscopy to examine enamel slabs conditioned with saliva (2 mg/mL), Busscher *et al.* (28) showed that proteinous films of multiple layers in thickness formed within 10 seconds and developed into heterogeneous structures after 5-10 minutes. Similarly, Vassilakos *et al.* (214) found that the kinetics of adsorption of saliva to silica was a very fast process. After 30 minutes exposure to 1% saliva in water, 0.2 $\mu g/cm^2$ of protein was detected on silica. Additional work by others also supported the rapid formation of a pellicle within 15-30 minutes, after which the protein composition does not drastically change (185, 214). Our results are consistent with these findings. We showed that significant amounts of protein could be recovered from EHA rods after immersion in BSA, diluted saliva or SA for only 15 minutes. In addition, we found that following conditioning in 1/10 diluted saliva 80% of salivary proteins could be retained on the EHA after a one hour incubation in a protein free buffer. This result is similar to that reported by Vassilakos *et al.* (214), that pellicles could be washed for 30 minutes with only a 10% loss of adherent protein. The stability of the pellicle suggests that the majority of the proteins firmly adhere to the surface. With respect to the constituents of the conditioning film formed on saliva-conditioned EHA rods, we found that

they correlate with those reported by Al-Hashimi and Levine (4), i.e., that sIgA, amylases and high molecular-weight mucins such as MG1 were recovered from 2 h *in vivo*-conditioned enamel.

In preparation for latter experiments requiring more specific mechanisms for the adherence of *S. mutans* to the substrata, EHA was conditioned with SA. In these instances, a less concentrated protein solution was used to condition EHA. However, the quantities of protein recovered from SA-conditioned rods was not dramatically affected, reaffirming that the deposition of proteins on EHA was a rapid and efficient process. Unfortunately the stability of the SA conditioning film on the EHA rods was not determined. It would have been interesting to compare the stability of the SA conditioning film to the stability of the whole saliva conditioning film. Since SA is known to adhere to enamel, the SA conditioning may have a greater stability than the saliva, a complex mixture of proteins which may have varying affinities for the EHA rods. Differential stability's of individual salivary proteins may also affects subsequent detachment of biofilm cells from the conditioned surface (see below).

Biofilm formation on conditioned EHA.

Our results of biofilm formation on EHA rods showed a decrease in adherence of *S. mutans* to surfaces after conditioning with salivary proteins. These results are consistent with previous work reported by others (1, 26, 27, 39, 40, 158, 216). The similarities also include the kinetics of adherence in which a rapid initial adherence followed by a period of slow or little increase in bacterial cell accumulation to unconditioned surfaces and a slow adhesion rate to conditioned surfaces. Interestingly, the accumulation of *S. mutans* cells on the saliva-coated

surface was lower than that on the BSA-coated surface, even though the rods had been conditioned with the same concentration of saliva and BSA. When monolayers were formed on EHA rods coated with 80 μg/ml SA, the number of *S. mutans* cells accumulated was higher than on the saliva-conditioned surface. The differences between the saliva-, BSA- and SA- samples were not, however, statistically significant. The results demonstrate how different surface pretreatments can affect subsequent bacterial adherence to surfaces.

Researchers examining the adherence of bacteria to a device to be implanted between the esophagus and the trachea found that preconditioning the surface with salivary proteins greatly decreased bacterial adherence to the surface (27). A correlation between the decreased lifespan of implanted devices observed in patients with decreased salivary flow, which was not observed in normal patients, suggests saliva plays a protective effect within the oral cavity to limit adhesion by depositing a pellicle of salivary proteins on enamel. Saliva may provide nonspecific mechanisms to limit adherence, but it is possible that some proteins or polysaccharides from saliva may behave as surfactants to limit adherence. The precise mechanism for the decreased bacterial adherence is unclear. Some reports suggest that the acquisition of a conditioning film makes the interaction electrostatically unfavorable due to charge repulsion between the negatively charged pellicle and bacterial surface (213). Others theorize that in the presence of a pellicle bacteria may adhere to the bare, positively charged, areas of the surface (1). While there may be some electrostatic repulsion, the idea of bacteria adhering to unconditioned "spots" on a conditioned surface was addressed by Gibbons and Etherdon (64). Experiments using bovine serum albumin as a blocking reagent following

conditioning with saliva diluted up to 1/25 did not affect adherence. However, increasing the dilution factor of saliva (1/125 and 1/625), prior to BSA blocking did result in decreased adherence. Decreased adherence may have been caused by a decreased number of binding sites resulting from sparse conditioning of the surface with salivary proteins. Two conclusions were drawn from this: (a) due to the efficiency of the formation of the conditioning film, a protein solution of relatively low concentration (1/25 diluted saliva) may be used to condition a surface such that there are few bare spots. In relation to the binding capacity of our rods this suggests that relatively small quantities of protein are required to provide a thin uniform layer of proteins on a surface. (b) BSA can be used to block any bare sites allowing one to measure adherence to surfaces conditioned with dilute protein solutions. These conclusions are critical when comparing the adherence of *S. mutans* NG8 and 834 to EHA conditioned with SA (1 - 80 μg/mL), since it was necessary to distinguish between specific and non-specific adherence. The equal adherence of NG8 and 834 to EHA conditioned with lower concentrations of SA, and the SA-dependent increase in adherence of NG8, but not 834, imply that the P1 - SA interaction mediates specific adherence to SA-conditioned EHA.

From a topographical point of view, a logical explanation for decreased bacterial adherence to conditioned surfaces is that the surface becomes irregular after a thick heterogeneous conditioning film forms on it, making it difficult for bacteria to adhere (26). In this instance the bacteria may reversibly associate with the surface prior to specific interactions with a component of the pellicle allowing firm attachment (213).

Detachment of adherent *S. mutans* NG8 from model biofilms.

Detachment of biofilm cells is considered a nonspecific event resulting from predator harvesting, shear-related removal, cell division, abrasion, or periodic sloughing of biofilm cells (5, 31, 38, 169). Recent research from this laboratory challenged this belief suggesting detachment of *S. mutans* from EHA rods conditioned with hog gastric mucin is induced by the activity of SPRE (123). However, the dental relevance of this detachment was unclear due to the conditioning films used in the model biofilms. The model biofilm developed in this study offers a more relevant system to examine *S. mutans* detachment than the hog gastric mucin model. Furthermore, additional advantages of the present model include: minimization of non-specific detachment due to shear forces, formation of monospecies biofilms to prevent competition for available binding sites or the possibilities of neighboring organisms secreting inhibitory compounds (29), and the cells used were viable, non-dividing bacteria to eliminate cell division as a source of error.

The optimal pH for detachment from saliva-conditioned EHA rods supported previous results demonstrating maximum detachment and surface protein release occurred between pHs of 5.5-6.0 (121). Detachment was also found to respond to increasing temperature. The increasing proportion of cells detaching as the temperature increased and the pH decreased may be mediated by SPRE.

At 10°C, 39 % of cells detached from the surface. This is similar to but slightly greater than the 25% detachment at pHs 7.0 and 7.5 at 37°C at which the SPRE activity is minimum. Hence, detachment at pH 7 at 37°C and pH 6 at 10°C may be the basal level of detachment in our system. Basal detachment could be attributed to SPRE-independent detachment of cells

reversibly or weakly associated with the substratum (46, 213). Unfortunately, the percentage of cells detaching from bare or BSA-conditioned rods was not determined. However if the percentage of cells detaching from the bare or BSA-conditioned rods was determined and found to be approximately 30%, it would support the theory of nonspecific detachment resulting from detachment of nonspecifically adherent cells. Alternatively, basal detachment may result from the loss of cells due to the detachment of the underlying conditioning film. In measuring the stability of the conditioning film we found 20% of the protein was lost during a one hour incubation in a protein free buffer. If a similar losses occur during the detachment experiment it is possible that cells adhering to the detaching conditioning film may also be lost. However, I favor the detachment of nonspecifically adherent cells to explain basal detachment. If there is a loss of a proportion of the conditioning film this loss would likely occur very quickly after removal of the rods from the protein solution in which they were conditioned, i.e during the biofilm formation phase of the experiment immediately following conditioning of the EHA rods.

The pH and temperature data collectively suggest that an active enzyme mediated process, in addition to a nonspecific phenomenon, results in the observed detachment. The dose-dependent release of biofilm cells by the SPRE and the abrogation of the SPRE activity by pretreatment of the SPRE with pronase further support the notion that SPRE functions enzymatically to release cells from biofilms. The active enzyme is likely to be the SPRE.

The complex nature of the salivary protein conditioning film made it difficult to draw conclusions on the mechanism of detachment as the specificity of cellular adherence to the substratum was uncharacterized. In monolayers formed on saliva-coated EHA, detachment

may be attributed not only to SPRE cleavage of P1 but also of other surface proteins, as a number of proteins (in addition to P1) can be released by SPRE (121). To impose specificity on adherence as to make conclusions regarding detachment, purified SA was used to condition EHA rods. The SA - P1 interaction was indicated by the increased adherence of *S. mutans* NG8, but not the isogenic P1-negative mutant 834, to EHA rods conditioned with SA. In this system where adherence is postulated to be facilitated by P1, detachment may be attributed to SPRE-mediated cleavage of P1 from the cell surface, allowing the bacterium to detach.

In the release of P1 from cells, SPRE apparently cleaves at or near the C-terminal structure that links P1 to the cell wall. This argument is made from the fact that P1 released from cells by SPRE is an intact 185 kDa molecule (Fig. 18), and that P1 is anchored to the *S. mutans* cell surface by its C terminus (83, 84). At this time, the exact site of P1 cleavage and the biochemical nature of the SPRE remain unknown.

Many surface proteins of gram-positive organisms share structural characteristics within the C-terminus which determines their surface localization. One of the characteristics is a LPXTGX consensus sequence (57). The conserved threonine within the hexapeptide repeat has been shown to anchor protein A of *S. aureus* to the cell wall and may play a similar function in other Gram-positive bacteria (83, 204). A significant proportion of surface proteins with the conserved C-terminal features are involved in adherence to surfaces via the recognition of specific surface structures, and have been reported to be released into the culture medium (53). It is tempting to speculate that SPRE may be a conserved enzyme among Gram-positive bacteria possessing similar C-terminal motifs and that it is responsible for cleaving

these surface proteins from the bacteria. If so, there would likely be a conserved sequence within the proteins which SPRE may recognize as its substrate. However, the LPXTGX is the only sequence conserved among all of the surface proteins. It is possible that SPRE may cleave within the LPXTGX thus cleaving the protein at the site of it's linkage to the cell wall. The possibility of a unique enzyme cleaving all gram-positive surface proteins with the LPXTGX motif may be ruled out since the enzyme that liberates M protein from *S. pyogenes* is different from SPRE in sensitivity to pH and inhibitors (121, 161). Other than within the protein, there are two additional sites at which SPRE may act. The enzyme may cleave the polysaccharide backbone of the peptidoglycan or it may cleave the stem peptide which the protein is covalently linked to. The later activity would be favored since it may be more efficient. By cleaving the stem peptide, the enzyme would only have to cleave one substrate to release the protein. Conversely, if the enzyme cuts within the polysaccharide backbone two enzymatic reactions may be required, one cleavage upstream and the other downstream of the N-acetyalmuramic acid residue the protein is linked to. Both of these activities are similar to that mediated by cellular autolysins (182).

While other researchers have targeted the degradation of extracellular polysaccharides encompassing the bacterium as a means to induce detachment of biofilm cells (93, 179), we have taken a different approach. Through our experiments we demonstrated that an endogenous enzyme detaches biofilm cells. Although we studied monospecies biofilms formed of resting cells that were not producing copious amounts of extracellular polysaccharides, it is possible that SPRE could detach more complex biofilms from surfaces. It has been said that the interaction between primary colonizers and the conditioning film is very strong (25).

Whether a biofilm will remain adhered to the surface then hinges upon the strength of the interaction between the substrata and the conditioning film. In experiments in which biofilm cells were detached by shear forces, an all-or-none phenomena was noted and there was no loss of proportions of the biofilm population. The detachment of the entire biofilm by a critical shear force may result from cohesive failure of the conditioning film (25). Since SPRE would disrupt the link between the conditioning film and the cells, SPRE activity would weaken the biofilm resulting in detachment of the biofilm at lower shear rates normally unable to induce detachment of the biofilm. This type of detachment may result in the clearing of the detached biofilms from the oral cavity, as large detaching clumps of biofilm cells may be cleared from the oral cavity. This type of detachment may provide an explanation for Byers' theory of the sloughing off of a large aggregates of biofilm cells resulting from uncharacterized intrinsic cellular processes (30). Conversely if the detaching bacterium was a secondary colonizer on the periphery of a biofilm, the bacterium may sense that the environment is becoming inhospitable and thus may employ the enzyme in order to detach and colonize another site.

Isolation and characterization of "SPRE-negative" mutants.

Once established, biofilms are extremely difficult to eradicate. In the conclusion of a literature review on biofilms, Gristina (69) stated that "The best strategy to prevent biofilm-resistant infection is to avoid microbial contamination." Without a doubt there would be immediate applications for an enzyme such as SPRE, which may be able to cleave proteins from numerous gram-positive bacteria. The cleavage could prevent planktonic organisms from

adhering to surfaces or possibly be instrumental in detachment of adherent populations. The enzyme only needs to be found! Once isolated, SPRE could be used daily as a component of a toothpaste or an oral rinse. However, use in toothpaste or oral rinses may not allow the enzyme sufficient time to function. An alternative may be to have dental professionals apply SPRE during regular dental check ups in a method similar to the application of fluoride. Fluoride is often administered as a paste dispensed onto a bite plate which is subsequently left in the mouth for a few minutes thus placing the paste and therefor the enzyme in direct contact with the enamel.

In this study, I have taken a molecular approach in an attempt to identify this enzyme. Using Tn*917*, two putative SPRE-negative mutants, A and E, were isolated. These mutants were identified by an increased surface - localised P1. Mutants A and E appear to be distinct mutants based on Southern hybridisation evidence. In comparison to the wild type, both mutants were impaired in their ability to release proteins, although the impairment was less pronounced for mutant E. Differences in surface protein release also translated into a decrease in detachment of biofilm cells. Detachment experiments showed that mutant A and mutant E detached less effectively that the wild type. These results strongly suggest that mutant A was SPRE - and detachment-deficient.

Genetic analysis of mutant A revealed that the transposon had inserted at an AT-rich region immediately upstream of the -35 region of an operon that we named *copYBZ* that appeared to be involved in copper transport in *S. mutans*. The role of this *cop* operon in detachment and cellular physiology will be discussed later.

The *cop* operon.

The *cop* operon of *S. mutans* JH1005 consists of three genes encoding a putative negative transcriptional regulatory protein (CopY), a cation transporting P-type ATPase (CopB), and a small globular protein (CopZ). To the best of our knowledge, this is the first report of a copper transport operon in the genus *Streptococcus*. The *cop* operon was also found in the genome of *S. mutans* UAB159, currently being sequenced at the University of Oklahoma. A comparison of the *S. mutans* JH1005 *cop* operon and the operon from strain UAB159 showed 98% sequence identity at the nucleotide level. The similarity began 380 bp upstream of *copY* and continued past the postulated terminator and into the beginning of the next open reading frame.

Overall, the *S. mutans cop* operon shares the most homology with the *E. hirae copYZAB* operon which has been demonstrated to confer high-level copper resistance to *E. hirae* (155-157). The *E. hirae cop* operon encodes two P-type ATPases, CopA and CopB, which respectively transport copper into and out of the cells, and CopY and CopZ, which regulate the expression of the ATPases and themselves (155). However, the genetic organization and the number of genes in the *S. mutans copYBZ* operon is different from that of *E. hirae* (*copYZAB*). Other characterized bacterial operons such as the *S. aureus cadAC* operon (49, 55, 119, 154) or the *H. pylori copAP* operon (61) encode structurally similar ATPase but, respectively, lack a *copZ* or a *copY* homologue.

The results of northern blotting suggest that the *cop* operon is transcribed as a single polycistronic message. A small hybridization band was observed at 1.4 kb, but this was too small to be the ATPase and too large to be *copY*. I thus concluded that this small

hybridization band was a degradation product. Of the larger signals, the 3.2 kb band matches the size of the *cop* operon while the 4 kb band may have resulted from inefficient termination. Primer extension results, which map the start site of transcription, reaffirmed the presence of the promoter at the -10 and -35 regions identified from the sequence.

Analysis of the open reading frames and function of the gene products.

CopB

The *S. mutans* CopB is a P-type ATPase which shares similarities with other ATPases that have specificity for copper or cadmium (11, 60, 154, 157, 162, 165). The similarities include a number of conserved structural and functional domains. The ATPases of *S. mutans, E. hirae, H. felis, H. pylori* and *L. sake* are each postulated to have eight transmembrane spanning hydrophobic regions as evidenced by hydropathy plots (Fig. 39). This group of heavy metal-transporting P-type ATPases are members of a larger superfamily of P-type ATPases. A recent study by Axelson and Palmgren (9) identified 211 P-type ATPases in the databases and sequence alignments showed 265 amino acids always aligned and contained minimal additions or deletions. The conserved amino acids were clustered around amino acids situated in the cytoplasmic loop between the fourth and fifth transmembrane segments, within the sixth transmembrane segment, and within the large cytoplasmic loop between transmembrane segments 6 and 7 (Fig. 40). These regions are responsible for binding ATP, phosphorylation of an aspartic acid, ion translocation and

Figure 39. Hydropathy plots of P-type ATPases, from *S. mutans*, *E. hirae*, *H. felis* and *L. sake*.

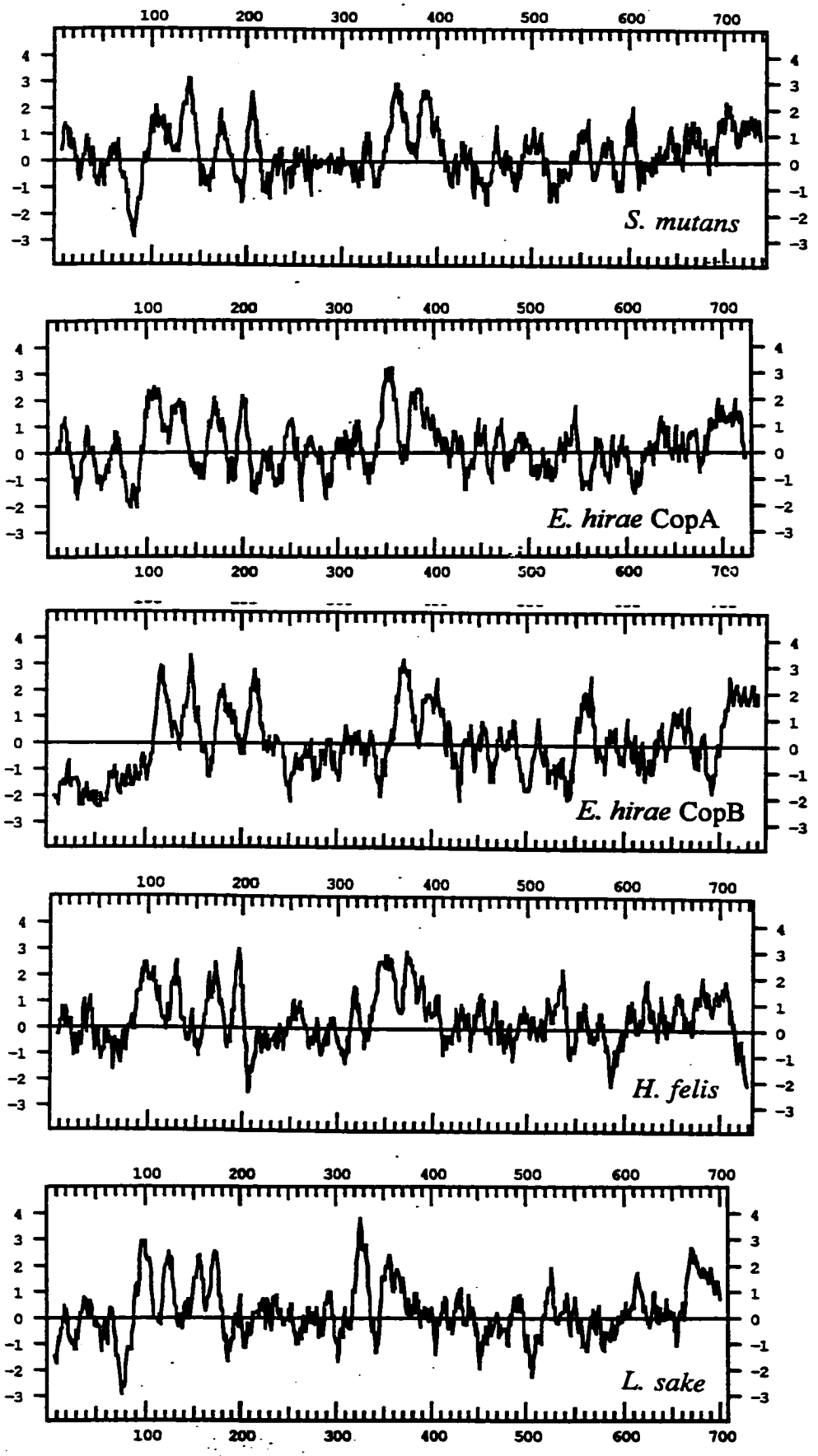
100
200
300
400
500
600
700
4
3
2
1
0
-1
-2
-3
S. mutans
E. hirae CopA
E. hirae CopB
H. felis
L. sake

Figure 40. Predicted membrane topology of *S. mutans* CopB. The amino acid sequence was input into TmPredict, which identified transmembrane regions indicated in Figure 26, allowing prediction of membrane topology.

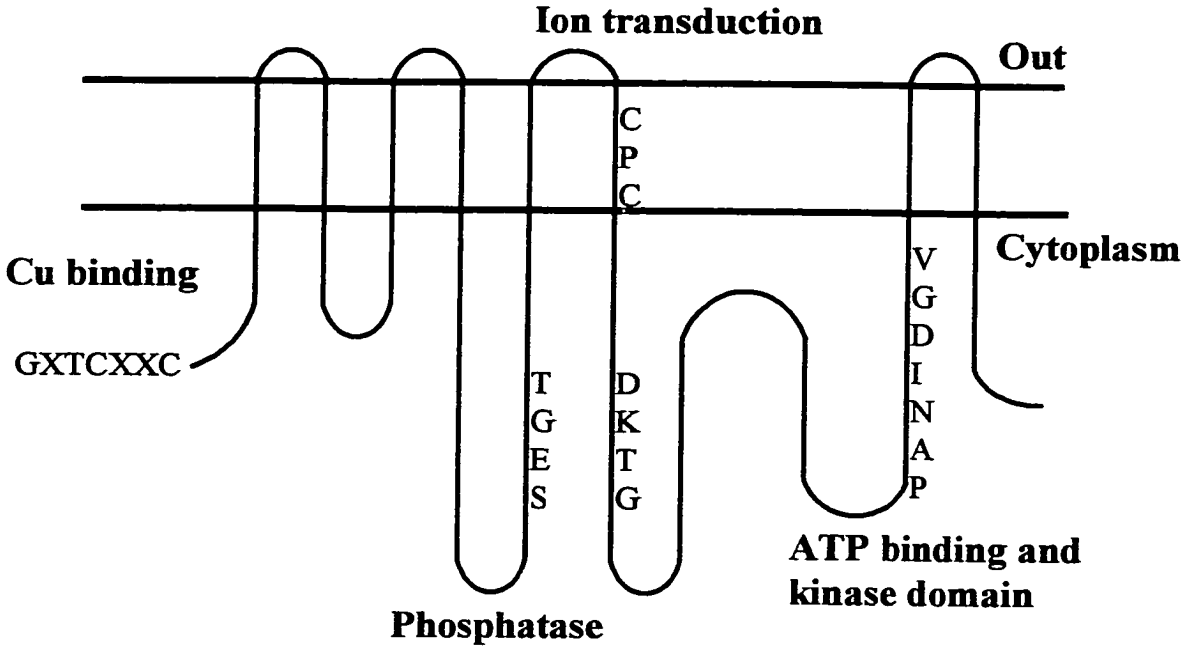
Ion transduction
Out
C
P
C
Cytoplasm
Cu binding
GXTCXXC
T
G
E
S
D
K
T
G
V
G
D
I
N
A
P
ATP binding and
kinase domain
Phosphatase

subsequent dephosphorylation of the aspartic acid. In relation to the topology of the protein, the conserved motifs can also be mapped to similar locations in each of the proteins. For example, the metal binding motif immediately precedes the first transmembrane domain, the TGES occurs just before the fifth transmembrane domain, the CPC transduction motif is within the sixth transmembrane domain, and a large cytoplasmic region between the sixth and seventh transmembrane domains contains the DKTG and the VGDGINAP motifs (Fig. 40). On average, the bacterial proteins are approximately 40% identical at the amino acid level. Not including the extended N-terminus in the comparison, the Menkes and Wilson proteins are 38% and 37% identical to CopB at the amino acid level. While the ATPases have similar sequences and structure, the ion specificity of the proteins may differ. CopB of *E. hirae* can transport Cu^{2+} and Ag^{2+}; CadA of *S. aureus* transports Cd^{2+}; and the CopA from *H. pylori* and *H. felis* transports Cu^{2+} (11, 154, 157). The results of our heavy metal susceptibility experiments suggest that CopB of *S. mutans* mainly transports copper. The ATPase enables the bacterium to tolerate extracellular copper concentrations of up to 8 mM. Without the ATPase, *S. mutans* S4 failed to grow in copper concentrations greater than 2 mM. Similar MIC's were noted for the wildtype *E. hirae* strain that could grow in 8 mM copper, but a *copB* knockout mutant was sensitive to 6 mM (155, 157). The ability of the wild type *S. mutans* strain to grow in higher copper concentrations than S4 implies that the *S. mutans* CopB functions to transport copper out of the cell.

CopY

CopY is similar to a few other bacterial negative transcriptional regulatory proteins. These proteins are bifunctional, with an N-terminal domain that interacts with DNA while the C-terminal domain allows the proteins to dimerize and interact with their respective effector molecule or ion. Examples of these regulatory proteins include MecI and BlaI of *S. aureus*, and BlaI and PenI of *B. licheniformis*, which regulate β-lactam resistance. The *S. mutans* CopY shares 31%, 29%, 28%, and 29% amino acid identity, respectively, to these proteins. However, CopY of *E. hirae* that regulates the expression of P-type ATPases which control intracellular copper homeostasis are of greater relevance to this analysis. CopY of *S. mutans* shares 35% amino acid identity to *E. hirae* CopY. These regulatory proteins have been shown to repress transcription by binding to inverted repeat sequences overlapping the promoter when the effector molecule (β-lactam antibiotics) or ions (Cu^{2+}) are respectively absent or at physiological levels . An ACA triplet at the promoter appears to be the recognition sequence for *E. hirae* CopY, the lambda repressor and *B. lichenformis* PenI (109, 192, 219, 222). For the ARC repressor of phage P22, the DNA sequence is AGA (103). The ACA triplet is also present within the inverted repeats of the *S. mutans cop* operon promoter. The regulatory proteins appear to have two different amino acid motifs that function to recognize the ACA in the promoter. The phage 434 repressor and *E. hirae* CopY have a glutamine pair at positions 30/31 and 29/30 respectively which are critical for DNA binding (109, 155). However, the glutamine pair is absent from *S. mutans* CopY, PenI, and the ARC repressor of phage P22. Research with the ARC repressor showed that the first nine amino acids of the

protein function to bind DNA (103), and PenI possess a similar sequence (218). Sequences similar to PenI and the ARC repressor are absent from the N-terminus of *S. mutans* CopY. However, *S. mutans* CopY does have a glutamine pair at position 82/83, and a glutamine-arginine-glutamine at positions 62-64, which may function similarly to *E. hirae* CopY if the protein adopts a slightly different tertiary structure.

The C-terminal $CXCX_4CXC$ motif is shared by heavy metal binding proteins such as CopY of *E. hirae*, CopP of *H. felis*, and the hypothetical protein encoded by *orfY* of *L. sake*. This motif may play an important role in de-repressing transcription of the *cop* operon as evidenced by studies with *E. hirae*. Results of experiment with CopY of *E. hirae* demonstrated that the binding of copper to CopY, presumably at the $CXCX_4CXC$ motif, caused dissociation of the protein-DNA complex as the copper concentration increased, thereby allowing transcription (155, 192, 222). As expected, this heavy metal binding motif is absent from transcriptional regulators (eg. MecI) not involved in heavy metal transport.

CopZ

CopZ is similar to the putative positive regulator CopZ of *E. hirae*. Cobine *et al.* (42) recently demonstrated the *E. hirae* CopZ protein could function as a chaperone delivering copper to CopY bound to the operator. In this capacity CopZ appears to function as an anti-repressor of the *cop* operon. However, previous results by the same group suggest that de-repression of the *cop* operon could be CopZ-independent at high concentrations of Cu^{2+} (192). In a gel mobility shift experiment, where increasing

concentrations of copper were added to a constant concentration of the promoter-CopY complex, the complex could be dissociated in the absence of CopZ (192). Our experiments with the CAT reporter gene showed that the growth of S4/CAT complemented with *copYBZ*, but not S4/CAT complemented with *copY*, could be restored by Cu^{2+}. This result indicates either CopB or CopZ can de-repress the *cop* promoter activity. Given the finding by Cobine *et al.* (42), CopZ is likely the anti-repressor. In our system, the role of CopZ in de-repression may be confirmed by constructing two additional plasmids, one expressing CopY and CopB, and the other expressing CopY and CopZ. Upon transformation of the plasmids into S4/CAT, these strains (plus those used in this study (Table 5) could be tested for growth in the presence of chloramphenicol and increasing concentrations of Cu^{2+}. If CopZ is the anti-repressor, we would expect that growth of S4/CAT complemented with *copYZ* would be induced at similar Cu^{2+} concentrations as S4/CAT complemented with *copYBZ*. Growth of S4/CAT complemented with *copYB* at higher Cu^{2+} would demonstrate two points: (i) the importance of CopZ for activation of transcription and (ii) that de-repression can be CopZ independent. Alternatively, the inability of S4/CAT complemented with *copYB* to grow at higher concentrations would imply CopZ is required for de-repression.

A possibility remains that CopZ could directly regulate the activity of the ATPase. In order to transduce ions, the ATPase must switch from the E1 (inactive) to the E2 (active) conformation. The E1 - E2 switch could be regulated by CopZ. Interaction between the Cu^{2+}-bound CopZ and the ATPase may induce the switch to E2. Alternatively, binding of CopZ alone to the ATPase may trap the ATPase in the E1

conformation and prevent ATP binding or the interaction between the large cytoplasmic loop containing the bound ATP and the phosphatase domain.

Regulation of the *S. mutans cop* operon.

The results of transcript analysis suggest that the expression of the *cop* operon is regulated. This statement is further supported by the results from the CAT reporter gene experiments (Table 5). In the transcript analysis experiments, we showed that a higher level of *cop* transcript was expressed by Cu^{2+}-induced cells than by the non-induced cells (Fig. 34). In the CAT reporter gene experiment, we showed that S4/CAT, but not S4/CAT complemented with *copY* or *copYBZ*, could grow in the presence of chloramphenicol. Furthermore, the growth of S4/CAT complemented with *copYBZ* could be restored by Cu^{2+}. These data collectively suggest that CopY is the negative regulator repressing the *cop* promoter activity. The repression can be de-repressed by Cu^{2+}. As indicated earlier, we suggest CopZ is the anti-repressor by delivering Cu^{2+} to CopY. In general, the mechanism of *cop* operon regulation in *S. mutans* is similar to that in *E. hirae*. This model of regulation, however, appears to be different from that of the *S. aureus cadAC* and the *H. pylori copAP*. The *S. aureus cadAC* does not have a CopZ analogue, so regulation may only be mediated at the level of transcription. The *H. pylori copAP* lacks a CopY homologue, hence, regulation may be controlled by some uncharacterized regulatory proteins. Alternatively, the expression of the *H. pylori* ATPase may be constitutive and CopP, the CopZ analogue, may regulate copper transport by controlling

the conformational state of the ATPase. In *S. mutans* and *E. hirae* there may be greater potential for more stringent regulation of intracellular copper, especially for *E. hirae* which also has an ATPase functional for copper import.

The results of the growth studies of mutant A also suggest that the *cop* promoter activity is regulated. We showed that mutant A is more resistant to Cu^{2+} than the wildtype (Fig. 36). The increase in resistance implies an increase in CopB activity. Such an increase may be due to an increase in transcription of the *cop* operon which may be the result of a decreased affinity of CopY for the inverted repeats overlapping the promoter. The decreased affinity of CopY to the promoter may be caused by the insertion of Tn*917* into the AT rich region immediately upstream of the promoter. In other systems, it is known that upstream sequences play a role in promoter activation (114). Hence, it is conceivable that the upstream sequence of the *cop* operon is also important for promoter activity. However, in this case, the upstream sequence is required for efficient binding by CopY.

Effect of the *cop* operon on physiology of *S. mutans*.

The primary function of the *cop* operon is likely to regulate intracellular copper concentrations. In this capacity the *cop* operon may be important for the ability of *S. mutans* to thrive in the oral cavity. Wataha *et al.* (217) have demonstrated that significant quantities (40 $\mu g/cm^2$) of copper ions could leech out of dental casting alloys. Similarly, Leirskar (129) showed that copper ions could also leech out from dental amalgam. In

light of these findings, it is safe to say that *S. mutans* is constantly exposed to Cu^{2+} and that by possessing a functional ATPase capable of pumping copper out of the cell, *S. mutans* would definitely have a competitive advantage over other bacteria.

As indicated in the literature review, P-type ATPase of *L. monocytogenes* and *P. mirabilis* are associated with virulence and swarming phenomena, respectively. These findings suggest that the *cop* operon may have other physiological roles in addition to copper transport. In *S. mutans*, one such role may be in modulation of SPRE activity. We demonstrated that the *cop* operon enables *S. mutans* to tolerate high concentrations of extracellular Cu^{2+}. The ATPase may also be important for the bacterium to tolerate the changing environment it occupies in the oral cavity. The cell depends on the ATPase to regulate the cytoplasmic concentration of heavy metals. Heavy metal concentrations must be within a range that is non-toxic and provides the copper as a cofactor necessary for cellular enzymes to function properly. The cell may also count on the ATPase to regulate copper or other metal ions in such a way that will allow the cell to sense how much copper is in the environment. For example if the copper concentration is high enough to induce the ATPase, the copper concentration may also be a signal for regulation of other genes such as the SPRE gene. So while the cell membrane allows cells to maintain a certain intracellular environment, changes in that environment as a result of extracellular process must be able to occur for the bacteria to respond to them. In this case, the response may be the induction of SPRE, allowing *S. mutans* to detach and colonize other sites.

Our results clearly showed that mutant A has a deficiency in SPRE activity, suggesting a role of the *cop* operon in this activity. However, the *cop*-knock-out mutant S4 did not show an altered SPRE activity (Table 6). This result makes it difficult to explain the relationship between the *cop* operon and SPRE activity. However, I think there are two possible mechanisms which could account for the decreased SPRE activity

in mutant A: (i) CopY could directly or indirectly affect the expression of SPRE or (ii) increased CopB production in mutant A may result in decreased cytoplasmic concentration of heavy metals resulting in decreased expression or activity of SPRE. As discussed earlier mutant A is likely to have an increased expression of the *cop* proteins due to the Tn*917* insertion. Excess copies of CopY in the cells may have negatively regulated the expression of SPRE, either by directly binding to the SPRE promoter or by repressing transcription of a factor that is required for SPRE expression. Alternatively, SPRE may require heavy metals for activity or its expression. With an increased expression of CopB, it is conceivable that mutant A may have a lower intracellular Cu^{2+}, or other heavy metal ion concentration, than the wildtype and mutant S4. This condition leads to a decrease in SPRE activity if SPRE is a metalloenzyme. Alternatively, the low intracellular metal ions may have affected the ability of ion-dependent factors to express SPRE. In the case of the wildtype cells, because of the tightly-regulated nature of the *cop* operon, excess copies of CopY and CopB are probably not present under low Cu^{2+} conditions to downregulate SPRE activity or expression. In S4, CopY and CopB are not present at all. These explanations may account for the same SPRE and detachment activity displayed by the wildtype and mutant S4 cells.

The *cop* operon also appears to have some effects on cell wall-related properties of *S. mutans*. We showed that mutant A was osmotically more fragile than the wild type. Osmotic fragility is a function of cell wall strength. Increased osmotic fragility will result from a weakened cell wall unable to tolerate osmotic shock. The observed difference in the cell wall strength between JH1005 and mutant A may be the result of a decreased activity of peptidoglycan synthases or an increased activity of autolysins. We did not find any difference in cellular autolysis between JH1005 and mutant A (Fig. 37), suggesting the total autolytic activity in mutant A has not been altered. On the other hand, a decrease in

peptidoglycan synthases activity is possible in mutant A. There are reports of cell wall carboxypeptidases that are metallo(zinc) enzymes (86, 221). In mutant A, functional cell wall metalloenzymes may not be able to function due to the increased CopB activity.

CONCLUSIONS

Improvements made to model biofilms provide evidence that detachment of biofilm cells is an active enzyme mediated process. Future purification of SPRE, the enzyme postulated to cause detachment, would be very beneficial as it may allow us to detach *S. mutans* from enamel. SPRE may also have the ability to detach other bacteria from a wide variety of surfaces. As with any enzyme, the cell must be able to control SPRE. Further study may allow us to learn more about the environmental stimuli and intracellular processes affecting SPRE activity.

A genetic locus, the *cop* operon, which appears to affect detachment, was identified. Further characterization of the *cop* proteins may be the first step in identifying environmental factors which influence cellular processes such as surface-protein release and detachment of cells from biofilms.

In itself, identification and characterization of the *cop* operon is a significant discovery. The *cop* operon may provide *S. mutans* with a competitive advantage in an environment in which it may be exposed to heavy metals leeching out of amalgam. Further *in-vitro* experimentation assaying the tolerance of the wild type and *cop* knock out strains adhered to surfaces containing copper, i.e. EHA-$CuSO_4$, may illustrate the importance of the *cop* operon for the survival of *S. mutans*. The same model may also give us an opportunity to examine the extent of detachment of *S. mutans* when exposed to copper. This may provide insights into the interactions between the *cop* operon and the SPRE, as well as the role SPRE plays in defining the sites *S. mutans* colonizes or detaches from.

With additional in-vivo experimentation to determine the ability of *cop* operon knock out to cause caries the ATPase may also be added to the list of attributes classifying *S. mutans*

as an ondontopathogen. In conclusion this work has taken preliminary steps to understand how environmental factors affect cellular processes that could lead to changes in oral ecology.

APPENDIX A

Resting Cell Buffer: The following solutions were prepared and autoclaved separately. Solutions 1, 2, and 3 were prepared as stock solutions and stored at -20°C. When required the basic solution was prepared and solutions 1, 2, and 3 were added as indicated.

Basic Solution (pH 7.2)	1 L
Potassium Phosphate Monobasic	6 g
Potassium Phosphate Dibasic	9 g
$CaCl_2$	20 mg
$MgSO_4$	200 mg
$NaCH_3COO$	300 mg
L-Glutamic Acid	1.5 g

- pH 7.2

Solution 1	1 L
PAB	200 mg
Thiamine	200 mg
Riboflavin	200 mg
Nicotinic Acid	200 mg
Pyridoxal Phosphate	200 mg
Inositol	200 mg
Ca Pantothenate	200 mg

- dissolve ingredients in deionized H_2O
- pH 7.0
- add 10 mL in 1 L of basic solution.

Solution 2	100 mL
DL-Thioctic Acid	10 mg
Biotin	10 mg
Haemin	10 mg
Folic Acid	20 mg

- dissolve haemin first in 1 drop dH_2O + 1 drop ammonium hydroxide
- add 1 mL to 1 L of basic solution.

Solution 3	100 mL
Ferrous Sulfate	400 mg
Manganous Sulfate	15 mg
Sodium Molybdate	15 mg

- add 1 mL to 1 L of basic solution.

REFERENCES

1. **Abbott, A., and M. L. Hayes.** 1984. The conditioning role of saliva in streptococcal attachment to hydroxyapatite surfaces. J. Gen. Microbiol. **130:**809-16.

2. **Abo, H., T. Matsumura, T. Kodama, H. Ohta, K. Fukui, K. Kato, and H. Kagawa.** 1991. Peptide sequences for sucrose splitting and glucan binding within *Streptococcus sobrinus* glucosyltransferase (water-insoluble glucan synthetase). J Bacteriol. **173:**989-96.

3. **Agranoff, D. D., and S. Krishna.** 1998. Metal ion homeostasis and intracellular parasitism. Mol. Microbiol. **28:**403-12.

4. **Al-Hashimi, I., and M. J. Levine.** 1989. Characterization of in vivo salivary-derived enamel pellicle. Arch. Oral. Biol. **34:**289-95.

5. **Allison, D. G., D. J. Evans, M. R. Brown, and P. Gilbert.** 1990. Possible involvement of the division cycle in dispersal of *Escherichia coli* from biofilms. J. Bacteriol. **172:**1667-9.

6. **Anderson, P., and J. C. Elliott.** 1985. Scanning X-ray microradiographic study of the formation of caries-like lesions in synthetic apatite aggregates. Caries Res. **19:**403-6.

7. **Archibald, A. R., I. C. Hancock, and C. R. Hardwood.** 1993. Cell Wall Structure, Synthesis, and Turnover., p. 381-410. *In* A. L. Sonenshein (ed.), *Bacillus subtilis* and other gram positive bacteria. ASM Press, Washington.

8. **Ashwell, G.** 1957. Colorimetric analysis of sugars. Methods of Enzymology **3:**73-105.

9. **Axelsen, K. B., and M. G. Palmgren.** 1998. Evolution of substrate specificities in the P-type ATPase superfamily. J. Mol. Evol. **46:**84-101.

10. **Ayakawa, G. Y., L. W. Boushell, P. J. Crowley, G. W. Erdos, W. P. McArthur, and A. S. Bleiweis.** 1987. Isolation and characterization of monoclonal antibodies specific for antigen P1, a major surface protein of mutans streptococci. Infect. Immun. **55:**2759-67.

11. **Bayle, D., S. Wangler, T. Weitzenegger, W. Steinhilber, J. Volz, M. Przybylski, K. P. Schafer, G. Sachs, and K. Melchers.** 1998. Properties of the P-type ATPases encoded by the *copAP* operons of *Helicobacter pylori* and *Helicobacter felis*. J. Bacteriol. **180:**317-29.

12. **Bearson, S., B. Bearson, and J. W. Foster.** 1997. Acid stress responses in enterobacteria. FEMS Microbiol. Lett. **147:**173-80.

13. **Belli, W. A., and R. E. Marquis.** 1991. Adaptation of *Streptococcus mutans* and *Enterococcus hirae* to acid stress in continuous culture. Appl. Environ. Microbiol. **57:**1134-8.

14. **Bender, G. R., S. V. Sutton, and R. E. Marquis.** 1986. Acid tolerance, proton permeabilities, and membrane ATPases of oral streptococci. Infect. Immun. **53:**331-8.

15. **Bockmann, R., C. Dickneite, B. Middendorf, W. Goebel, and Z. Sokolovic.** 1996.

Specific binding of the *Listeria monocytogenes* transcriptional regulator PrfA to target sequences requires additional factor(s) and is influenced by iron. Mol. Microbiol. **22:**643-53.

16. **Bowen, W. H., K. Schilling, E. Giertsen, S. Pearson, S. F. Lee, A. Bleiweis, and D. Beeman.** 1991. Role of a cell surface-associated protein in adherence and dental caries. Infect. Immun. **59:**4606-9.

17. **Bradford, M. M.** 1976. A rapid and sensitive method for the quantitation of microgram quantities of protein utilizing the principle of protein-dye binding. Anal. Biochem. **72:**248-54.

18. **Bradshaw, D. J., K. A. Homer, P. D. Marsh, and D. Beighton.** 1994. Metabolic cooperation in oral microbial communities during growth on mucin. Microbiology **140:**3407-12.

19. **Bradshaw, D. J., P. D. Marsh, K. M. Schilling, and D. Cummins.** 1996. A modified chemostat system to study the ecology of oral biofilms. J. Appl. Bacteriol. **80:**124-30.

20. **Bradshaw, D. J., A. S. McKee, and P. D. Marsh.** 1990. Prevention of population shifts in oral microbial communities in vitro by low fluoride concentrations. J. Dent. Res. **69**(2):436-41.

21. **Brady, L. J., D. G. Cvitkovitch, C. M. Geric, M. N. Addison, J. C. Joyce, P. J. Crowley, and A. S. Bleiweis.** 1998. Deletion of the central proline-rich repeat domain results in altered antigenicity and lack of surface expression of the *Streptococcus mutans* P1 adhesin molecule. Infect. Immun. **66:**4274-82.

22. **Brady, L. J., D. A. Piacentini, P. J. Crowley, P. C. Oyston, and A. S. Bleiweis.** 1992. Differentiation of salivary agglutinin-mediated adherence and aggregation of mutans streptococci by use of monoclonal antibodies against the major surface adhesin P1. Infect. Immun. **60:**1008-17.

23. **Brown, A. T., and C. L. Wittenberger.** 1971. The occurrence of multiple glyceraldehyde-3-phosphate dehydrogenases in cariogenic streptococci. Biochem. Biophys. Res. Commun. **43:**217-24.

24. **Burne, R. A.** 1997. Oral Streptococci, products of their environment. J. Dent. Res. **77:**445-48.

25. **Busscher, H. J., R. Bos, and H. C. van der Mei.** 1995. Initial microbial adhesion is a determinant for the strength of biofilm adhesion. FEMS Microbiol. Lett. **128:**229-34.

26. **Busscher, H. J., G. I. Doornbusch, and H. C. Van der Mei.** 1992. Adhesion of mutants streptococci to glass with and without a salivary coating as studied in a parallel-plate flow chamber. J. Dent. Res. **71:**491-500.

27. **Busscher, H. J., G. I. Geertsema-Doornbusch, and H. C. van der Mei.** 1997. Adhesion to silicone rubber of yeasts and bacteria isolated from voice prostheses: influence of salivary conditioning films. J. Biomed. Mater. Res. **34:**201-9.

28. **Busscher, H. J., H. M. Uyen, I. Stokroos, and W. L. Jongebloed.** 1989. A transmission electron microscopy study of the adsorption patterns of early developing artificial pellicles on human enamel. Arch. Oral Biol. **34:**803-10.

29. **Busscher, H. J., and H. C. van der Mei.** 1997. Physico-chemical interactions in

initial microbial adhesion and relevance for biofilm formation. Adv. Dent. Res. **11:**24-32.

30. **Byers, J. D.** 1988. Modeling biofilm accumulation., p. 109-144. *In* M. Bazin, J. and J. I. Prosser (ed.), Physiological Models in Microbiology, vol. vol. 2. CRC, Boca Raton.

31. **Caldwell, D. E.** 1987. Microbial colonization of solid-liquid interfaces. Ann. NY Acad. Sci. **506:**274-80.

32. **Carlsson, J., H. Grahnen, G. Jonsson, and S. Wikner.** 1970. Establishment of *Streptococcus sanguis* in the mouths of infants. Arch. Oral Biol. **15:**1143-8.

33. **Carlsson, J., and C. J. Griffith.** 1974. Fermentation products and bacterial yields in glucose-limited and nitrogen-limited cultures of streptococci. Arch. Oral Biol. **19:**1105-9.

34. **Characklis, W. G.** 1990. Biofilm Processes, p. 195-231. *In* W. G. Characklis and K. C. Marshall (ed.), Biofilms. John Wiley & Sons, NY., New York.

35. **Cheung, H. Y., and E. Freese.** 1985. Monovalent cations enable cell wall turnover of the turnover-deficient *lyt*-15 mutant of *Bacillus subtilis*. J. Bacteriol. **161:**1222-5.

36. **Childers, N. K., F. R. Denys, N. F. McGee, and S. M. Michalek.** 1990. Ultrastructural study of liposome uptake by M cells of rat Peyer's patch: an oral vaccine system for delivery of purified antigen. Reg Immunol **3**(1):8-16.

37. **Childers, N. K., S. S. Zhang, and S. M. Michalek.** 1994. Oral immunization of humans with dehydrated liposomes containing *Streptococcus mutans* glucosyltransferase induces salivary immunoglobulin A2 antibody responses. Oral

Microbiol. Immunol. **9:**146-53.

38. **Christersson, C. E., P. O. Glantz, and R. E. Baier.** 1988. Role of temperature and shear forces on microbial detachment. Scand. J. Dent. Res. **96:**91-8.

39. **Clark, W. B., L. L. Bammann, and R. J. Gibbons.** 1978. Comparative estimates of bacterial affinities and adsorption sites on hydroxyapatite surfaces. Infect. Immun. **19:**846-53.

40. **Clark, W. B., and R. J. Gibbons.** 1977. Influence of salivary components and extracellular polysaccharide synthesis from sucrose on the attachment of *Streptococcus mutans* 6715 to hydroxyapatite surfaces. Infect. Immun. **18:**514-23.

41. **Clarke, J. K.** 1924. On the bacterial factor in the aetiology of dental caries. British J. Exp. Path. **5:**141-47.

42. **Cobine, P., W. A. Wickramasinghe, M. D. Harrison, T. Weber, M. Solioz, and C. T. Dameron.** 1999. The *Enterococcus hirae* copper chaperone CopZ delivers copper(I) to the CopY repressor. FEBS Lett. **445:**27-30.

43. **Cole, M. F., G. H. Bowden, D. C. Korts, and W. H. Bowen.** 1978. The effect of pyridoxine, phytate and invert sugar on production of plaque acids in situ in the monkey (M. fascicularis). Caries Res. **12:**190-201.

44. **Costerton, J. W., K. J. Cheng, G. G. Geesey, T. I. Ladd, J. C. Nickel, M. Dasgupta, and T. J. Marrie.** 1987. Bacterial biofilms in nature and disease. Annu. Rev. Microbiol. **41:**435-64.

45. **Costerton, J. W., B. Ellis, K. Lam, F. Johnson, and A. E. Khoury.** 1994. Mechanism of electrical enhancement of efficacy of antibiotics in killing biofilm

bacteria. Antimicrob. Agents Chemother. **38:**2803-9.

46. **Cowan, M. M., K. G. Taylor, and R. J. Doyle.** 1986. Kinetic analysis of *Streptococcus sanguis* adhesion to artificial pellicle. J. Dent. Res. **65:**1278-83.

47. **Crowley, P. J., L. J. Brady, S. M. Michalek, and A. S. Bleiweis.** 1999. Virulence of a *spaP* mutant of *Streptococcus mutans* in a gnotobiotic rat model. Infect. Immun. **67:**1201-6.

48. **Crowley, P. J., L. J. Brady, D. A. Piacentini, and A. S. Bleiweis.** 1993. Identification of a salivary agglutinin-binding domain within cell surface adhesin P1 of *Streptococcus mutans*. Infect. Immun. **61:**1547-52.

49. **Crupper, S. S., V. Worrell, G. C. Stewart, and J. J. Iandolo.** 1999. Cloning and expression of *cadD*, a new cadmium resistance gene of *Staphylococcus aureus*. J. Bacteriol. **181:**4071-5.

50. **Dameron, C. T., and M. D. Harrison.** 1998. Mechanisms for protection against copper toxicity. Am. J. Clin. Nutr. **67:**1091S-1097S.

51. **Dashper, S. G., and E. C. Reynolds.** 1992. pH regulation by *Streptococcus mutans*. J. Dent. Res. **71:**1159-65.

52. **Demuth, D. R., P. Berthold, P. S. Leboy, E. E. Golub, C. A. Davis, and D. Malamud.** 1989. Saliva-mediated aggregation of *Enterococcus faecalis* transformed with a *Streptococcus sanguis* gene encoding the SSP-5 surface antigen. Infect. Immun. **57:**1470-5.

53. **Dramsi, S., P. Dehoux, and P. Cossart.** 1993. Common features of gram-positive bacterial proteins involved in cell recognition [letter]. Mol. Microbiol. **9:**1119-21.

54. **Dunny, G. M., L. N. Lee, and D. J. LeBlanc.** 1991. Improved electroporation and cloning vector system for gram-positive bacteria. Appl. Environ. Microbiol. **57:**1194-201.

55. **Endo, G., and S. Silver.** 1995. CadC, the transcriptional regulatory protein of the cadmium resistance system of *Staphylococcus aureus* plasmid pI258. J. Bacteriol. **177:**4437-41.

56. **Ericson, T., and J. Rundegren.** 1983. Characterization of a salivary agglutinin reacting with a serotype c strain of *Streptococcus mutans*. Eur. J. Biochem. **133:**255-61.

57. **Fischetti, V. A., V. Pancholi, and O. Schneewind.** 1990. Conservation of a hexapeptide sequence in the anchor region of surface proteins from gram-positive cocci. Mol. Microbiol. **4:**1603-5.

58. **Francis, M. S., and C. J. Thomas.** 1997. The *Listeria monocytogenes* gene *ctpA* encodes a putative P-type ATPase involved in copper transport. Mol. Gen. Genet. **253:**484-91.

59. **Francis, M. S., and C. J. Thomas.** 1997. Mutants in the CtpA copper transporting P-type ATPase reduce virulence of *Listeria monocytogenes*. Microb. Pathog. **22:**67-78.

60. **Ge, Z., K. Hiratsuka, and D. E. Taylor.** 1995. Nucleotide sequence and mutational analysis indicate that two *Helicobacter pylori* genes encode a P-type ATPase and a cation-binding protein associated with copper transport. Mol. Microbiol. **15:**97-106.

61. **Ge, Z., and D. E. Taylor.** 1996. *Helicobacter pylori* genes *hpcop*A and *hpcop*P

constitute a cop operon involved in copper export. FEMS Microbiol. Lett. **145:**181-8.

62. **Geddes, D. A.** 1975. Acids produced by human dental plaque metabolism in situ. Caries. Res. **9:**98-109.

63. **Ghuysen, J. M.** 1991. Serine beta-lactamases and penicillin-binding proteins. Annu. Rev. Microbiol. **45:**37-67.

64. **Gibbons, R. J., and I. Etherden.** 1985. Albumin as a blocking agent in studies of streptococcal adsorption to experimental salivary pellicles. Infect. Immun. **50:**592-4.

65. **Goffin, C., and J. M. Ghuysen.** 1998. Multimodular penicillin-binding proteins: an enigmatic family of orthologs and paralogs. Microbiol. Mol. Biol. Rev. **62:**1079-93.

66. **Goldmann, D. A., and G. B. Pier.** 1993. Pathogenesis of infections related to intravascular catheterization. Clin. Microbiol. Rev. **6:**176-92.

67. **Grenby, T. H., and M. G. Saldanha.** 1986. Studies of the inhibitory action of intense sweeteners on oral microorganisms relating to dental health. Caries Res. **20:**7-16.

68. **Gristina, A. G.** 1994. Biofilms and chronic bacterial infections. Clinical Microbiology Newsletter **16:**171-78.

69. **Gristina, A. G.** 1987. Biomaterial-centered infection: microbial adhesion versus tissue integration. Science **237:**1588-95.

70. **Gutierrez, J. A., P. J. Crowley, D. P. Brown, J. D. Hillman, P. Youngman, and A. S. Bleiweis.** 1996. Insertional mutagenesis and recovery of interrupted genes of

Streptococcus mutans by using transposon Tn*917*: preliminary characterization of mutants displaying acid sensitivity and nutritional requirements. J. Bacteriol. **178:**4166-75.

71. **Hajishengallis, G., M. W. Russell, and S. M. Michalek.** 1998. Comparison of an adherence domain and a structural region of *Streptococcus mutans* antigen I/II in protective immunity against dental caries in rats after intranasal immunization. Infect. Immun. **66:**1740-3.

72. **Hamilton, I. R., and G. H. Bowden.** 1992. Oral Microbiology, p. 269-281, Encyclopedia of Microbiology, vol. 3. Academic Press.

73. **Hamilton, I. R., and N. D. Buckley.** 1991. Adaptation by *Streptococcus mutans* to acid tolerance. Oral Microbiol. Immunol. **6:**65-71.

74. **Hamilton, I. R., and G. Svensater.** 1998. Acid-regulated proteins induced by *Streptococcus mutans* and other oral bacteria during acid shock. Oral Microbiol. Immunol. **13:**292-300.

75. **Hanada, N., and H. K. Kuramitsu.** 1988. Isolation and characterization of the *Streptococcus mutans gtfC* gene, coding for synthesis of both soluble and insoluble glucans. Infect. Immun. **56:**1999-2005.

76. **Hanada, N., and H. K. Kuramitsu.** 1989. Isolation and characterization of the *Streptococcus mutans gtfD* gene, coding for primer-dependent soluble glucan synthesis. Infect. Immun. **57:**2079-85.

77. **Harokopakis, E., G. Hajishengallis, T. E. Greenway, M. W. Russell, and S. M. Michalek.** 1997. Mucosal immunogenicity of a recombinant *Salmonella*

typhimurium-cloned heterologous antigen in the absence or presence of coexpressed cholera toxin A2 and B subunits. Infect. Immun. **65:**1445-54.

78. **Harper, D. S., and W. J. Loesche.** 1983. Effect of pH upon sucrose and glucose catabolism by the various genogroups of *Streptococcus mutans*. J. Dent. Res. **62:**526-31.

79. **Hay, D. I.** 1967. The adsorption of salivary proteins by hydroxyapatite and enamel. Arch. Oral Biol. **12:**937-46.

80. **Hazlett, K. R., S. M. Michalek, and J. A. Banas.** 1998. Inactivation of the *gbpA* gene of *Streptococcus mutans* increases virulence and promotes in vivo accumulation of recombinations between the glucosyltransferase B and C genes. Infect. Immun. **66:**2180-5.

81. **Heijenoort, J.-V.** 1994. Biosynthesis of the bacterial peptidoglycan unit., p. 39-54. *In* G. J.-M. and R. Hackenbeck (ed.), Bacterial Cell Wall. Elsevier.

82. **Holtje, J. V.** 1998. Growth of the stress-bearing and shape-maintaining murein sacculus of *Escherichia coli*. Microbiol. Mol. Biol. Rev. **62:**181-203.

83. **Homonylo-McGavin, M. K., and S. F. Lee.** 1996. Role of the C terminus in antigen P1 surface localization in *Streptococcus mutans* and two related cocci. J. Bacteriol. **178:**801-7.

84. **Homonylo-McGavin, M. K., S. F. Lee, and G. H. Bowden.** 1999. Subcellular localization of the *Streptococcus mutans* P1 protein C terminus. Can. J. Microbiol. **45:**536-9.

85. **Honda, O., C. Kato, and H. K. Kuramitsu.** 1990. Nucleotide sequence of the

Streptococcus mutans gtfD gene encoding the glucosyltransferase-S enzyme. J. Gen. Microbiol. **136:**2099-105.

86. **Hourdou, M. L., M. Guinand, M. J. Vacheron, G. Michel, L. Denoroy, C. Duez, S. Englebert, B. Joris, G. Weber, and J. M. Ghuysen.** 1993. Characterization of the sporulation-related gamma-D-glutamyl-(L)meso- diaminopimelic-acid-hydrolysing peptidase I of *Bacillus sphaericus* NCTC 9602 as a member of the metallo(zinc) carboxypeptidase A family. Modular design of the protein. Biochem. J. **292:**563-70.

87. **Hudson, M. C., and G. C. Stewart.** 1986. Differential utilization of *Staphylococcus aureus* promoter sequences by *Escherichia coli* and *Bacillus subtilis*. Gene **48:**93-100.

88. **Isokangas, P., J. Tenovuo, E. Soderling, H. Mannisto, and K. K. Makinen.** 1991. Dental caries and mutans streptococci in the proximal areas of molars affected by the habitual use of xylitol chewing gum. Caries. Res. **25:**444-8.

89. **Iwami, Y., and T. Yamada.** 1980. Rate-limiting steps of the glycolytic pathway in the oral bacteria *Streptococcus mutans* and *Streptococcus sanguis* and the influence of acidic pH on the glucose metabolism. Arch. Oral Biol. **25:**163-9.

90. **Jayaraman, G. C., J. E. Penders, and R. A. Burne.** 1997. Transcriptional analysis of the *Streptococcus mutans hrcA*, *grpE* and *dnaK* genes and regulation of expression in response to heat shock and environmental acidification. Mol. Microbiol. **25:**329-41.

91. **Jenkinson, H. F.** 1994. Cell surface protein receptors in oral streptococci. FEMS

Microbiol. Lett. **121:**133-40.

92. **Jenkinson, H. F., R. A. Baker, and G. W. Tannock.** 1996. A binding-lipoprotein-dependent oligopeptide transport system in *Streptococcus gordonii* essential for uptake of hexa- and heptapeptides. J. Bacteriol. **178:**68-77.

93. **Johansen, C., P. Falholt, and L. Gram.** 1997. Enzymatic removal and disinfection of bacterial biofilms. Appl. Environ. Microbiol. **63:**3724-8.

94. **Joliffe, L. K., R. J. Doyle, and U. N. Streips.** 1981. The energized membrane and cellular autolysis in *Bacillus subtilis*. Cell **25:**753-763.

95. **Jolliffe, L. K., R. J. Doyle, and U. N. Streips.** 1980. Extracellular proteases modify cell wall turnover in *Bacillus subtilis*. J. Bacteriol. **141:**1199-208.

96. **Kashket, S., and E. R. Kashket.** 1985. Dissipation of the proton motive force in oral streptococci by fluoride. Infect. Immun. **48:**19-22.

97. **Kato, C., and H. K. Kuramitsu.** 1990. Carboxyl-terminal deletion analysis of the *Streptococcus mutans* glucosyltransferase-I enzyme. FEMS Microbiol. Lett. **60:**299-302.

98. **Kato, C., and H. K. Kuramitsu.** 1991. Molecular basis for the association of glucosyltransferases with the cell surface of oral streptococci. FEMS Microbiol. Lett. **63:**153-7.

99. **Kato, C., Y. Nakano, M. Lis, and H. K. Kuramitsu.** 1992. Molecular genetic analysis of the catalytic site of *Streptococcus mutans* glucosyltransferases. Biochem. Biophys. Res. Commun. **189:**1184-8.

100. **Katz, J., C. C. Harmon, G. P. Buckner, G. J. Richardson, M. W. Russell, and S.**

M. Michalek. 1993. Protective salivary immunoglobulin A responses against *Streptococcus mutans* infection after intranasal immunization with *S. mutans* antigen I/II coupled to the B subunit of cholera toxin. Infect. Immun. **61:**1964-71.

101. **Kelly, C., P. Evans, L. Bergmeier, S. F. Lee, A. Progulske-Fox, A. C. Harris, A. Aitken, A. S. Bleiweis, and T. Lehner.** 1989. Sequence analysis of the cloned streptococcal cell surface antigen I/II. FEBS Lett. **258:**127-32.

102. **Kirchner, G., M. A. Kemper, A. L. Koch, and R. J. Doyle.** 1988. Zonal turnover of cell poles of *Bacillus subtilis*. Ann. Inst. Pasteur. Microbiol. **139:**645-54.

103. **Knight, K. L., and R. T. Sauer.** 1989. DNA binding specificity of the Arc and Mnt repressors is determined by a short region of N-terminal residues. Proc. Natl. Acad. Sci. U.S.A. **86:**797-801.

104. **Kobayashi, H., T. Suzuki, and T. Unemoto.** 1986. Streptococcal cytoplasmic pH is regulated by changes in amount and activity of a proton-translocating ATPase. J. Biol. Chem. **261:**627-30.

105. **Koch, A. L., and R. J. Doyle.** 1985. Inside-to-outside growth and turnover of the wall of gram-positive rods. J. Theor. Biol. **117:**137-57.

106. **Koch, A. L., G. Kirchner, R. J. Doyle, and I. D. Burdett.** 1985. How does a Bacillus split its septum right down the middle? Ann. Inst. Pasteur Microbiol. **136A:**91-8.

107. **Kohler, B., D. Birkhed, and S. Olsson.** 1995. Acid production by human strains of *Streptococcus mutans* and *Streptococcus sobrimus*. Caries Res. **29:**402-6.

108. **Kolenbrander, P. E., and J. London.** 1993. Adhere today, here tomorrow: oral

bacterial adherence. J. Bacteriol. **175:**3247-52.

109. **Koudelka, G. B., S. C. Harrison, and M. Ptashne.** 1987. Effect of non-contacted bases on the affinity of 434 operator for 434 repressor and Cro. Nature **326:**886-8.

110. **Kroczek, R. A., and E. Siebert.** 1990. Optimization of northern analysis by vacuum-blotting, RNA-transfer visualization, and ultraviolet fixation. Anal. Biochem. **184:**90-5.

111. **Labischinski, H., and H. Maidhof.** 1994. Bacterial peptidoglycan:overview and evolving concepts., p. 23-38. *In* G. J.-M. and R. Hackenbeck (ed.), Bacterial Cell Wall. Elsevier.

112. **Laemmli, U. K.** 1970. Cleavage of structural proteins during the assembly of the head of bacteriophage T4. Nature **227:**680-5.

113. **Lai, H. C., D. Gygi, G. M. Fraser, and C. Hughes.** 1998. A swarming-defective mutant of *Proteus mirabilis* lacking a putative cation-transporting membrane P-type ATPase. Microbiology **144:**1957-61.

114. **Lamond, A. I., and A. A. Travers.** 1983. Requirement for an upstream element for optimal transcription of a bacterial tRNA gene. Nature **305:**248-250.

115. **Lamont, R. J., D. R. Demuth, C. A. Davis, D. Malamud, and B. Rosan.** 1991. Salivary-agglutinin-mediated adherence of *Streptococcus mutans* to early plaque bacteria. Infect. Immun. **59**(10)**:**3446-50.

116. **Lamont, R. J., and B. Rosan.** 1990. Adherence of mutans streptococci to other oral bacteria. Infect. Immun. **58:**1738-43.

117. **Lawrence, J. R., and D. E. Caldwell.** 1987. Behavior of bacterial stream

populations within the hydrodynamic boundry layers of surface microenvironments. Microbial. Ecology **14:**15-27.

118. **Lawrence, J. R., P. J. Delaquis, and D. R. Krober.** 1987. Behavior of *Pseudomonas fluorescens* within the hydrodynamic boundry layers of surface microenvironments. Microbial. Ecology **14:**1-14.

119. **Lebrun, M., A. Audurier, and P. Cossart.** 1994. Plasmid-borne cadmium resistance genes in *Listeria monocytogenes* are similar to *cadA* and *cadC* of *Staphylococcus aureus* and are induced by cadmium. J. Bacteriol. **176:**3040-8.

120. **Lee, S. F.** 1995. Active release of bound antibody by *Streptococcus mutans*. Infect. Immun. **63:**1940-6.

121. **Lee, S. F.** 1992. Identification and characterization of a surface protein-releasing activity in *Streptococcus mutans* and other pathogenic streptococci. Infect. Immun. **60:**4032-9.

122. **Lee, S. F.** 1999. Unpublished results.

123. **Lee, S. F., Y. H. Li, and G. H. Bowden.** 1996. Detachment of *Streptococcus mutans* biofilm cells by an endogenous enzymatic activity. Infect. Immun. **64:**1035-8.

124. **Lee, S. F., R. J. March, S. A. Halperin, G. Faulkner, and L. Gao.** 1999. Surface expression of a protective recombinant pertussis toxin S1 subunit fragment in *Streptococcus gordonii*. Infect. Immun. **67:**1511-6.

125. **Lee, S. F., A. Progulske-Fox, and A. S. Bleiweis.** 1988. Molecular cloning and expression of a *Streptococcus mutans* major surface protein antigen, P1 (I/II), in

Escherichia coli. Infect. Immun. **56:**2114-9.

126. **Lee, S. F., A. Progulske-Fox, G. W. Erdos, D. A. Piacentini, G. Y. Ayakawa, P. J. Crowley, and A. S. Bleiweis.** 1989. Construction and characterization of isogenic mutants of *Streptococcus mutans* deficient in major surface protein antigen P1 (I/II). Infect. Immun. **57:**3306-13.

127. **Lehner, T., J. Caldwell, and R. Smith.** 1985. Local passive immunization by monoclonal antibodies against streptococcal antigen I/II in the prevention of dental caries. Infect. Immun. **50:**796-9.

128. **Leimeister-Wachter, M., C. Haffner, E. Domann, W. Goebel, and T. Chakraborty.** 1990. Identification of a gene that positively regulates expression of listeriolysin, the major virulence factor of *Listeria monocytogenes*. Proc. Natl. Acad. Sci. U. S. A. **87**(21)**:**8336-40.

129. **Leirskar, J.** 1974. On the mechanism of cytotoxity of silver and copper amalgams in a cell culture system. Scand. J. Dent. Res. **82:**74-81.

130. **Li, Y. H., and G. H. Bowden.** 1994. Characteristics of accumulation of oral gram-positive bacteria on mucin- conditioned glass surfaces in a model system. Oral Microbiol. Immunol. **9:**1-11.

131. **Li, Y. H., and G. H. Bowden.** 1994. The effect of environmental pH and fluoride from the substratum on the development of biofilms of selected oral bacteria. J. Dent. Res. **73:**1615-26.

132. **Lindahl, T., and B. Nyberg.** 1972. Rate of depurination of native deoxyribonucleic acid. Biochemistry **11:**3610-8.

133. **Loesche, W. J.** 1986. Role of *Streptococcus mutans* in human dental decay. Microbiol. Rev. **50:**353-80.

134. **Loesche, W. J., J. Rowan, L. H. Straffon, and P. J. Loos.** 1975. Association of *Streptococcus mutans* with human dental decay. Infect. Immun. **11:**1252-60.

135. **Lunsford, R. D.** 1995. Recovery of RNA from oral streptococci. Biotechniques **18:**412-4.

136. **Ma, J. K., A. Hiatt, M. Hein, N. D. Vine, F. Wang, P. Stabila, C. van Dolleweerd, K. Mostov, and T. Lehner.** 1995. Generation and assembly of secretory antibodies in plants [see comments]. Science **268:**716-9.

137. **Ma, J. K., T. Lehner, P. Stabila, C. I. Fux, and A. Hiatt.** 1994. Assembly of monoclonal antibodies with IgG1 and IgA heavy chain domains in transgenic tobacco plants. Eur. J. Immunol. **24:**131-8.

138. **Ma, J. K., R. Smith, and T. Lehner.** 1987. Use of monoclonal antibodies in local passive immunization to prevent colonization of human teeth by *Streptococcus mutans*. Infect. Immun. **55:**1274-8.

139. **Mandel, I. D.** 1987. The functions of saliva. J. Dent. Res. **66:**623-7.

140. **Marsh, P. D., C. W. Keevil, A. S. McDermid, M. I. Williamson, and D. C. Ellwood.** 1983. Inhibition by the antimicrobial agent chlorhexidine of acid production and sugar transport in oral streptococcal bacteria. Arch. Oral Biol. **28:**233-40.

141. **Massidda, O., R. Kariyama, L. Daneo-Moore, and G. D. Shockman.** 1996. Evidence that the PBP 5 synthesis repressor (psr) of *Enterococcus hirae* is also

involved in the regulation of cell wall composition and other cell wall-related properties. J. Bacteriol. **178:**5272-8.

142. **Matsuhashi, M.** 1994. Utilization of lipid-linked precurusors and the formation of peptidoglycan in the process of cell growth and division: membrane enzymes involved in the final steps of peptidoglycan synthesis and the mechanism of their regulation., p. 55-71. *In* J.-M. Ghuysen and R. Hakenbeck (ed.), Bacterial Cell wall. Elsevier.

143. **May, T. B., D. Shinabarger, R. Maharaj, J. Kato, L. Chu, J. D. DeVault, S. Roychoudhury, N. A. Zielinski, A. Berry, R. K. Rothmel, and et al.** 1991. Alginate synthesis by *Pseudomonas aeruginosa*: a key pathogenic factor in chronic pulmonary infections of cystic fibrosis patients. Clin. Microbiol. Rev. **4:**191-206.

144. **Mazmanian, S. K., G. Liu, H. Ton-That, and O. Schneewind.** 1999. *Staphylococcus aureus* sortase, an enzyme that anchors surface proteins to the cell wall. Science **285:**760-3.

145. **Minah, G. E., and W. J. Loesche.** 1977. Sucrose metabolism by prominent members of the flora isolated from cariogenic and non-cariogenic dental plaques. Infect. Immun. **17:**55-61.

146. **Minah, G. E., and W. J. Loesche.** 1977. Sucrose metabolism in resting-cell suspensions of caries associated and non-caries-associated dental plaque. Infect. Immun. **17:**43-54.

147. **Moore, W. E., L. V. Holdeman, R. M. Smibert, D. E. Hash, J. A. Burmeister, and R. R. Ranney.** 1982. Bacteriology of severe periodontitis in young adult

humans. Infect. Immun. **38:**1137-48.

148. **Mooser, G., S. A. Hefta, R. J. Paxton, J. E. Shively, and T. D. Lee.** 1991. Isolation and sequence of an active-site peptide containing a catalytic aspartic acid from two *Streptococcus sobrinus* alpha- glucosyltransferases. J. Biol. Chem. **266:**8916-22.

149. **Munro, C., S. M. Michalek, and F. L. Macrina.** 1991. Cariogenicity of *Streptococcus mutans* V403 glucosyltransferase and fructosyltransferase mutants constructed by allelic exchange. Infect. Immun. **59:**2316-23.

150. **Munro, G. H., P. Evans, S. Todryk, P. Buckett, C. G. Kelly, and T. Lehner.** 1993. A protein fragment of streptococcal cell surface antigen I/II which prevents adhesion of *Streptococcus mutans*. Infect. Immun. **61:**4590-8.

151. **Nakai, M., N. Okahashi, H. Ohta, and T. Koga.** 1993. Saliva-binding region of Streptococcus mutans surface protein antigen. Infect. Immun. **61:**4344-9.

152. **Navarre, W. W., and O. Schneewind.** 1999. Surface proteins of gram-positive bacteria and mechanisms of their targeting to the cell wall envelope. Microbiol. Mol. Biol. Rev. **63:**174-229.

153. **Navarre, W. W., H. Ton-That, K. F. Faull, and O. Schneewind.** 1998. Anchor structure of staphylococcal surface proteins. II. COOH-terminal structure of muramidase and amidase-solubilized surface protein. J. Biol. Chem. **273:**29135-42.

154. **Nucifora, G., L. Chu, T. K. Misra, and S. Silver.** 1989. Cadmium resistance from *Staphylococcus aureus* plasmid pI258 cadA gene results from a cadmium-efflux ATPase. Proc. Natl. Acad. Sci. U.S.A. **86:**3544-8.

155. **Odermatt, A., and M. Solioz.** 1995. Two trans-acting metalloregulatory proteins

controlling expression of the copper-ATPases of *Enterococcus hirae*. J. Biol. Chem. **270.:**4349-54.

156. **Odermatt, A., H. Suter, R. Krapf, and M. Solioz.** 1992. An ATPase operon involved in copper resistance by *Enterococcus hirae*. Ann. NY Acad. Sci. **671:**484-6.

157. **Odermatt, A., H. Suter, R. Krapf, and M. Solioz.** 1993. Primary structure of two P-type ATPases involved in copper homeostasis in *Enterococcus hirae*. J. Biol. Chem. **268:**12775-9.

158. **Orstavik, D.** 1978. The in-vitro attachment of an oral *Streptococcus sp.* to the acquired tooth enamel pellicle. Arch. Oral Biol. **23:**167-73.

159. **Palmer, R. J., and D. C. White.** 1997. Developmental biology of biofilms: implications for treatment and control. T. in Microbiol. **5:**435-40.

160. **Palmgren, M. G., and K. B. Axelsen.** 1998. Evolution of P-type ATPases. Biochim Biophys. Acta. **1365**(1-2):37-45.

161. **Pancholi, V., and V. A. Fischetti.** 1989. Identification of an endogenous membrane anchor-cleaving enzyme for group A streptococcal M protein. Its implication for the attachment of surface proteins in gram-positive bacteria. J. Exp. Med. **170:**2119-33.

162. **Payne, A. S., and J. D. Gitlin.** 1998. Functional expression of the menkes disease protein reveals common biochemical mechanisms among the copper-transporting P-type ATPases. J. Biol. Chem. **273:**3765-70.

163. **Penderson, P. L., and E. Carafoli.** 1987. Ion motive ATPases. I. Ubiquity , properties, and significance to cell function. T. in Biological Sciences **12:**146-50.

164. **Perry, D., and H. K. Kuramitsu.** 1981. Genetic transformation of *Streptococcus mutans*,. Infectm Immunm **32:**1295-7.

165. **Petrukhin, K., S. Lutsenko, I. Chernov, B. M. Ross, J. H. Kaplan, and T. C. Gilliam.** 1994. Characterization of the Wilson disease gene encoding a P-type copper transporting ATPase: genomic organization, alternative splicing, and structure/function predictions. Hum. Mol. Genet. **3:**1647-56.

166. **Pruitt, K. M., R. C. Caldwell, A. D. Jamieson, and R. E. Taylor.** 1969. The interaction of salivary proteins with tooth surface. J Dent Res **48**(5):818-23.

167. **Quivey, R. G., Jr., R. C. Faustoferri, K. A. Clancy, and R. E. Marquis.** 1995. Acid adaptation in *Streptococcus mutans* UA159 alleviates sensitization to environmental stress due to RecA deficiency. FEMS Microbiol Lett **126**(3):257-61.

168. **Redfield, A. R., and C. W. Price.** 1996. General stress transcription factor sigmaB of *Bacillus subtilis* is a stable protein. J Bacteriol **178**(12):3668-70.

169. **Rittmenn, B. E.** 1989. Detachment from biofilms. *In* W. G. Characklis and P. A. Wilder (ed.), Structure and Function of Biofilms. Jon Wiley & sons Ltd.

170. **Roth, J. A.** 1995. Virulence mechanisms of bacterial pathogens, 2nd ed. ASM Press, Washington, D.C.

171. **Rundegren, J., and R. R. Arnold.** 1987. Differentiation and interaction of secretory immunoglobulin A and a calcium-dependent parotid agglutinin for several bacterial strains. Infect. Immun. **55:**288-92.

172. **Russell, R. R., A. C. Donald, and C. W. Douglas.** 1983. Fructosyltransferase activity of a glucan-binding protein from *Streptococcus mutans*. J Gen Microbiol

129:3243-50.

173. **Sack, R. A., S. Sathe, L. A. Hackworth, M. D. Willcox, E. A. Holden, and C. A. Morris.** 1996. The effect of eye closure on protein and complement deposition on Group IV hydrogel contact lenses: relationship to tear flow dynamics. Curr Eye Res **15**(11):1092-100.

174. **Sambrook, J., E. F. Fritsch, and T. Maniatis.** 1989. Molecular cloning : a laboratory manual, 2nd ed. Cold Spring Harbor Laboratory, Cold Spring Harbor, NY.

175. **Scheie, A. A.** 1989. Modes of action of currently known chemical anti-plaque agents other than chlorhexidine. J.of D. R. **68:**1609-16.

176. **Schilling, K. M., and W. H. Bowen.** 1992. Glucans synthesized in situ in experimental salivary pellicle function as specific binding sites for *Streptococcus mutans*. Infect. Immun. **60.:**284-95.

177. **Schneewind, O., D. Mihaylova-Petkov, and P. Model.** 1993. Cell wall sorting signals in surface proteins of gram-positive bacteria. Embo. J. **12:**4803-11.

178. **Schneewind, O., P. Model, and V. A. Fischetti.** 1992. Sorting of protein A to the staphylococcal cell wall. Cell **70:**267-81.

179. **Selan, L., F. Berlutti, C. Passariello, M. R. Comodi-Ballanti, and M. C. Thaller.** 1993. Proteolytic enzymes: a new treatment strategy for prosthetic infections? Antimicrob. Agents Chemother. **37:**2618-21.

180. **Serrano, R., and F. Portillo.** 1990. Catalytic and regulatory sites of yeast plasma membrane H(+)-ATPase studied by directed mutagenesis. Biochim. Biophys. Acta.

1018:195-9.

181. **Shiroza, T., S. Ueda, and H. K. Kuramitsu.** 1987. Sequence analysis of the *gtfB* gene from *Streptococcus mutans*. J Bacteriol **169**(9):4263-70.

182. **Shockman, G. D., and J.-V. Holtje.** 1994. Microbial peptidoglycan (murien) hydrolases., p. 131-166. *In* G. J.-M. and R. Hackenbeck (ed.), Bacterial Cell Wall. Elsevier.

183. **Sissons, C. H., T. W. Cutress, M. P. Hoffman, and J. S. Wakefield.** 1991. A multi-station dental plaque microcosm (artificial mouth) for the study of plaque growth, metabolism, pH, and mineralization. J. Dent. Res. **70:**1409-16.

184. **Sissons, C. H., L. Wong, E. M. Hancock, and T. W. Cutress.** 1994. The pH response to urea and the effect of liquid flow in 'artificial mouth' microcosm plaques. Arch. Oral Biol. **39:**497-505.

185. **Skjorland, K. K., M. Rykke, and T. Sonju.** 1995. Rate of pellicle formation in vivo. Acta. Odontol. Scand. **53:**358-62.

186. **Smith, D. J., H. Akita, W. F. King, and M. A. Taubman.** 1994. Purification and antigenicity of a novel glucan-binding protein of *Streptococcus mutans*. Infect Immun **62:**2545-52.

187. **Smith, D. J., M. A. Taubman, C. F. Holmberg, J. Eastcott, W. F. King, and P. Ali-Salaam.** 1993. Antigenicity and immunogenicity of a synthetic peptide derived from a glucan-binding domain of mutans streptococcal glucosyltransferase. Infect. Immun. **61:**2899-905.

188. **Solioz, M., A. Odermatt, and R. Krapf.** 1994. Copper pumping ATPases:

common concepts in bacteria and man. FEBS Lett. **346:**44-7.

189. **Southern, E. M.** 1975. Detection of specific sequences among DNA fragments separated by gel electrophoresis. J. Mol. Biol. **98:**503-17.

190. **Staat, R. H., S. D. Langley, and R. J. Doyle.** 1980. Streptococcus mutans adherence: presumptive evidence for protein- mediated attachment followed by glucan-dependent cellular accumulation. Infect. Immun. **27(2):**675-81.

191. **Stephan, R. M.** 1945. The pH of carrious lesions. J. Dent. Res. **24:**202.

192. **Strausak, D., and M. Solioz.** 1997. CopY is a copper-inducible repressor of the *Enterococcus hirae* copper ATPases. J Biol. Chem. **272:**8932-6.

193. **Sturr, M. G., and R. E. Marquis.** 1992. Comparative acid tolerances and inhibitor sensitivities of isolated F- ATPases of oral lactic acid bacteria. Appl. Environ. Microbiol. **58:**2287-91.

194. **Svanberg, M.** 1980. *Streptococcus mutans* in plaque after mouth-rinsing with buffers of varying pH value. Scand. J. Dent. Res. **88:**76-8.

195. **Svanberg, M., and D. Birkhed.** 1991. Effect of dentifrices containing either xylitol and glycerol or sorbitol on mutans streptococci in saliva. Caries. Res. **25:**449-53.

196. **Takahashi, N., M. Horiuchi, and T. Yamada.** 1997. Effects of acidification on growth and glycolysis of *Streptococcus sanguis* and *Streptococcus mutans*. Oral. Microbiol. and Immun. **10:**72-76.

197. **Tanzer, J. M., M. I. Krichevsky, and P. H. Keyes.** 1969. The metabolic fate of glucose catabolized by a washed stationary phase caries-conducive streptococcus. Caries Res. **3:**167-77.

198. **Terleckyj, B., N. P. Willett, and G. D. Shockman.** 1975. Growth of several cariogenic strains of oral streptococci in a chemically defined medium. Infect. Immun. **11:**649-55.

199. **Theilade, E., and J. Theilade.** 1985. Formation and ecology of plaque at different locations in the mouth. Scand. J. Dent. Res. **93:**90-5.

200. **Tipper, D. J.** 1969. Structures of the cell wall peptidoglycans of *Staphylococcus epidermidis* Texas 26 and *Staphylococcus aureus* Copenhagen. II. Structure of neutral and basic peptides from hydrolysis with the Myxobacter al-1 peptidase. Biochemistry **8:**2192-202.

201. **Tipper, D. J., and M. F. Berman.** 1969. Structures of the cell wall peptidoglycans of *Staphylococcus epidermidis* Texas 26 and *Staphylococcus aureus* Copenhagen. I. Chain length and average sequence of cross-bridge peptides. Biochemistry **8:**2183-92.

202. **Tipper, D. J., and J. L. Strominger.** 1968. Biosynthesis of the peptidoglycan of bacterial cell walls. XII. Inhibition of cross-linking by penicillins and cephalosporins: studies in Staphylococcus aureus in vivo. J. Biol. Chem. **243:**3169-79.

203. **Tobian, J. A., M. L. Cline, and F. L. Macrina.** 1984. Characterization and expression of a cloned tetracycline resistance determinant from the chromosome of *Streptococcus mutans*. J. Bacteriol. **160:**556-63.

204. **Ton-That, H., K. F. Faull, and O. Schneewind.** 1997. Anchor structure of staphylococcal surface proteins. A branched peptide that links the carboxyl

terminus of proteins to the cell wall. J Biol Chem **272**(35):22285-92.

205. **Ton-That, H., G. Liu, S. K. Mazmanian, K. F. Faull, and O. Schneewind.** 1999. Purification and characterization of sortase, the transpeptidase that cleaves surface proteins of *Staphylococcus aureus* at the LPXTG motif [In Process Citation]. Proc Natl. Acad. Sci. U.S.A **96:**12424-9.

206. **Ton-That, H., and O. Schneewind.** 1999. Anchor structure of staphylococcal surface proteins. IV. Inhibitors of the cell wall sorting reaction. J. Biol. Chem. **274**(34):24316-20.

207. **Towbin, H., T. Staehelin, and J. Gordon.** 1979. Electrophoretic transfer of proteins from polyacrylamide gels to nitrocellulose sheets: procedure and some applications. Proc. Natl. Acad.Sci. U S A **76:**4350-4.

208. **Tsumori, H., and H. Kuramitsu.** 1997. The role of the *Streptococcus mutans* glucosyltransferases in the sucrose-dependent attachment to smooth surfaces: essential role of the GtfC enzyme. Oral. Microbiol. Immunol. **12:**274-80.

209. **Tsumori, H., T. Minami, and H. K. Kuramitsu.** 1997. Identification of essential amino acids in the *Streptococcus mutans* glucosyltransferases. J Bacteriol **179:**3391-6.

210. **Ueda, S., T. Shiroza, and H. K. Kuramitsu.** 1988. Sequence analysis of the *gtfC* gene from *Streptococcus mutans* GS-5. Gene **69:**101-9.

211. **Vadeboncoeur, C., and L. Gauthier.** 1987. The phosphoenolpyruvate: sugar phosphotransferase system of Streptococcus salivarius. Identification of a IIIman protein. Can. J. Microbiol. **33:**118-22.

212. **Vadeboncoeur, C., and M. Pelletier.** 1997. The phosphoenolpyruvate:sugar phosphotransferase system of oral streptococci and its role in the control of sugar metabolism. FEMS Microbiol. Rev. **19:**187-207.

213. **van Loosdrecht, M. C., J. Lyklema, W. Norde, and A. J. Zehnder.** 1990. Influence of interfaces on microbial activity. Microbiol. Rev. **54:**75-87.

214. **Vassilakos, N., T. Arnebrant, and P. O. Glantz.** 1992. Adsorption of whole saliva onto hydrophilic and hydrophobic solid surfaces: influence of concentration, ionic strength and pH. Scand. J. Dent. Res. **100:**346-53.

215. **Venkitaraman, A. R., A. M. Vacca-Smith, L. K. Kopec, and W. H. Bowen.** 1995. Characterization of glucosyltransferaseB, GtfC, and GtfD in solution and on the surface of hydroxyapatite. J. Dent. Res. **74:**1695-701.

216. **Vickerman, M. M., and G. W. Jones.** 1995.. Sucrose-dependent accumulation of oral streptococci and their adhesion- defective mutants on saliva-coated hydroxyapatite. Oral Microbiol. Immunol. **10:**175-82.

217. **Wataha, J. C., and P. E. Lockwood.** 1998. Release of elements from dental casting alloys into cell-culture medium over 10 months. Dent. Mater. **14:**158-63.

218. **Wittman, V., H. C. Lin, and H. C. Wong.** 1993. Functional domains of the penicillinase repressor of *Bacillus licheniformis*. J. Bacteriol. **175:**7383-90.

219. **Wittman, V., and H. C. Wong.** 1988. Regulation of the penicillinase genes of *Bacillus licheniformis*: interaction of the pen repressor with its operators. J. Bacteriol. **170:**3206-12.

220. **Wong, C., S. A. Hefta, R. J. Paxton, J. E. Shively, and G. Mooser.** 1990. Size and

subdomain architecture of the glucan-binding domain of sucrose:3-alpha-D-glucosyltransferase from *Streptococcus sobrinus*. Infect. Immun. **58:**2165-70.

221. **Wu, Z., G. D. Wright, and C. T. Walsh.** 1995. Overexpression, purification, and characterization of VanX, a D-, D- dipeptidase which is essential for vancomycin resistance in *Enterococcus faecium* BM4147. Biochemistry **34:**2455-63.

222. **Wunderli-Ye, H., and M. Solioz.** 1999. Effects of promoter mutations on the in vivo regulation of the cop operon of *Enterococcus hirae* by copper(I) and copper(II). Biochem. Biophys. Res. Commun. **259:**443-9.

223. **Yamada, T., and J. Carlsson.** 1973. Phosphoenolpyruvate carboxylase and ammonium metabolism in oral streptococci. Arch. Oral Biol. **18:**799-812.

224. **Yamashita, Y., W. H. Bowen, R. A. Burne, and H. K. Kuramitsu.** 1993. Role of the *Streptococcus mutans gtf* genes in caries induction in the specific-pathogen-free rat model. Infect. Immun. **61:**3811-7.